POLITECNICO DI MILANO

School of Industrial and Information Engineering

Master of Science in Materials Engineering and Nanotechnology

DEVELOPMENT OF NOVEL COATINGS FOR GENE-ELUTING STENT APPLICATIONS

Supervisor: Prof. Gabriele CANDIANI
Co-supervisor: Prof. Diego MANTOVANI
Dott. Daniele PEZZOLI

Candidate:
Leonardo BOAROTTO   Matr. 854058

Academic year: 2016/2017

TABLE OF CONTENTS

LIST OF FIGURES

LIST OF TABLES

ABSTRACT

The overall goal of this thesis was the development of novel coatings for AISI 316L substrates, to be applied in gene-eluting stent applications for the treatment of artery-related diseases. Particularly, it aimed at the realization of platforms able to directly anchor non-viral gene delivery particles on their surface and exert surface-mediated gene delivery. The major challenges toward the realization of a reliable gene-eluting stent (GES) apparatus are the realization of stable, biocompatible and anti-thrombogenic biomaterial surfaces capable to immobilize gene delivery vectors and allow their interaction with cells upon implantation. In this context, AISI 316L was chosen as starting material, since it is the most commonly used austenitic stainless-steel metal for stents and biomedical applications in general; then, an electropolishing process was performed to decrease its superficial roughness, and finally, two superficial modifications were investigated in parallel. The first concerned the deposition of a reactive polydopamine (PDA) coating, while the second one was based on the functionalization of the former with glutaric anhydride (GLU), to introduce carboxylic acids on the surface. The choice of these treatments was done according to the overall goal of this work of being able to attach on them PEI-based polyplexes, thus positively charged structures, bearing amine groups at surface. Particularly, the main hypothesis at the base of the work are that PEI-based polyplexes react with PDA forming covalent bonds, while, with GLU through electrostatic interactions. The developed surface treatments were characterized in terms of morphological and physicochemical properties, from which the success of the different modification protocols was confirmed and a good cytocompatibility was observed, making them promising for biomedical applications. Furthermore, PDA and GLU ability to immobilize on the surface amine-bearing sub-micrometric particles was investigated and the stability of the deposition was assessed by either simple washing in PBS and under flow reproducing quasi-physiological shear stresses occurring *in vivo* in coronary arteries. Both PDA and GLU surfaces allowed to increase particle deposition with respect to unmodified electropolished stainless steel, with GLU reaching very high surface coverage values of about 80%; furthermore, the particles demonstrated to be quite stably attached to the surfaces even under flow. Finally, preliminary surface-mediated transfection tests were performed using bPEI-based polyplexes on HeLa cells, but with limitedly satisfactory results. Hence, further optimization of the polyplex type and of the polyplex deposition will be necessary to take advantage of the properties of the well-developed coatings for surface-mediated gene delivery.

SOMMARIO

Le componenti essenziali del sistema cardiovascolare umano sono il cuore, il sangue e i vasi sanguigni. L' azione combinata di tali componenti garantisce la circolazione sanguigna e il trasporto di nutrienti e ossigeno da e verso le cellule all' interno dell'organismo. Sfortunatamente, diverse malattie cardiovascolari ne compromettono il regolare funzionamento, causando, nel solo 2015, 15 milioni di morti. Tra di esse, l'aterosclerosi è la condizione più diffusa e si manifesta tramite la formazione di placche ateromatose, in seguito al deposito di grassi e coaguli di sangue nelle pareti delle arterie. La principale conseguenza di tale accumulo è la parziale o totale ostruzione al normale flusso sanguigno (stenosi), che può portare per esempio all'insorgere di infarti se le arterie interessate sono quelle coronarie e di ictus se i vasi ostruiti sono quelli cerebrali. Solamente negli USA, circa 1.4 milioni di procedure chirurgiche vengono compiute annualmente per la cura e il trattamento di malattie del sistema coronarico (World Health Organization (WHO), dati aggiornati al 2011), e tale numero è destinato ad aumentare, in relazione all' aumento dei fattori di rischio associati alla patologia (fumo di sigaretta, obesità e ipertensione) e all' incremento dell'aspettativa di vita media della popolazione.

Ad oggi, tra i trattamenti disponibili, l'angioplastica percutanea transluminale (PTCA) rappresenta il metodo più utilizzato, in particolare quando associato all'impiego di stent. Essa consiste nell'inserimento di un palloncino montato su un catetere guida, e nella sua espansione nella regione di restringimento del vaso sanguigno. In aggiunta, uno stent è posto *in situ* per garantire il supporto meccanico alle pareti dell'arteria, riducendo sia i rischi a breve che a lungo termine di restenosi. Lo stent è una protesi metallica tubulare a maglie aperte, che permette di alleviare gli effetti dell'aterosclerosi e di supportare meccanicamente le pareti arteriose, garantendo l'allargamento della sezione del lume e il suo mantenimento nel tempo.

In generale, i requisiti necessari per l'impiego di stent sono la capacità di sottoporsi a deformazione plastica e di mantenerla una volta espansi, biocompatibilità e proprietà anti-trombogeniche. Inoltre, essi dovrebbero garantire un'efficiente proliferazione delle cellule endoteliali per consentire la formazione di neointima sulla loro superficie, evitando così la formazione di iperplasia neointimale. Tale complicazione si riferisce ad un'eccessiva proliferazione e migrazione di cellule muscolari lisce primarie nella tunica intima, con conseguente ispessimento delle pareti arteriose e riduzione del lume: la cosiddetta restenosi intra stent (ISR).

Per quanto riguarda gli stent metallic tradizionali (Bare metal stent o BMS), i materiali più comunemente usati sono: acciaio inossidabile AISI, cobalto-cromo, nichel-titanio e leghe di platino-iridio; mentre, ferro puro e leghe di magnesio stanno guadagnando rilevanza come materiali per la produzione di stent degradabili. Tuttavia, sebbene l'utilizzo di stent abbia contribuito a ridurre l'incidenza di restenosi coronarica, il rischio non è risolto completamente; infatti, l'ISR si verifica ad un tasso compreso tra il 20% e il 30% entro i primi sei mesi dopo l'impianto di BMS.

Così, nuove tecnologie sono state sviluppate. Tra di esse, l'innovazione è stata guidata dagli stent medicati (Drug Eluting Stent), ovvero BMS rivestiti con materiale polimerico, utilizzati come substrati e serbatoi per il rilascio di farmaci, tra cui agenti pro-endoteliali e agenti antiproliferativi, con l'obiettivo di diminuire il tasso di restenosi. Tuttavia, malgrado i progressi ottenuti nel trattamento clinico di cardiopatie coronariche, l'insorgenza di trombosi tardiva e iperplasia neointimale, ha spinto, ancora una volta, la medicina verso la realizzazione di nuovi trattamenti.

In questo progetto, l'idea di combinare il supporto meccanico degli stent con la possibilità di utilizzarli come piattaforme per il rilascio controllato di geni, è stata proposta come possibile soluzione al problema. In particolare, lo scopo di questo studio è quello di sviluppare rivestimenti superficiali per substrati in acciaio inossidabile AISI316L, atti ad immobilizzare vettori non-virali per il rilascio di materiale genetico esogeno da superficie (surface-mediated gene delivery).

Le sfide che caratterizzano la realizzazione di tali dispositivi (Gene-eluting stent o GES) sono la realizzazione di un biomateriale stabile, biocompatibile e anti-trombogenico, in grado di immobilizzare e mantenere i vettori in superficie, al fine di promuovere e sostenere la loro associazione e internalizzazione cellulare. In questo lavoro, l'acciaio inossidabile AISI 316L è stato scelto come materiale di partenza, dal momento che è il metallo austenitico più comunemente usato per la produzione di stent e in generale per applicazioni biomediche. Infatti, esso combina adeguate proprietà meccaniche ad un'eccellente resistenza alla corrosione, le quali sono principalmente garantite dalla presenza di cromo nella sua composizione.

Inizialmente, il processo di lucidatura elettrochimica è stato utilizzato per diminuire la rugosità dello strato di ossido superficiale, ed ottenere una superficie più pulita e chimicamente più omogenea. Poi, a partire da tali superfici, due rivestimenti superficiali sono stati indagati parallelamente: il primo è stato realizzato con deposizione di sola polidopamina (PDA), mentre il secondo, mediante una funzionalizzazione del precedente con anidride glutarica (GLU).

La scelta di questi trattamenti è stata eseguita al fine di sfruttare le proprietà adesive, la stabilità e la reattività chimica della polidopamina (PDA), con l'obiettivo finale di immobilizzare su di essi, poliplessi generati mediante l'utilizzo di polietilenimmina (PEI), ovvero strutture cariche positivamente, aventi gruppi amminici in superficie. In particolare, l'ipotesi principale alla base del lavoro è che tali complessi reagiscano con il rivestimento in PDA formando legami chimici covalenti, mentre, con il PDA funzionalizzato (GLU) attraverso interazioni elettrostatiche.

Il lavoro sperimentale di questa tesi è stato condotto presso il Laboratorio di Biomateriali e Bioingegneria (LBB, Québec, Canada), e i suoi obiettivi specifici sono divisi nelle seguenti quattro diverse fasi:

1) Ottenimento di substrati in acciaio inossidabile AISI 316L, lisci e chimicamente omog-enei, mediante lucidatura elettrochimica

2) Sviluppo e caratterizzazione di rivestimenti superficiali in polidopamina (PDA) e PDA-funzionalizzata con anidride glutarica (GLU), partendo dai substrati precedentemente ottenuti nella fase 1

3) Deposizione di particelle sub-micrometriche aventi ammine primarie in superficie, per simulare il comportamento di poliplessi, al fine di convalidare le ipotesi d' interazione rivestimento/particelle

4) Test preliminari di trasfezione su cellule HeLa, utilizzando poliplessi a base di PEI

Relativamente alla prima fase, con l'obiettivo di ottenere superfici metalliche in acciaio inossidabile più lisce e prive di imperfezioni, è stato eseguito un processo di lucidatura elettrochimica, seguendo un protocollo precedentemente sviluppato al LBB. La microscopia a forza atomica (AFM) e la microscopia a scansione elettronica (SEM) hanno confermato la buona riuscita del processo mostrando superfici lisce accompagnate dalla formazione di bordi grano. Inoltre, una diminuzione sia della rugosità (RMS) che dei valori dell'angolo di contatto, ha evidenziato l'ottenimento di superfici più lisce, più idrofiliche e quindi ben elettrolucidate. Infine, l'analisi XPS ha confermato l'ottenimento di uno strato di ossido spesso e omogeneo, dovuto al processo di elettrolucidatura, dimostrando un aumento del contenuto di ossigeno e composti metallici in superficie.

Per quanto riguarda la seconda fase di questo lavoro invece, sia le superfici ottenute in PDA che quelle in GLU sono state analizzate morfologicamente, fisico-chimicamente e infine anche biologicamente, come suggerito dall'obiettivo finale di applicarle come rivestimenti per GES. Dall'imaging AFM, è possibile apprezzare la formazione di protrusioni (punti bianchi) sulle superfici PDA e GLU, che non erano presenti su campioni EP; mentre, dall'analisi SEM, è ancora possibile osservare la struttura dei bordi dei grani tipica delle superfici EP, a prova del fatto che sono stati ottenuti rivestimenti sottili e dunque che non hanno alterato eccessivamente la morfologia superficiale. Successivamente, l'analisi RMS ottenuta dalle immagini AFM ha mostrato: un leggero aumento dei valori dopo il rivestimento in PDA e un aumento rilevante dopo la funzionalizzazione con GLU. Ciò è dovuto alla formazione di protrusioni superficiali dopo le modifiche superficiali apportate, e tale aspetto è sottolineato dalle misure dell'angolo di contatto, le quali diminuiscono moderatamente per entrambe le superfici PDA e GLU, rispetto ai campioni EP, evidenziando l'arricchimento superficiale in composti idrofili come NH_3^+ e COO^-. Sono stati eseguiti saggi di colorimetria per quantificare la reale quantità di composti depositati in superficie, ma non sono state fornite informazioni sulla loro natura chimica. Pertanto, tecniche spettroscopiche come FT-IR e XPS sono state impiegate per ottenere informazioni sulla composizione elementare superficiale. In particolare, l'analisi FT-IR ha mostrato la comparsa di nuove bande, tipiche dei rivestimenti in polidopamina (PDA); mentre, l'XPS, ha registrato un aumento del contenuto di carbonio e di azoto, come suggerito dalla natura organica chimica di entrambi i rivestimenti, e una diminuzione di quelli dell'ossigeno e dei composti metallici, il che dimostra il fatto che uno spesso strato (circa 50 nm, secondo i dati della letteratura) di polidopamina è stata depositata in superficie. Inoltre, l'analisi XPS eseguita dopo derivatizzazione chimica con vapori di 4- (trifluorometil) benzaldeide ha evidenziato, come previsto, una

quantità importante di ammine primarie su campioni di PDA, che sono poi quasi completamente scomparsi dopo la funzionalizzazione della PDA con GLU.

Infine, la biocompatibilità e la citotossicità di PDA e GLU sono state testate attraverso test di vitalità diretta e indiretta, utilizzando cellule HeLa e HUVEC. Non sono state notate differenze tra le due tipologie cellulari, in cui entrambi i trattamenti sono apparsi non citotossici, mostrando inoltre risultati promettenti in termini di adesione e proliferazione cellulare, specialmente sulle cellule endoteliali (HUVEC), ovvero quelle cellule che sono in contatto diretto con gli stent. Come prospettiva futura, gli stessi test dovrebbero essere eseguiti in punti di tempo più lunghi (7 e 14 giorni) e su altre linee cellulari, come le cellule muscolari lisce (SMC), che sono coinvolte nei processi di restenosi arteriosa. In particolare, i trattamenti dovrebbero bloccare la loro adesione e proliferazione, al fine di ridurre l'insorgenza di iperplasia neointimale.

Una volta che le superfici sono state sviluppate e completamente caratterizzate, su di esse sono state depositate particelle sub-micrometriche, aventi ammine primarie in superficie, al fine di simulare l'interazione tra le superfici trattate e i poliplessi. Come confermato dalla microscopia a luce visibile, sono stati ottenuti buoni risultati in termini di attaccamento, in particolare sui campioni GLU, dove, rispetto ai semplici rivestimenti in PDA, la deposizione è stata incrementata di circa quattro volte. Inoltre, sia sul PDA che sul GLU, dopo 7 giorni di test dinamici sotto flusso, riproducendo sforzi di taglio quasi fisiologici che si verificano *in vivo* nelle arterie coronarie, è stata osservata un'elevata resistenza adesiva.

Alla luce di questi risultati molto promettenti in termini di deposizione e stabilità delle particelle, l'ultima fase di questo lavoro ha riguardato esperimenti preliminari di transfezione superficiale su cellule HeLa; per i quali, poliplessi preparati miscelando 250 kDa bPEI e pGLuc-Basic Vector at N /P=2.5 sono stati depositati su entrambe superfici trattate. Il saggio Luciferase è stato utilizzato per valutare l'efficienza della trasfezione. Inaspettatamente, dall'analisi registrata a 24 ore, 72 ore, 5 giorni e 7 giorni dopo la trasfezione, sono stati ottenuti segnali piuttosto bassi in tutti i campioni testati, senza differenze rispetto ai campioni EP non trattati. Questi risultati, che sono bassi se confrontati con quelli ottenuti nelle transfezioni classiche in soluzione, suggeriscono come sia necessaria un'ulteriore ottimizzazione sia del tipo di poliplessi che della loro strategia di deposizione. In questo lavoro, infatti, sono stati eseguiti solo test preliminari, impiegando un solo tipo di polimero cationico e transfettando una tipologia di cellule soltanto. Ad ogni modo, supponendo che il bPEI sia la scelta migliore, poiché è considerato il miglior polimero cationico per le applicazioni di gene delivery, le sue caratteristiche dovrebbero essere modulate per ottenere efficienze di trasfezione superiori.

In conclusione, sebbene siano necessari ulteriori miglioramenti, in questo lavoro sono state sviluppate e caratterizzate due modifiche superficiali, PDA e GLU, che hanno mostrato risultati promettenti per la loro futura applicazione come piattaforme da utilizzare in tecniche di gene delivery da superficie. Infatti, i protocolli impiegati per la realizzazione dei rivestimenti hanno permesso di ottenere con buona riproducibilità dei rivestimenti biocompatibili e in grado di immobilizzare efficacemente le particelle sub-micrometriche in superficie.

1. Introduction

The purpose of this thesis is to develop novel strategies for surface mediated gene delivery, to be applied in cardiovascular stent applications for the treatment of artery-related diseases. In this context, the aim of this chapter is to describe the role of arteries in the vascular system, by giving an overview of their structure and of the main related diseases.

1.1. The cardiovascular system

The human cardiovascular system (Figure 1.1) is a closed system, composed by heart, blood and blood vessels, which all together guarantee blood circulation and transport of nutrients and oxygen towards all the organs and cells in the body.[1] It can be divided in two main closed systems: systemic and pulmonary circulation. The former consists of a "loop" through the body that provides oxygenated blood to tissues; while, the latter one a "loop" through the lungs where blood is re-oxygenated. Moreover, a third system, which is heart-specific, is present to guarantee the blood supply to the heart: the coronary system.
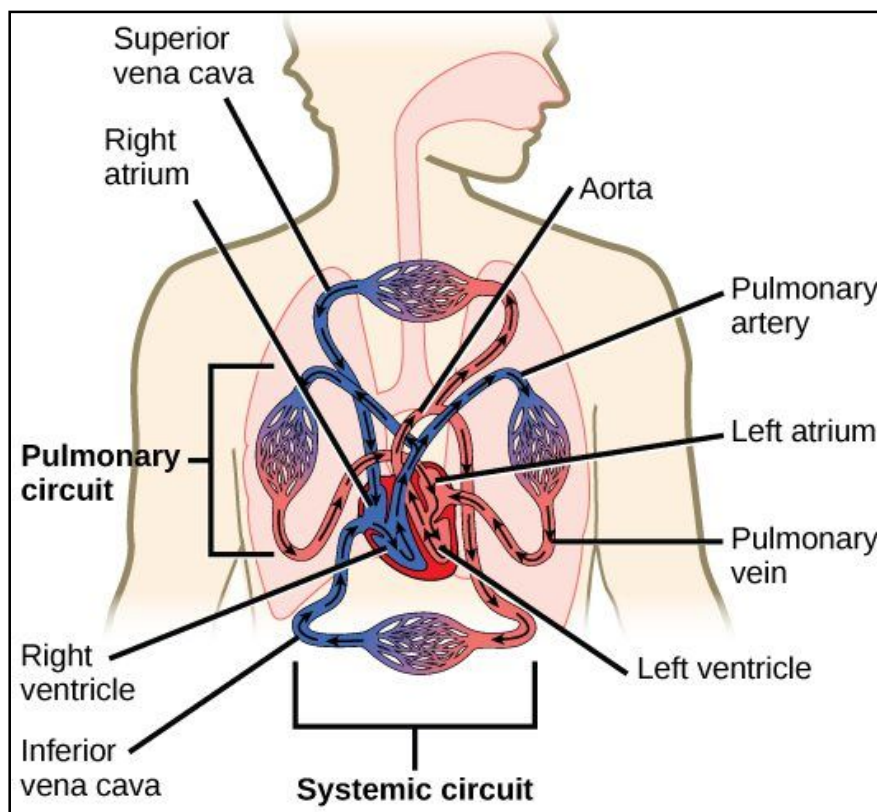
Figure 1.1: Schematization of the human cardiovascular system[1]

The heart is a muscular organ, which pumps blood to the blood vessels of the circulatory system, through to automatic and rhythmic contractions. It is divided into four chambers called left and right atria and right and left ventricles.

The complex network of blood vessels, instead, is composed by arteries, which branch and narrow along the system into arterioles and then further into capillaries. Furthermore, capillaries widen to become venules, which in turn converge to become veins.

Since, the oxygenated blood is ejected at high pressure (80-120 mmHg) from the heart by the left ventricle to the aorta and is then distributed to the organs by the systemic arteries, arterial walls must withstand elevated levels of pressure, and thus, must be thick, elastic, and when active contraction is needed, muscular.[2]

1.1.1. The structure of arteries

Arteries are hollowed-cylindrical structures composed mainly by three adjacent concentric layers, which are, from the core to the external part (Figure 1.2):

- *Tunica intima*: it is the innermost layer, directly in contact with the blood flow that streams in the inner cavity called *lumen.* It is composed by a monolayer of endothelial cells (ECs, endothelium), which are flattened cells whose role is to impair blood coagulation and translating mechanical signals coming from the blood flow into physiological signals (i.e. mechano-transduction).[3] The endothelium lies on an extracellular matrix (ECM) called the basal membrane that in turn is placed over the so called internal elastic lamina.[4]

- *Tunica media*: it is the mid-layer and it is mainly composed by smooth muscle cells (SMCs) immersed in an elastic ECM. SMCs are responsible for the vasoconstriction and vasodilation of the arteries in response to biological stimuli. The media ECM provides support and mechanical stability to the vessel and thus it is rich in connective tissue (collagen type-I and proteoglycans) as well as elastic fibers (elastin) responsible for vessel elasticity. The thickness of the media layer is variable inside the circulatory system, and it is directly proportional to the diameter of the vessel and in arteries is higher than in veins.[5]

- *Tunica adventitia*: it is the outer layer, separated from the tunica media by the external elastic lamina. It is a connective tissue composed of an ECM mainly made of collagen type III and elastin and populated by fibroblasts. Its main role is connecting blood vessels to the surrounding tissues and, in case of thick vessels, it features nerves and capillaries.[5]
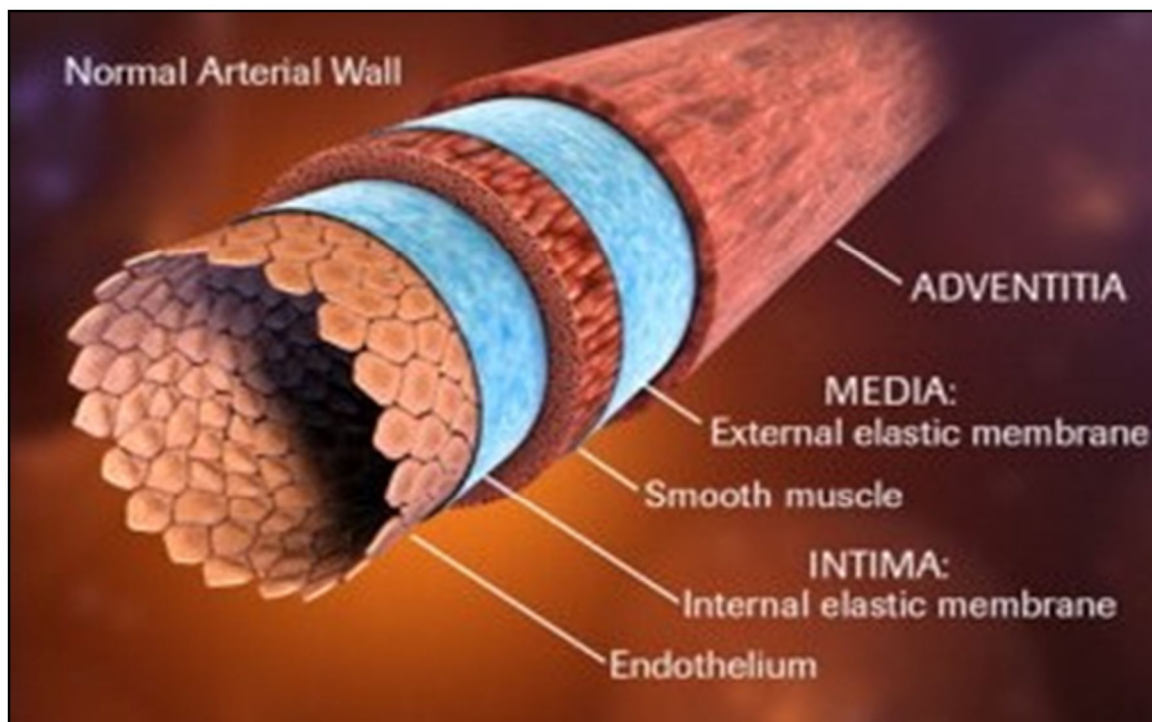
Figure 1.2: Schematic representation of distinct layers of arterial wall[6]

1.2. Cardiovascular Diseases (CVDs)

Cardiovascular diseases (CVDs) are the main cause of mortality in the world. In fact, as estimated by the World Health Organization (WHO) statistics, approximately 17.5 million of people die each year because of CVDs representing, as shown in Figure 1.3, 31% of the cause of the all deaths worldwide.[7,8]
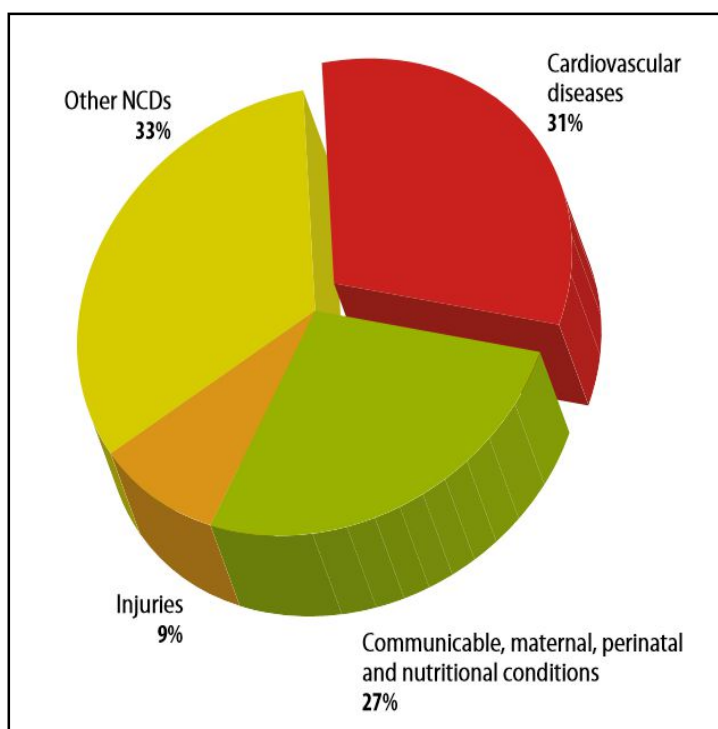
Figure 1.3: Distribution of the major causes of death including CVDs[8]

The term CVDs refers to a general category of diseases representative of many heart and blood vessel disorders that are caused by different phenomena. Among them, atherosclerosis is the main responsible for coronary heart diseases, cerebrovascular diseases and many other artery dysfunctions: in 2011, the WHO organization estimated that these atherosclerosis-related diseases caused 80% (Figure 1.4) of the overall CVD related deaths.[8,9]
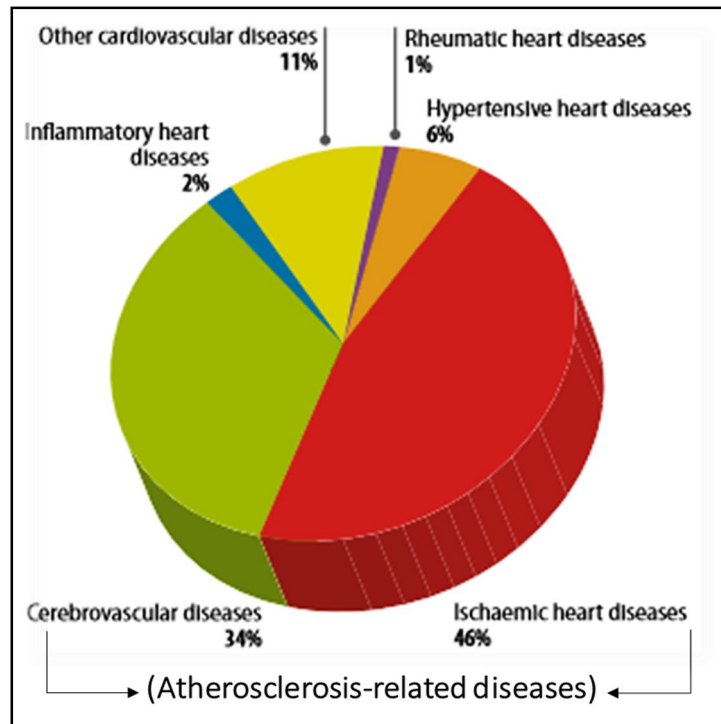
Figure 1.4: Distribution of CVD deaths due to heart attacks, strokes and other types, in males[8]

In light of these data, huge funding has been allocated by governments worldwide to the research in the prevention, control and treatment of atherosclerosis, aiming to decrease CVDs occurrence and mortality rate.[10,11]

1.3. Atherosclerosis

Atherosclerosis is a disease of the blood arterial walls that occurs at specific susceptible sites of blood vessels. It is characterized by a very slow and complex process that starts very early in infancy and whose complications evolve during decades, finally possibly causing disability and mortality.[5]

1.3.1. Physiopathology

The atherosclerotic process is initiated by the deposition and accumulation of the so called "atheromatous plaques" in the arterial walls, and its prolonged by a chronic inflammatory process.[7] Atherosclerotic plaques are mainly composed by lipids, connective tissue and debris, structured in a cholesterol-rich core (atheroma) and wrapped in a fibrous layer (sclerosis).[5]

Although the overall mechanism of plaque formation is not deeply understood yet, the principal cause of their formation is recognized to be the high blood concentrations of cholesterol, in particular the one carried by low-density lipoproteins (LDL).[12]

To date, many studies affirm that the process is triggered by LDLs accumulation, oxidation and modification within the intimal layer, and therefore sustained by the ability of these substances to stimulate the migration and proliferation of SMCs. In turn, these cells are capable of producing other chemo-attractive proteins that lead to the *in-situ* accumulation of white blood cells that ultimate the process by generating a chronic immunological response.[13]

The main consequences of plaque accumulation are the partial or total narrowing of the arterial lumen (stenosis) and the reduction of the blood flow (ischemia). Moreover, since some plaques are even vulnerable to rupture, they can ultimately provoke occlusive thrombosis inside vessels due to the formation of travelling blood clots.[14]

When vessel obstruction limits the blood flow and thus the supply of oxygen and nutrients towards the heart, it causes ischemia of the myocardial cells and their death, leading to myocardial infarction (i.e. heart attack), heart muscle damage and heart muscle death. When it occurs in the brain, an analogous mechanism of small cerebral blood vessels damaging will lead to ischaemic stroke or haemorrhagic stroke, in case of blockage or vessel rupture, respectively.[14]

Figure 1.5 schematically represents the progression of atherosclerosis from an initial lesion to the final stages of a fibrous plaque that can lead to complicated lesion or rupture.[15]
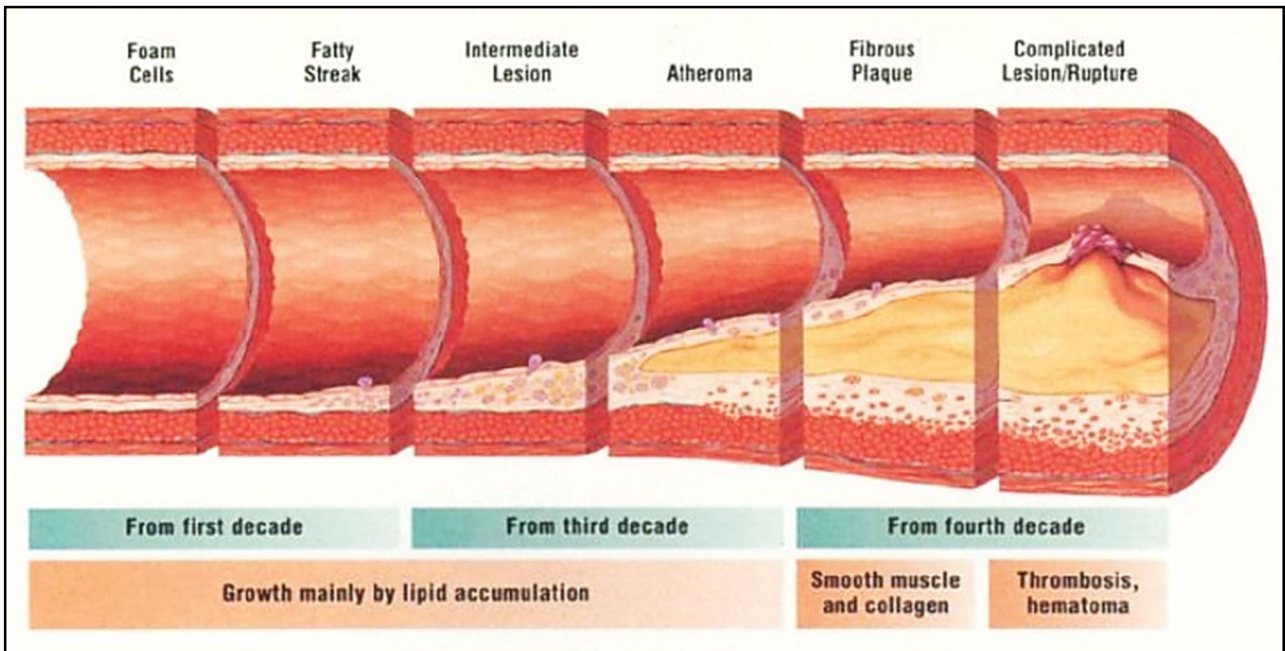
Figure 1.5: Atherosclerosis timeline, showing the progression of atherosclerotic process[15]

1.3.2. Current clinical treatments

Atherogenesis is affected by several risk factors, among which there are: hypertension, tobacco smoking, diabetes mellitus, obesity and genetic predisposition. According to the severity of the arterial damaging, different medical procedures are recommended to threat diseased vessels. Although lifestyle changes may help in preventing or limiting atherosclerosis, for example, via smoking cessation, diet restrictions and regular physical activity, in some case, i.e. once the plaque is formed, there is no way to remove it and medical intervention is necessary.[13]

The traditional ones include: angioplasty with or without vascular stenting and artery by-pass grafting.

Angioplasty is in both cases a minimally invasive procedure performed to restore blood flow in blocked arteries, while artery by-pass grafting is a surgical invasive technique which includes the substitution of the damaged portion of the vessel with a vascular graft.[16]

Since the aim of this work is to develop new strategies for surface-mediated gene delivery to be applied in stenting application, the next section will focus only on the angioplasty procedures.

1.3.2.1. Angioplasty and stenting

Angioplasty (without stenting) consists in the temporarily positioning of an expandable balloon catheter in the site of the arterial narrowing and in its following inflation (Figure 1.6).[17] Specifically, through to its mechanical action on the vessel wall, the inflated balloon allows the permanent deformation of the blood vessel, finally allowing to sufficiently reopen the lumen.[16]

Although this procedure is successful for the elimination, at least partially, of the arterial stenosis, its long-term efficacy is affected by a series of problems among which restenosis represents the most relevant issue.[18,19,20] Restenosis is the recurrence of stenosis of the vessel lumen, at the same site of the original occlusion and it is prevalently due to SMCs migration and proliferation along the vessel walls.[21,22]
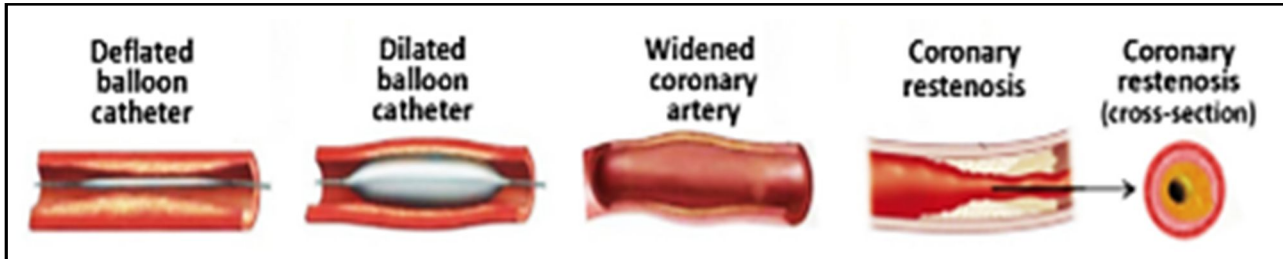
Figure 1.6: Schematic representation of percutaneous transluminal coronary angioplasty procedure and of coronary restenosis[17]

Since survey statistics report that, after simple angioplasty, restenosis occurs in almost the 35% of the cases within the six months after the intervention, balloon artery angioplasty has been improved by the additional application of stents (Figure 1.7), tiny wire meshes that provide mechanical support aiming to maintain the lumen open.[22–25]
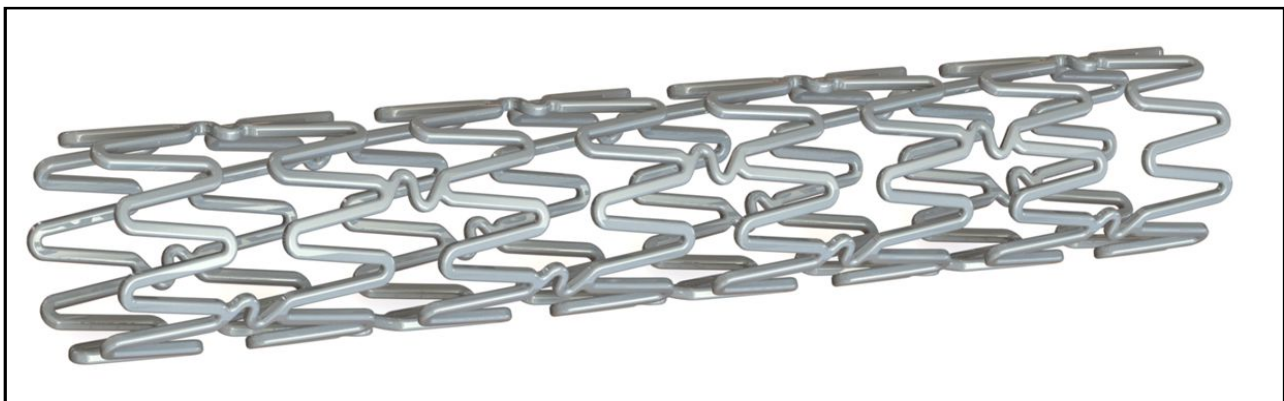
Figure 1.7: Example of a metallic stent structure[25]

1.3.3. Typologies of stents

As a strategy to reduce both the short and long-term risks of restenosis by ensuring the enlargement of the section of the lumen and its maintenance in time, different typologies of stents have been developed during the last decades. The main two generations of permanent stents are: bare metal stents (BMS) and drug-eluting stents (DES).[26]

In general, the requirements needed for stents employment are the capacity to undergo plastic deformation and to maintain it once inflated and deployed (Figure 1,8), biocompatibility, anti-thrombogenic properties and sufficient magnetic resonance imaging (MRI) resolution. Moreover, they should guarantee an efficient proliferation of endothelial cells to allow the formation of a neointima on their surface, while avoiding the

neointimal hyperplasia, which refers to an excessive proliferation and migration of vascular smooth muscle cells (VSMCs) in the tunica intima, resulting in the thickening of arterial walls and decreased lumen space, the so called in-stent restenosis. Thus, their chemical and physical properties at the surface, such as surface energy, roughness and oxide composition stability, must be perfectly engineered.[27–29]

A. Bare Metal Stent (BMS)

Concerning bare metal stents (BMS), the most commonly used materials are: AISI 316L stainless steel, cobalt-chromium (Co-Cr), nickel-titanium (Ni-Ti) and platinum-iridium (Pt-Ir) alloys; while, pure iron (Fe) and magnesium (Mg) alloys are gaining relevance as alloys for degradable stent applications.[30]

Among them, AISI 316L (Fe/Cr18/Ni10/Mo3)[31] is the most commonly used austenitic stainless steel metal for stents and biomedical applications in general, due to its well-suited mechanical properties and excellent corrosion resistance, given by the presence of chromium in its composition. However, it is non-MRI compatible and poorly fluoroscopic visible, due to its low density and its non-ferromagnetic nature. Moreover, its biocompatibility is compromised by the presence of nickel in the alloy's composition; in fact, its ions' release inside the organism can provoke allergic reactions and trigger further local immune and inflammatory responses, which in turn can induce intimal hyperplasia and in-stent restenosis.[32]

Thus, although stents have helped to reduce the incidence of restenosis in coronary surgery, the risk is not avoided completely; in fact, in-stent restenosis (Figure 1.8) occurs at a rate between 20% and 30% in bare metal stents within the first six months after implantation.[17,24,33]

Considering these data, innovative platforms for the percutaneous treatment of coronary artery diseases have been developed. In the next section, drug eluting stent (DES) will be presented as a smart modification of the traditional BMS technology.
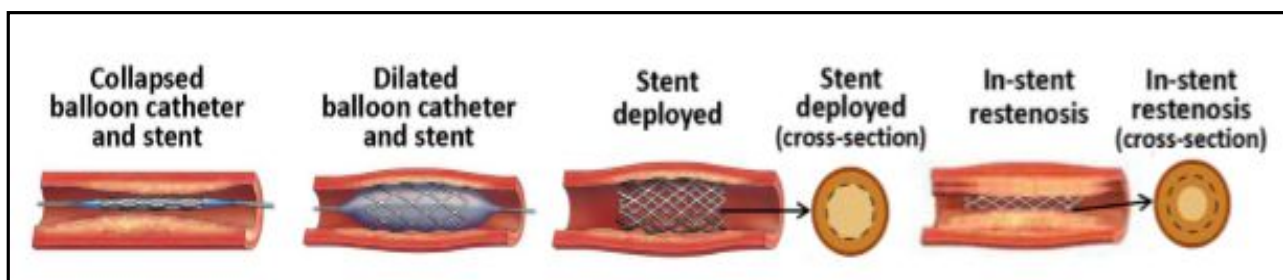
Figure 1.8: Schematic representation of stenting procedure and of in-stent restenosis[17]

B. Drug Eluting Stent (DES)

Drug eluting stents (DES) consist of a metallic stent covered by a polymeric drug delivery substrate containing a pharmacological agent. These devices are intended to release *in-situ* pro-endothelialisation agents and anti-SMC-proliferative agents with the aim of decreasing the rate of restenosis.[28,34]

The DES apparatus is mainly composed by three components (Figure 1.9):

- *Metallic stent platform*: the most common used materials are the ones already mentioned for BMS, i.e. AISI 316L stainless steel, Co-Cr, Ni-Ti and Pt-Ir alloys. The parameters that mostly affect the good outcomes of the whole structure are its thickness and roughness, that must be as lower as possible to reduce all the negative effects, such as thrombogenicity.[28,35]

- *Polymeric coating*: it is deposed onto the metallic surface and it acts as the drug delivery system. According to its application in biological systems, it must be biocompatible and sufficiently lasting over time to avoid the release of dangerous debris into the organism. The categories of polymers that have been employed in the realization of the coating can be classified into: non-biodegradable (PET, PEI) and biodegradable (PLA, PLL, PLGA) materials. Although some non-biodegradable polymer-coated DES have been claimed to be safe at long-lasting, there remains caution regarding their inflammatory response. Thus, up to now, biodegradable polymers are the most investigated materials for DES applications.[35]

- *Pharmacological agents*: they are biologically active substances that are loaded into the polymeric layer and whose controlled release over time favors the re-endothelization and the healing of the arterial walls in the post-implantation period, while avoiding the progressive SMC proliferation.[34,35]

  The main pharmacological agents used in the development of DES are: sirolimus (immunosuppressant used to prevent organ rejection and reduce SMC migration and proliferation)[36], paclitaxel (arrest SMC proliferation and neointimal formation by arresting the cell cycle)[36] and zotarolimus (immunosuppressant and potent antiproliferative agent that inhibits SMC migration and proliferation)[17,37].
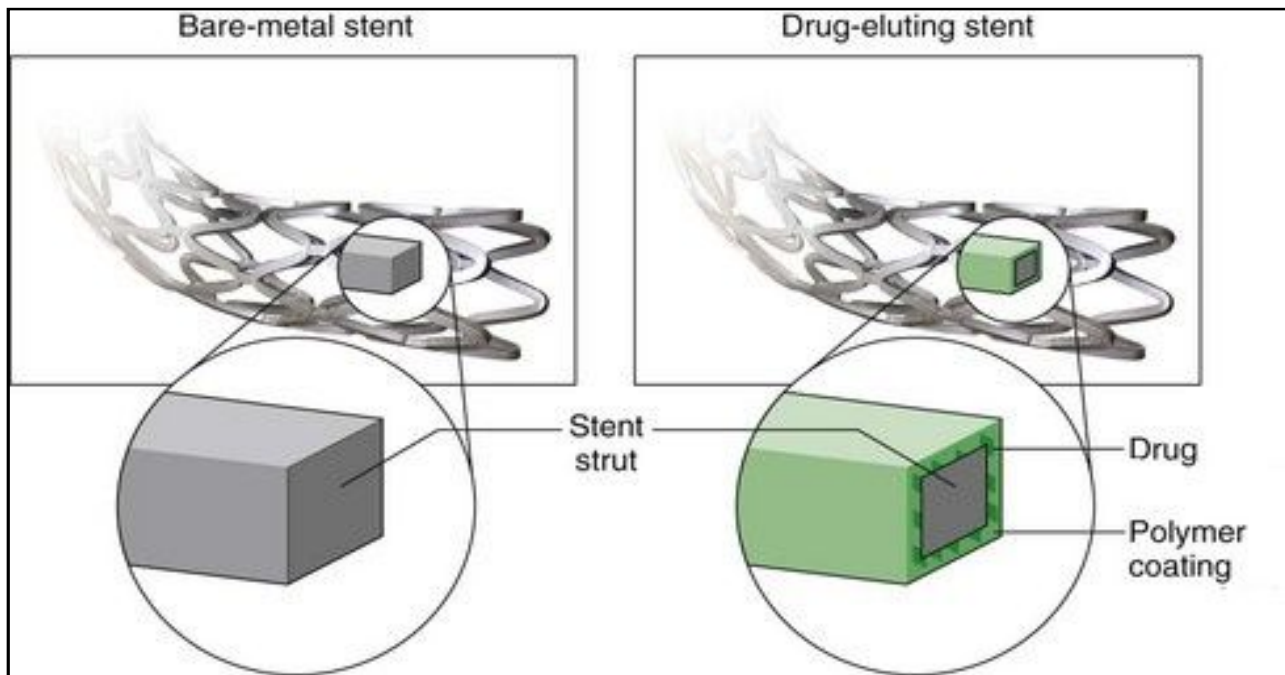
Figure 1.9: Comparison between BMS and DES structure, illustrating the 3 components of a DES apparatus: the stent strut, the polymer coating and the delivered drug[34]

However, despite all these promising properties of DES therapy, undesired outcomes due to their implantation are still not totally overcome. In fact, if on one hand the risk of restenosis is reduced with respect to BMS, it still occurs at a significant rate of about 10%, up to five years from DES implantation.[38] Moreover in-stent thrombosis (IST) or late-stent thrombosis (LST) often due to the lack of re-endothelization and the presence of inflammation, continue to represent serious risks of post-intervention failure.[28,34,39]

To overcome such DES limitations, the research has moved towards the innovative concept of gene therapy and its application in the treatment of cardiovascular diseases. In this regard, Gene Eluting Stents (GES) represent a promising strategy in cardiovascular research.

1.3.4. Gene Eluting Stent (GES)

GES represents a potential treatment strategy, proposed for the prevention of restenosis, in alternative to DES. The innovative concept of such stents relies in the stent surface-mediated delivery of therapeutic genes (in substitution to pharmacological agents), which are nucleic acid (such as DNA or RNA) sequences that, once delivered by cells, can provide benefits by either promoting the expression by vascular cells themselves of therapeutic proteins or by blocking the expression of a deleterious one.

Concerning GES, the selection of appropriate delivered genes must provide, for example, a long-lasting therapeutic modification of the vascular tissue and a selective inhibition of SMC proliferation and migration, while enhancing re-endothelialisation.[40]

An ideal GES should then sustains and controls the delivery of therapeutic genetic material over time, while protecting and facilitating its association with cells at the vessel wall.[34]

The apparatus, similarly to what described for DES, is composed by a metallic stent, whose subsequent superficial functionalization must allow the entrapment of gene carriers on its surface.[41,42] The use of gene carriers (gene delivery vectors), that will be described in the next chapter, is necessary to guarantee the protection of the genetic material from degradation and to facilitate their internalization by target cells. Nowadays, common stent surface modifications involve the application of inorganic or organic coatings, and physico-chemical modifications often obtained through physical vapor deposition (PVD), chemical vapor deposition (CVD) or plasma treatments.[43,44] Alternatively, many researches have investigated the possibility of tethering gene vectors directly to the metal stent surface.[17]

Since the first research concerning gene-eluting stent in 2000, great advances have been reached. Nowadays, the research community is working at developing new designs and strategies for the formulation of an appropriate GES apparatus capable of preventing restenosis and favoring vascular healing.[45]

In this concern, the following chapter will discuss about the possible surface-mediated gene delivery strategies that have been investigated up today, with the aim of localizing the overall gene delivery mechanism and getting it more efficient and clinically applicable.

2. Surface-mediated gene delivery

The aim of this paragraph is to provide an overview of the state-of-the-art concerning human gene therapy and gene delivery strategies. Great attention will be given to the techniques nowadays employed for surface-mediated gene delivery. Finally, the paragraph will focus on polydopamine coatings, proposed in this work as a tool for the functionalization of material surfaces for surface-mediated gene delivery purposes.

2.1. Gene therapy

Human gene therapy is an experimental and innovative therapeutic procedure which uses genetic material to cure and prevent many diseases, such as cancer and CVDs. It is based on gene delivery, consisting in the insertion of nucleic acids (DNA and RNA) into target cells in order to modify their protein expression.[46,47]

Genes are DNA structural sequences, that contain the necessary and fundamental information for the production of proteins; therefore, when for some reason they are altered, the encoded proteins are not able to be expressed correctly and this dysfunction can lead to the appearance of genetic disorders.[48] Hence, gene therapy is based on the insertion of therapeutic DNA (or RNA) encoding for a specific gene into target cell nuclei, with the aim of either promoting the expression of a therapeutic protein or the silencing (blocking the expression) of a deleterious one, respectively, for the enhancement or the inhibition of some functionalities in the target organ or tissue.[46,49]

Nowadays, there exist several fields of application for gene therapy, among which the most important are those concerning cancer and cardiovascular treatments; with the former ones representing the 64.6% of the overall clinical trials, while the latter ones still only the 8.5%.[49]

For a better comprehension of the mechanism of protein expression, the next section will provide a description of the flow of genetic information within a biological system.

2.2. The central dogma of molecular biology
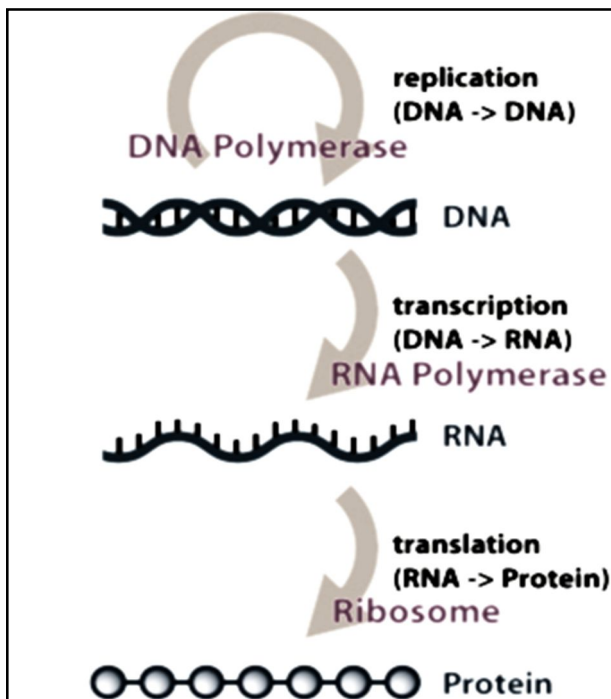
In 1970, Francis Crick formulated the so called "central dogma of molecular biology", in order to explain the flow of genetic information within a biological system (Figure 2.1).[50,51] In general, it states that the genetic information flows from DNA to DNA (replication), for the transmission of genetic information; and from DNA to RNA, and further to the proteins. Moreover, once the information arrives at the proteins level, it is not able to flow back to the level of nucleic acids; thus, the central dogma has been alternatively and simply described as "DNA makes RNA and RNA makes protein".[52]

Figure 2.1: Schematic representation of the genetic information's flow within a biological system[51]

As already mentioned, genes are DNA structural sequences, that contain the necessary and fundamental genetic instructions for the synthesis of proteins. The multi-step process that makes it possible is called *gene expression*.[47] The first step occurs in cell nucleus and is called *transcription*, through which the information contained in a specific portion of DNA is replicated in a newly complementary piece of messenger RNA (mRNA), leading to the formation of a mature mRNA at the end of the entire transcription process. Once this mature mRNA chain reaches the ribosome (outside the nucleus, in the cytoplasm), which is a complex molecular machine that living cells use as the site of biological protein synthesis, it is translated into a series of amino acids and finally into a protein. [53]

2.3. Cardiovascular gene therapy

Cardiovascular gene therapy gained relevance in gene-based medicine in the late 1980s, when it was shown that direct intra-arterial gene transfer was possible with endovascular catheter techniques.[54]

Inspired by the pioneering work of Isner et al.,[55] who used DNA gene transfer to treat severe peripheral vascular disease, and pushed by the necessity of limiting the huge amount of deaths due to CVDs, cardiovascular gene therapy has significantly evolved during the last three decades, until becoming nowadays a protagonist in the field of advanced biotherapies.[46]

The main potential targets of cardiovascular gene therapy are classified in three different levels, as reported in Figure 2.2. At the systemic and liver level, it aims at preventing the appearance of atherosclerosis, by regulating the expression of those proteins, whose dysfunction could alter the normal blood concentrations of cholesterol; at the cardiac one, its main goals are the prevention and treatment of some coronary blood vessel dysfunctions such as ischemia and in-stent restenosis, which could lead to heart failure; at the peripheral one, cardiovascular gene therapy mainly aims at decreasing the incidence of complications due to either by-pass graft or stent implantation failures.
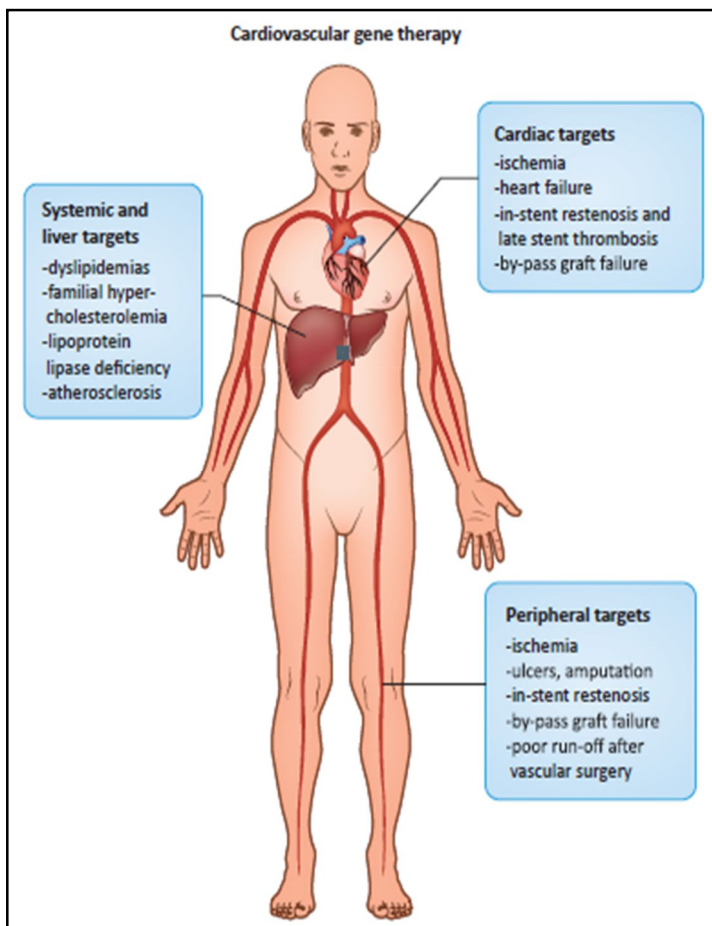
Figure 2.2: Schematic representation of the possible targets for cardiovascular gene therapy[54]

Specifically, to the case of stent failure, the targets for cardiovascular gene therapy are vascular cells, in particular ECs and SMCs. Several proteins whose enhanced expression can prevent restenosis and other stenting-related and atherosclerosis-related drawbacks have been identified. Some of their examples are represented by the eNOS (endothelial Nitric Oxide Synthase) that features anti-inflammatory and antithrombotic functionalities or by the VEGF (vascular endothelial growth factor) whose overexpression has positive outcomes in lowering the neointima hyperplasia and improving the re-endothelization.[56]

The success of cardiovascular gene therapy is mostly related to the possibility to induce durable transgene expression into cells. To guarantee this, suitable delivery systems are needed.[57,58]

2.3.1. Gene delivery systems

The direct delivery of naked nucleic acids to cells is an inefficient approach to gene delivery. In fact the anionic nature of the DNA phosphate backbone, together with its relative large size, make internalization by cells, featuring a negatively charged surface, very difficult.[58,59]

For these reasons, several gene delivery strategies have been developed in the last 30 years. On the one hand, different physical techniques such as gene gun delivery, hydrodynamic injection and electroporation, have been tested but with bad outcomes in terms of cytocompatibility and *in vivo* applicability; on the other, the use of gene delivery vectors, have emerged as very promising in terms of delivery efficiency, cost and applicability, in both *in-vivo* and *in-vitro* procedures.[59–61]

An ideal gene delivery vector should be able to carry to cells a sufficiently high amount of genetic material while protecting it from extracellular and intracellular degradation, without exerting cytotoxic effects.[58,62]

To elicit their therapeutic effects gene delivery vectors must overcome several barriers to reach cell cytoplasm or enter cell nucleus and then they should safely release the carried nucleic acids containing the encoded genetic informations.[59,63]

In details, as shown in Figure 2.3,[64] once the gene-vector construct meets the external cellular membrane, it must be internalized. Depending on cell type and vector used, there exist several different routes of internalization among which endocytosis is the most common one, while pinocytosis and phagocytosis are less probable alternative ways.

Endocytosis is a process by which cells internalize large polar particles and macromolecules that cannot pass through the hydrophobic cell membrane, by engulfing them into vesicles named endosomes.

Once these steps are performed, the complex is entrapped in the so called endocytic pathway, which is a process that involves a series steps: the early endosomes evolve into late endosomes, where pH lowers to facilitate the degradation of the endosomal content and finally is possibly transferred to lysosomes, organelles containing hydrolytic enzymes that can break down many kinds of biomolecules and are supposed to digest unwanted material.

Therefore, although inside these vesicles the gene delivery vector can be transported through the cytosol, it must rapidly find a way to escape from them to safely reach the nucleus without being damaged. In fact, degradation mechanisms are typical of these compartments where both the pH drop to the range of 4.5-6 and the enzymatic processes can deteriorate the nucleic acids and compromise the whole gene delivery process.

Then, once released in proximity of the nuclear region, the last barrier is represented by the double bilayer nuclear membrane, which can be easily overcome through its pores by nano- or micro-metric particles, while bigger complexes need the help of specific nuclear import proteins or have to wait that nuclear membrane integrity is lost during cell division. Finally, once the vector manages to enter the nucleus, it must be able to release the transgene cargo in-situ for its following expression.[49,65]
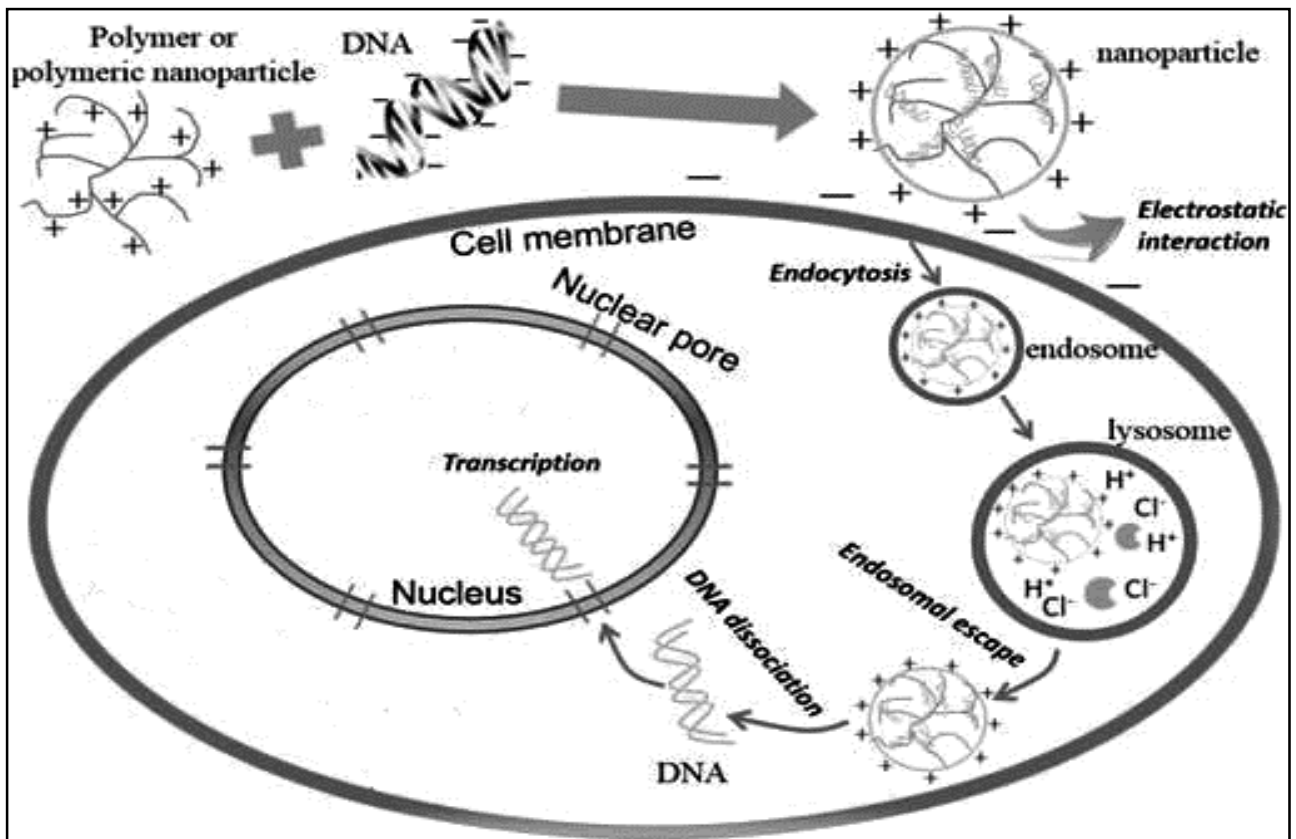
Figure 2.3: Schematic representation of the process of internalization of non- viral carriers into the cell and of the pathway leading to the transcription of their genetic content inside the nucleus[64]

Currently, two main classes of gene carriers have been developed: viral and non-viral vectors. An overview of these two classes, of their advantages and disadvantages will be presented in the following sections, particularly focusing on non-viral vectors, that were employed in this work.[66]

2.3.2. Viral vectors

Viruses are biological agents employed in gene delivery techniques for their capacity of entering inside cells and for the facility of expressing their own genetic cargo. Because of their pathogenic nature, they must be modified and made non-dangerous to be used as gene vehicles. For instance, the pathogenic part of their native genetic payload and the genes related to viral replication have to be removed and replaced by the gene of interest.[58,59]

To now, viral vectors, compared to non-viral ones, show much higher efficiency in terms of transgene delivery in-vivo, and for this reason they are the most used platforms in clinical trials.[67] The main typologies of virus employed for gene delivery are adenoviruses, lentiviruses, retroviruses, adeno-associated viruses and herpes simplex viruses.[58,67,68]

 Since viral vectors are not the subject of this work, their main features are summarized in Table 2.1, but no further insights will be provided herein below.

Gene delivery agent	Mechanism of delivery	Advantages	Disadvantages
Adenovirus	RME	• Characterized by complexity, stability, and integrity	• Capsid proteins causes inflammatory immune responses
		• Integration of host genome does not occur	• Short-term expression
Retrovirus	Interaction between viral envelope protein and cell surface receptors on the target cell	• In the treatment of inherited and chronic diseases	• Low transfection efficienc
			• Low vector titer
			• Instability
			• Inability to concentrate
Lentivirus	Interact with the nuclear import mechanism of the target cell and manage active transport of PIC via nucleopores	• Ability to infect both proliferating and quiescent cells	• Poor liver and muscle cell transgene activity
		• Long term expression	
		• Low immune reactions	
Adeno-associated virus	All the internal coding sequences are removed and co-transfected with a helper virus like adenovirus, HSV, etc.	• Long-lasting expression	• Small packaging efficiency
		• High stability, safety and efficacy	
		• Wide host range	
HSV	Cloning therapeutic gene to a plasmid containing HSV and infecting with HSV virus	• Large cloning capacity for foreign genes	• Turns off most of the genes on latency
		• Large number of genes can be incorporated	

RME: Receptor-mediated endocytosis, PIC: Pre-integration complex, HSV: Herpes simplex virus

Table 2.1: Shorth summary of the viral gene delivery strategies, their advantages and disadvantages[58]

In general, even if viral vector-based techniques for gene delivery applications have so far advanced significantly, their progress in clinical trials is still hampered by a series of limitations. Among them, there is the necessity of increase viruses carrying capacity, the lack of long-term effectiveness and, most importantly, important safety issues related to virus pathogenicity still need to be solved.[59,69]

For these reasons, the novel alternative and safer class of non-viral gene delivery vectors was developed by researchers.

2.3.3. Non-viral vectors

Non-viral gene delivery vectors were introduced at the end of the 1980s, when a study performed by Felgner *et al.* showed promising results in terms of *in-vitro* gene transfer by the use of cationic lipids.[70] During the following years, many other materials have been developed as gene vectors and, currently, two main classes of non-viral gene delivery vectors can be identified: cationic lipids and cationic polymer. These materials are also called transfectants and their gene delivery process is defined as transfection.[58,71]

The revolutionary idea of condensing DNA with a cationic structure by natural electrostatic and entropic interactions in solution, introduced by Felgner and colleagues for lipids and by Wu and colleagues for polymers,[70,72] allowed the realization of complexes (i.e. lipoplexes and polyplexes respectively) whose overall

positive charge enhanced their interaction with the anionic mammalian cellular membrane favoring their cellular internalization.[73]

In general, the advantages of non-viral vectors, with respect to the viral ones, are the ease of handling and manipulation, the ease of large-scale production, lower costs, the possibility of safely transport higher amounts of genetic material and, importantly a much safer profile for users and patients. Instead, the major drawback related to their use in clinics is represented by their still lower ability of delivering the genetic cargo into host cells with respect to viruses.[58,59,74]

For this reason, aiming to optimize the efficiency of non-viral gene vectors, the main parameters that influence their overall physicochemical and biological properties have been thoroughly investigated in the last years. Furthermore, the mechanisms of interaction between either lipids or polymers and nucleic acids, the cellular uptake of complexes, and in general the transfection pathway were almost completely elucidated.[75]

A. Cationic lipids

The first class of non-viral carriers that will be described in this chapter is represented by cationic lipids, which, in aqueous solutions, are able to self-assemble with negatively charged nucleic acids by electrostatic interactions ultimately forming complexes named lipoplexes, with dimensions between 100 and 1,000 nm.[69]

Cationic lipids (Figure 2.4) are composed by one or more positively charged groups named "heads", which are linked to one or more lipidic hydrophobic counterparts named "tails", through to the linkages furnished by one or more neutral groups (esters, amides, ethers, etc) named "linkers".[69]
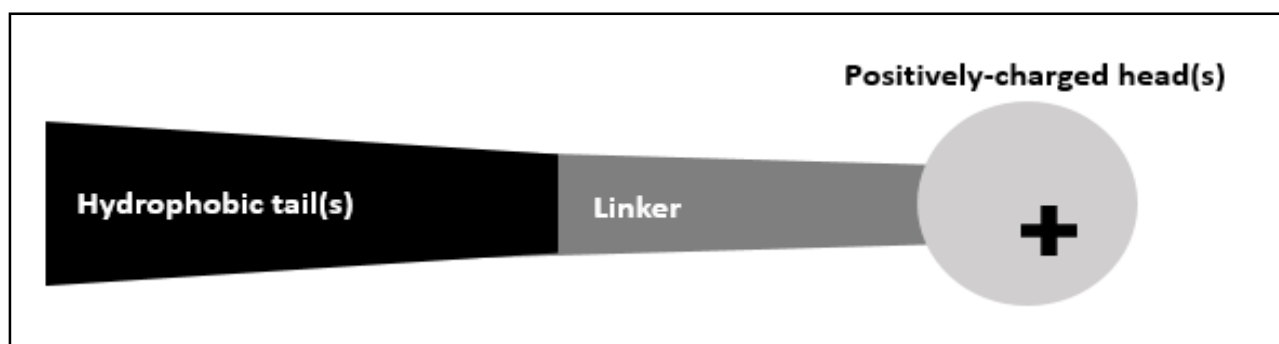
Figure 2.4: Schematic representation of the cationic lipid structure[69]

The main parameters that affect their efficacy as carrier's components are the chain length, both the charge and size of the cationic headgroup, and finally, the chemical nature of the linker backbone. As aforementioned, the overall positive charge enhances lipoplex interaction with the anionic mammalian cellular membrane and their following internalization by endocytosis.[76] Consequently, in general, an excess of cationic lipids is used in preparing lipid/DNA complexes, finally forming positively charged lipoplexes with a specific superficial topography and dimension that allow to carry nucleic acids inside the cell.[73] Anyway, since it depends on a lot

of factors, the mechanism of complexation is very difficult to be generalized: temperature, DNA/lipid ratio, kinetics of mixing and lipid formulation are the main parameters that can influence the formation of one structure rather than another.[77]

The most important commercially available lipidic gene delivery systems are 1,2-bis (oleoyloxy)-3-(trimethylammonium)propane (DOTAP, example in Figure 2.5), N-[2-({2,5-bis[(3-aminopropyl) amino]-1-oxopentyl}amino)ethyl]N,N-dimethyl-2,3-bis[(1-oxo-9-octadecenyl)oxy] chloride (DOSPA), DC-Cholesterol (3b[N-(N′,N′-dimethylaminoethane)carbamoyl] cholesterol) and Lipofectamine™ (a 3:1 mixture of DOSPA and DOPE) that are commonly used in laboratory practice to study gene expression, gene function, protein function and cell signaling.
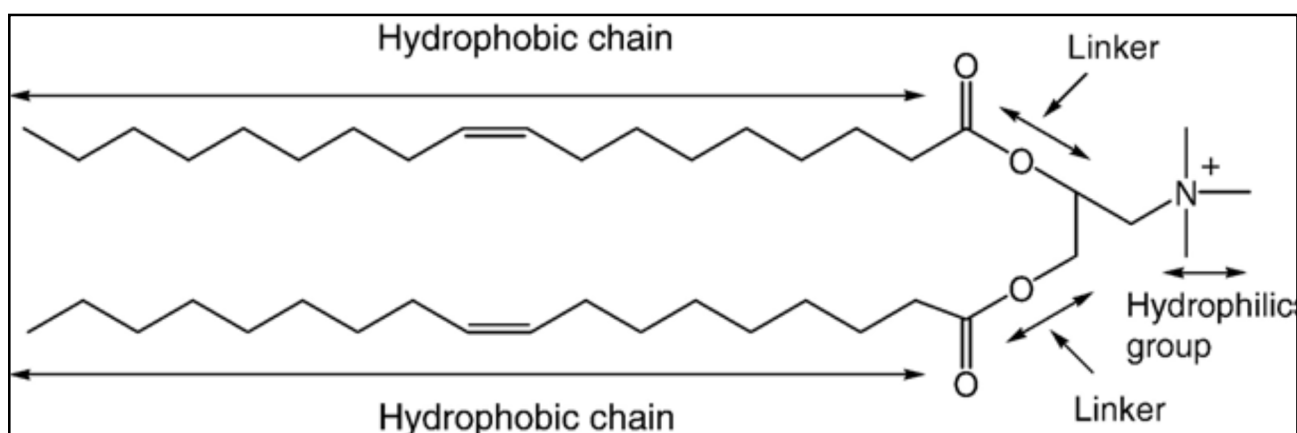
Figure 2.5: 1,2-bis (oleoyloxy)-3-(trimethylammonium)propane (DOTAP) chemical structure[59]

B. Cationic polymers

The second class of non-viral gene delivery vectors is represented by cationic polymers that, similarly to cationic lipids, are able to spontaneously self-assemble in aqueous solution with nucleic acids, forming particles named polyplexes with size varying from 30-50 nm to more than 1 µm, depending on the polymer chemistry and on the complexation parameters.[78,77]

Since the introduction of polyL-lysine (PLL) as gene carrier in 1987,[72] many polymers for gene transfer have been developed and studied, either synthetic polymers, such as polyethylenimine (PEI), either in its linear and branched configuration, or natural polymers, such as chitosan (Figure 2.6).[59,76]
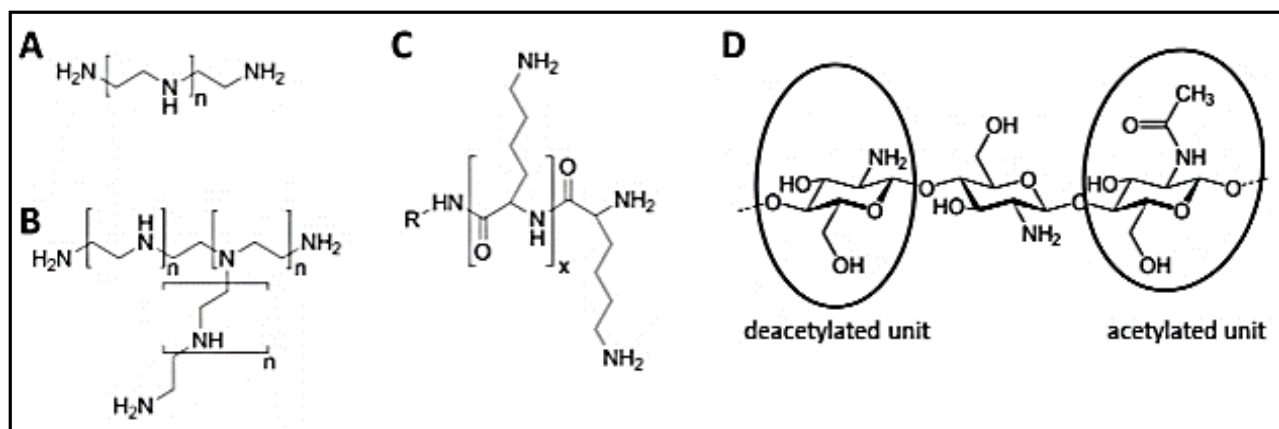
Figure 2.6: Chemical structure of (A) linear poly(ethylenimine) (lPEI), (B) branched poly(ethylenimine) (bPEI), (C) poly(L-lysine) (PLL), (D) chitosan[59]

Even if they all possess great potentialities as delivery vectors, their overall efficacy is related to an elevated number of parameters, such as molecular weight (MW), polydispersity (PD), superficial charge and degree of branching, whose combinations characterize their molecular diversity.[79]

One of the main parameter influencing the final properties of polyplexes is the ratio between the number of nitrogen atoms belonging to the cationic polymer in the solution and the one of the phosphate units of nucleic acids (N/P ratio).[80–82] Homogeneous populations of relatively small and positively charged polyplexes are usually formed when working at high ratios while at ratios close to neutrality larger colloidal aggregates have been reported to occur.[60]

Moreover, since the employment of cationic polymers as synthetic non-viral gene carriers has been constrained by the compromise between the efficiency of gene-delivery and the risk of cytotoxicity, their physicochemical characteristics must be properly modulated in order to make them biocompatible and biodegradable .[83]

Since in this work PEI was used as cationic polymer for gene delivery, its properties will be briefly summarized in the next section.

-Polyethyleneimine (PEI), which is one of the most studied and employed non-viral gene carriers and is considered the gold standard cationic polymer for gene delivery applications because of its high transfection efficiency.[82,84]

One of its major characteristics is the high charge density, which, on one hand is responsible for its great ability of binding DNA, on the other causes its relatively high cytotoxicity, hampering its application.

As previously shown in Figure 2.6, PEI can assume a linear configuration (lPEI) or a branched one (bPEI), ranging in molecular weight (MW) from 0.8 to 1,000 kDa.[84]

While the former contains only secondary amines at its extremities, the latter contains primary, secondary and tertiary amino groups at variable ratios, depending on the degree of branching.[59]

Comparative transfection studies have shown that the two classes are both effective for gene delivery, even though bPEI ability of DNA compaction is higher, due to the presence of primary ammines in its structure, and the resulting polyplexes are more stable.[69] In contrast, lPEI is less cytotoxic than bPEI at comparable MW, and, given its good ability in gene transfection, especially *in vivo*, several lPEI-based transfection reagents are nowadays commercially available.

Transfection efficiency and cytotoxicity of PEI are both dependent on MW and degree of branching, which in turn regulate the overall dimension of the carrier. A complete condensation of DNA (N/P $\geq$ 2) is necessary to obtain significant transfection and small-sized vectors are obtained by increasing N/P up to 30. Generally for both bPEI and lPEI, MW between 10 kDa and 250 kDa are considered the most effective for transfection but at the same time they exert a higher citotoxycity.[85] However, in *in vitro* experiments, it is possible to play with the DNA dose delivered to cells, the cell seeding density and the volume of the culture medium to identify a range of optimal transfection conditions roughly specific to each PEI, maximising the compromise between high transfection and low cytotoxicity.[86]

2.4. Surface-mediated gene delivery strategies

Surface-mediated gene delivery is a novel approach intended to localize the gene delivery process, by immobilizing and maintaining a huge number of vectors at a biomaterial surface, in order to promote and sustain over time their uptake by cells in contact with the surface.[87]

The major advantages carried by these approaches are the direct contact between carriers and cells, thus decreasing the drawbacks related to the mass transport, while increasing the concentration of DNA at cell surfaces and localizes the overall delivery and ultimately its efficiency.[88]

The several possible strategies concern the bulk encapsulation of naked nucleic acids into degradable polymer matrices, the alternated layer-by-layer adsorption of DNA and cationic polymers on surfaces to produce multi-layered structures, and the immobilization of pre-formed complexes to surfaces through either non-specific or specific tethering.[89,90]

A. Bulk encapsulation

The bulk encapsulation is a strategy based on the incorporation of plasmid DNA or gene vectors directly into degradable polymer matrices, which are deposited on the surface of materials as coatings (Figure 2.7). Since DNA and vectors are trapped in the structure, their release is obtained and controlled through a combination

of diffusion and polymer degradation. The degradation process can be triggered in several ways, and for this reason can be modulated over longer or shorter periods, in order to obtain the desired vector release rates.[88] An extended delivery over days or months aims at maintaining the amount of gene delivery vectors available for cellular uptake at appropriate moderate levels; while, a short-lasting release, provides only a rapid increase of vector concentration in the surrounding tissues, followed by a fast decline as soon as it is all cleared or degraded.

A)   **B)**
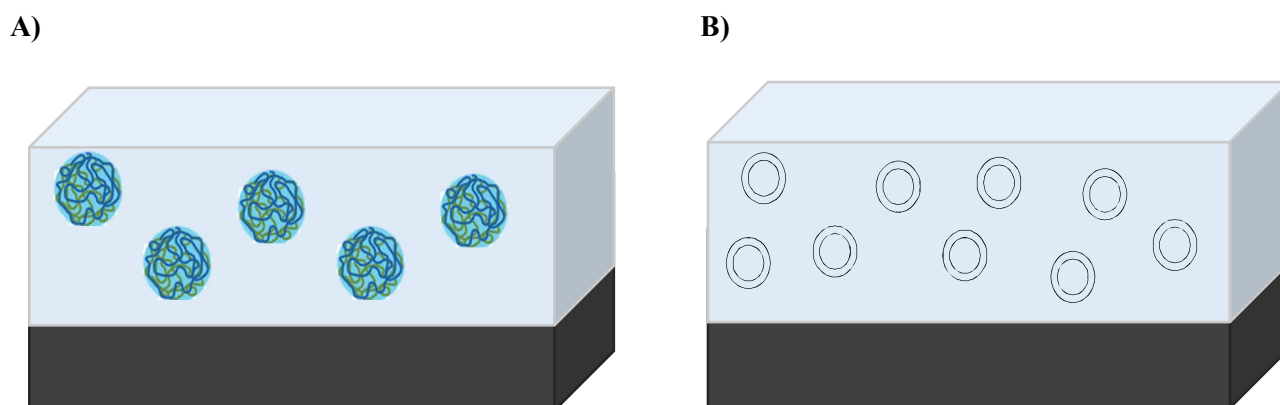
Figure 2.7: Schematic representation of the encapsulation inside a polymeric coating of (A) polyplexes and (B) plasmid DNA

This surface-mediated delivery approach has been investigated in various applications, such as suture coatings, bone implants and tissue engineering scaffolds.[91,92] Moreover, in the cardiovascular field, and more particularly in stent applications, many studies have reported the use of polymeric coatings for the encapsulation of DNA to be released *in-situ*. In this context, synthetic biodegradable polymers such as poly(lactic-co-glycol-acid) (PLGA) and polyanhydrides have been widely employed as materials for coating, because they are biocompatible and available in a wide range of copolymer ratios, that makes possible the control of their degradation. However, since organic solvents are used during their production, with a risk of DNA degradation, natural compounds such as gelatine and collagen have been proposed as alternatives, even if their degradation rate is usually fast and much less controllable.[89,90]

B. Layer-by-layer assembly

The layer-by-layer deposition of oppositely charged polyelectrolytes on surfaces is a well-established method for the "bottom-up" fabrication of thin multi-layered polymeric coatings (Figure 2.8).[89] This technique is based on the repetitive dipping of substrates in dilute polycation and polyanion solutions, exploiting the reciprocal electrostatic attraction for the growth of thin films. Concerning the gene delivery field, the employment of a DNA anionic solution and a cationic polymeric one allows the creation of multi-layered films composed of alternating charged layers, characterized by thicknesses that typically range from tens or hundreds of nanometers to up to several micrometers, depending on the number of layers deposited and the solution conditions.[93]

Layer-by-layer methods of assembly are continuously advancing in the general areas of biology, medicine, and biotechnology, as they provide ease of preparation (entirely aqueous-based multi dipping processes), a quite good accuracy over the DNA load amount and good control over its release in time and space (nanometer-scale control over composition and thickness of the composite structure).[89,93] Nevertheless, the fact that the DNA is not encapsulated inside vectors makes it relatively fragile and exposed to degradation.
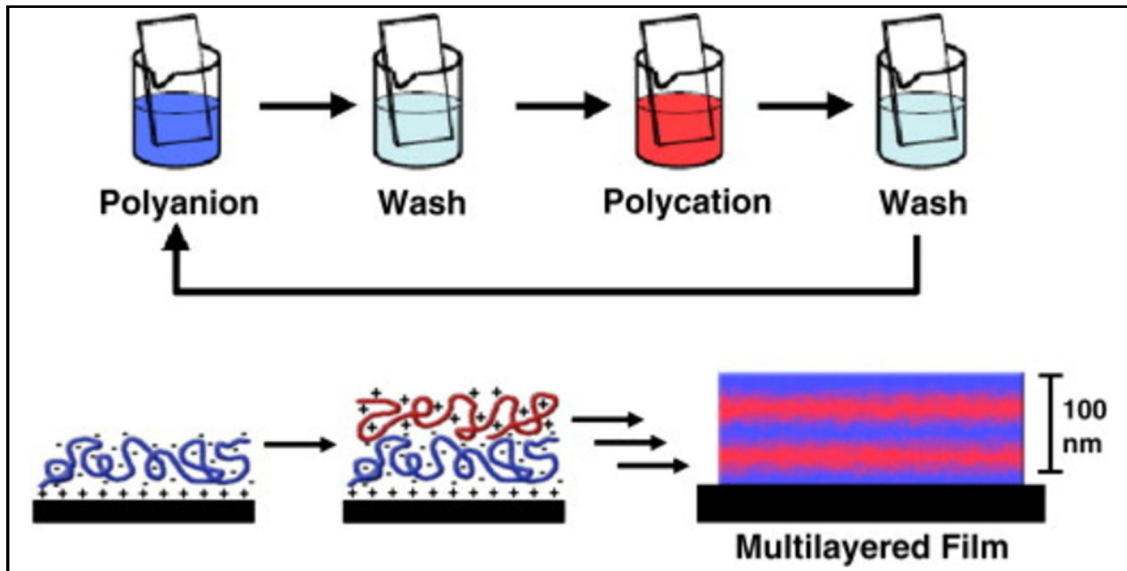
Figure 2.8: Formation of a multi-layered structure from "layer-by-layer" deposition[89]

Since the pioneering work of Lvov *et al.*,[94] who fabricated multi-layered structures from sturgeon sperm DNA and poly(allylamine), many other formulations have been proposed. Among the cationic polymers, the most employed are: polyamines such as poly(β-amino ester)s which is hydrolytically degradable in physiologically media,[95] polyethyleneimine (PEI) especially in hyper-branched configurations,[96] and poly(l-lysine) (PLL) which degrades in presence of enzymes.[97]

C. Direct immobilization of complexes on the surface

The direct immobilization of pre-formed complexes at surface relies on the interaction between the two counterparts through either non-specific or specific tethering. Considering the delivery mechanism of vectors, its difficulty lies in controlling the dissociation of the bonds created between the surface and the vector, which must not be too weak interactions or too strong, as in the case of covalent bonds. Instead, the great advantage is represented by the fact that pre-formed DNA/vector complexes are added directly on the already functionalised surface, usually in aqueous solutions, and thus they are not exposed to the risk of being degraded during deposition.

Concerning the electrostatic interaction between cationic complexes and negatively-charged substrate, their association is mainly obtained thanks to either ionic or hydrogen bonding. In the former case, the bond is generated by attractive forces between the two counterparts (Figure 2.9);[89] while, in the latter, it is weaker and obtained through dipole-dipole attractions.
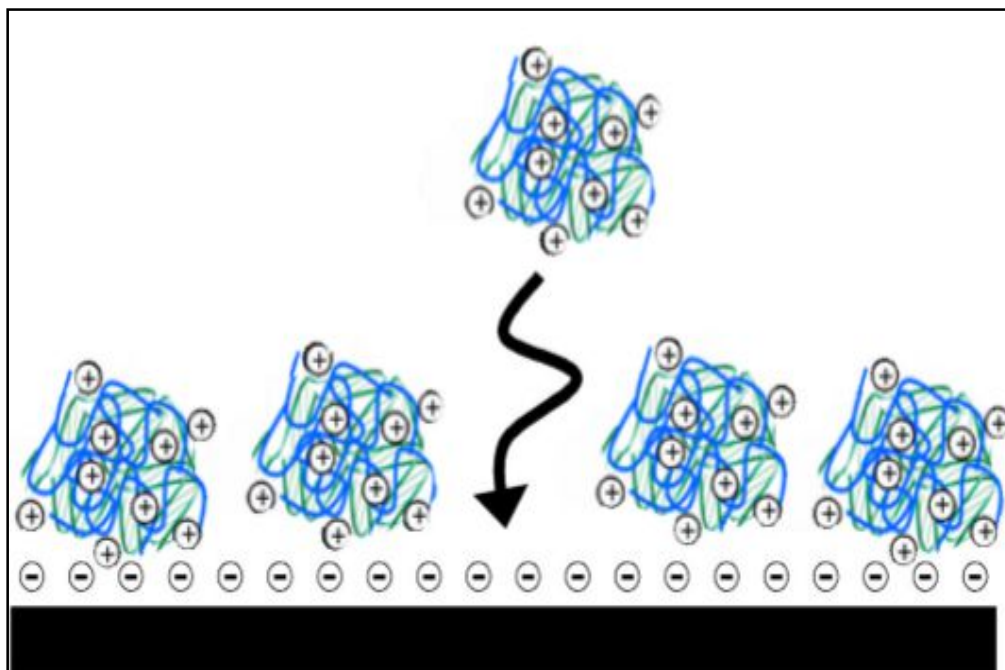
Figure 2.9: Direct immobilization of preformed DNA complexes at surface, through electrostatic interaction[89]

Instead, the covalent interactions between complexes and surface are generated thanks to the sharing of electron pairs between the chemical groups that are situated at the two surfaces (Figure 2.10).
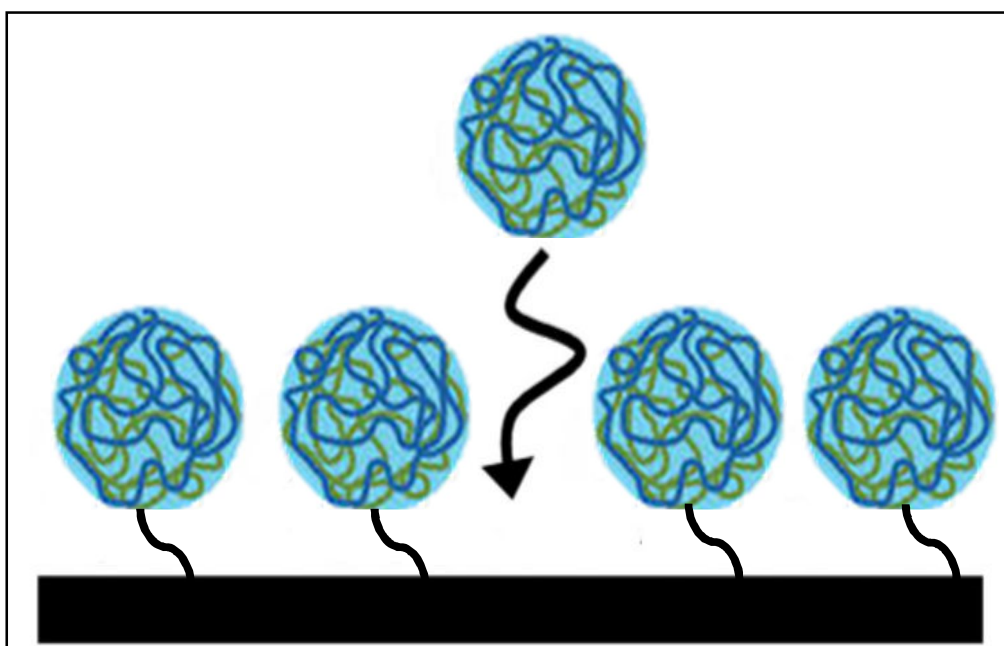
Figure 2.10: Direct immobilization of preformed DNA complexes at surface, through covalent bond interaction

One of the most employed non-covalent interactions between complexes and surface consists on the stable linkages occurring between streptavidin and biotin. Streptavidin is a homo-tetrameric protein able to bind, in aqueous solutions, four molecules of biotin (also known as vitamin B7), creating a stable complex characterized by a low dissociation constant (K_d on the order of ≈10−14 mol/L); thus, by functionalising the gene delivery vector with biotin it is possible to bind vectors on streptavidin modified surfaces of synthetic polymers or natural materials such as collagen and hyaluronic acid. In these latter cases, either poly-amidoamine dendrimers (PMAM) or poly(l-lysine) (PLL) were used for complexing DNA.[91,98]

While, among covalent interactions, common surface modifications included the employment of biocompatible materials such as poly(lactic-co-glycolic acid) (PLGA) or hydrogel of collagen and fibronectin, which were both tested, for example, by Bielinska et al.,[99] for the local and controlled delivery of DNA to eukaryotic dermal cells *in vitro* and *in vivo* using dendrimer PMAM/DNA complexes. Furthermore, Zheng *et al.*,[100] coated a glass platform with a porous foam made of highly crosslinked polycarbazole (PCBZL) (with or without PGLA inclusions), by solvent casting and salt leaching, in order to increase the amino groups present at surface. In fact, their idea was to take advantage of these surface amino groups, for exploiting the attachment of molecules capable of carrying DNA. For instance, PEI was covalently attached to PCBZL films using the bifunctional reagent BS3, which cross-links amino groups; then, plasmid DNA was deposited on PEI-coated surfaces.

Nowadays, the study of natural compounds whose employment enables to improve the adhesion ability of synthetic surfaces has inspired much research towards the development of alternative novel functionalized delivery substrates.

In this context, an interesting and innovative surface modification approach is represented by polydopamine (PDA) coatings. Since the discovery of the important role played by dopamine and its derivatives in the attachment of mussels in the most inhospitable marine regions, dopamine-based compounds have been widely studied for the development of stable mussel-inspired synthetic coatings, which can be exploited for the successive immobilization of other molecules or particles on the material surface.[101]

Since in this work polydopamine has been used for the functionalization of surfaces, a focus on its chemical characteristics will be presented in the following section.

2.4.1 Polydopamine (PDA) coatings

Dopamine belongs to the category of catecholic compounds, which are natural small molecules, characterized by the presence of catechol groups in their chemical structure (Figure 2.11).[101]
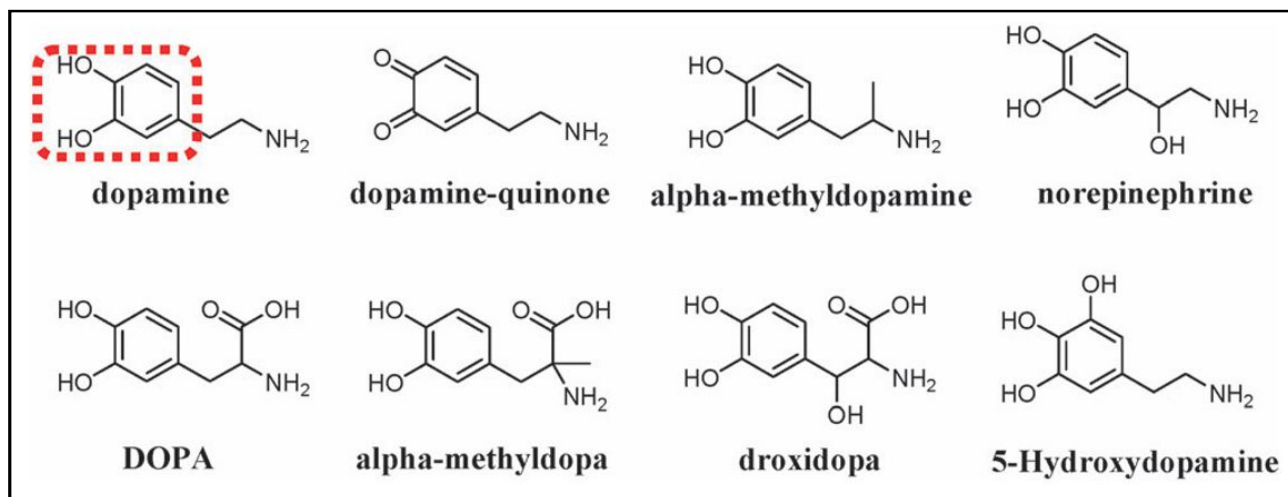
Figure 2.11: Examples of catecholic compounds which derive from dopamine.The catechol groups are highlighted in red[101]

Since the first work published by Messersmith et al,[102] the attachment strategy based on polymerized catecholic amines (i.e. polydopamine) has been widely investigated by many researches, with the aim of exploiting such natural compounds for enhancing the interfacial adhesion of synthetic materials.

Due to their ability of self-assembling onto a wide range of inorganic and organic materials, including noble metals, metal oxides, polymers and ceramics, simply by dip-coating of objects in an aqueous solution, catecholamines such as dopamine represent novel and promising alternatives for surface immobilization approaches.[101,103,104]

In particular, according to Saidin et al, once in aqueous solution at neutral to alkaline pH, catecholamines are easily oxidized into highly reactive quinones, which therefore undergo a multi-step self-polymerization, including intramolecular cyclisation and structural rearrangements, which lead to the obtainment of a thick (about 50 nm) and stable polymeric layer (Figure 2.12).[105]
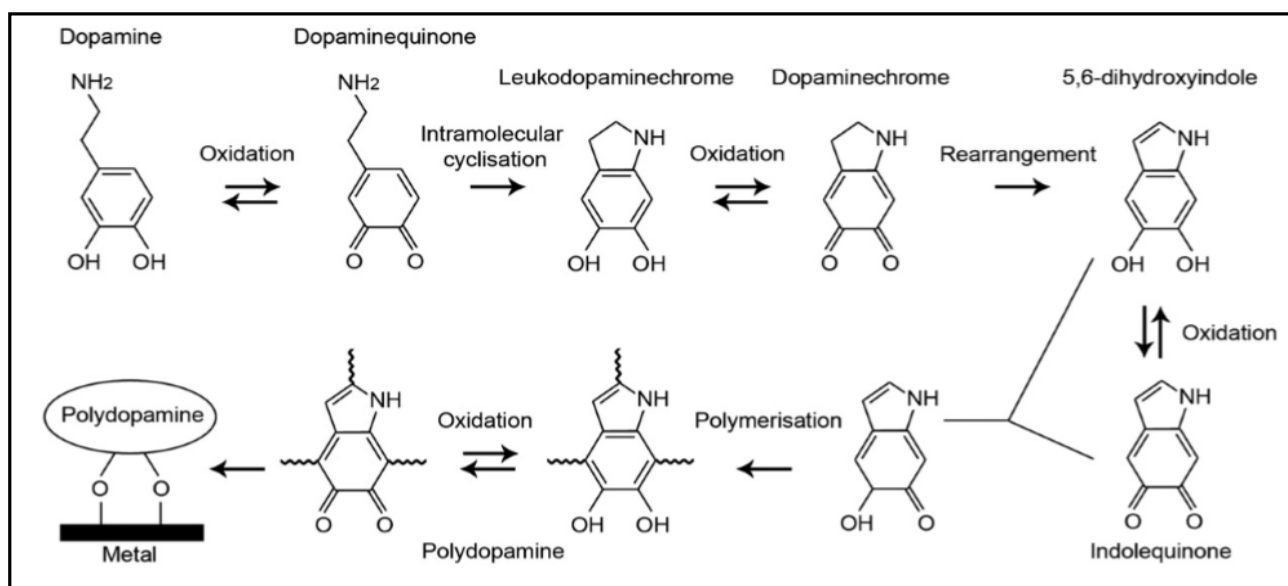
Figure 2.12: Schematic representation of the overall polymerisation process of dopamine[105]

For instance, when the polymerization process occurs in the presence of substrates, a strongly adherent PDA film is deposited onto them, thanks to the stability of the linkages formed with the catechol groups. In fact, although the exact adhesion mechanism and the chemistry behind the process are not fully understood so far, many studies have stated that catechol is the only functional element required for both adhesion and cross-linking onto substrates.[101,106] The result is the creation of a thick mixture of cross-linked products, bearing free amines and quinone groups exposed at surface (Figure 2.13),[104] whose presence allows the PDA coatings to be used as a versatile anchoring platform for secondary reactions with either organic or inorganic compounds and with micro/nanoparticles, for the obtainment of various functional uses. Thus, a proper choice of secondary reactants will transform PDA coatings into surfaces tethering specific chemical, physical and/or biological properties.[107]
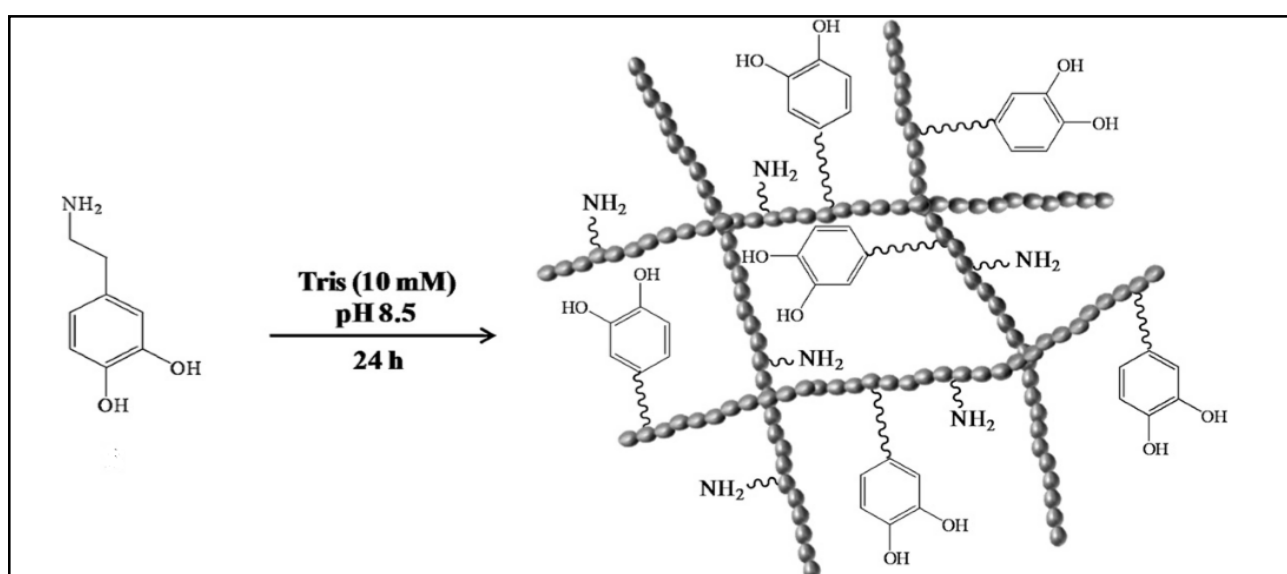
Figure 2.13: Exemplified representation of the polydopamine (PDA) network, resulting from self-polymerisation of dopamine[104]

PDA is employed as coating in several applications, including energy, environment, and sensing disciplines, as well as the biological and biomedical fields.

Concerning the environmental engineering, PDA is employed for wastewater treatment processes such as ultrafiltration (UF) or forward osmosis (FO),[108] while, in energy applications as impermeable membrane in Li-ion battery operations.[109]

Moreover, in the biomedical research, an example of application of PDA in the field of bone tissues regeneration, is reported by the work of Saidin et al.,[105] who exploited PDA properties for the immobilization of either antibacterial silver nanoparticles and hydroxyapatite molecules at surface, in order to promote the osteointegration and at the same time to avoid the appearance of bacterial infections. While, in the field of cardiovascular stent applications, Campelo et al.,[110] proposed the use of polydopamine as the anchor base for the obtainment of further chitosan anti-adhesive coatings on such metallic devices in contact with blood.

Furthermore, many works reported the creation of PEG-functionalized substrates, using either single or multiple catechols as anchor groups, for the realization of anti-fouling coatings to be applied in different fields.[111,112]

Aiming at the superficial modification of AISI 316L stainless steel (SS) substrates, for the realization of surface-mediated gene delivery platforms, in this work, polydopamine has been proposed as a promising solution for enhancing the immobilization of polyplexes at stent surface, either directly by a secondary reaction with gene delivery particles or through further modification with glutaric anhydride.

3. Aim of the project

The World Health Organization (WHO) estimated that in 2015, cardiovascular diseases (CVD) were the leading cause of death globally, causing 31% of all deaths per year. Among these deaths, an estimated 7.4 million were due to coronary heart diseases (CHD).[7] In this light, worldwide researchers in life sciences are struggling to improve the performance of medical and surgical therapies for the prevention and control of CHD.[11]

Since the first coronary angioplasty in 1977, percutaneous coronary intervention has become one of the most performed medical procedures. From the balloon angioplasty in fact, the technique has been improved by the addition of bare metal stents (BMS) for avoiding the risk of vessel recoil. Anyway, despite their employment lowered the restenosis rates, the occurrence of early stent thrombosis and neointimal hyperplasia, pushed the biomedical research to the realization of novel technologies. Firstly, the idea of combining the mechanical stent support with the possibility of using them as drug delivery platforms leaded to the realization of drug eluting stent (DES) for the *in-situ* release of anti-proliferative or pro-endothelialisation drugs. DES can reduce in-stent restenosis rates, but further improvement is still possible. A possible alternative to DES are gene eluting stents (GES), that aim to combine a gene therapy approach to stent technology by exploiting the device itself as surface-mediated gene delivery system.

The major challenge toward the development of a reliable GES apparatus is the realization of a stable, biocompatible and anti-thrombogenic biomaterial on which gene delivery vectors can be immobilized, in order to promote and sustain their activity on the surrounding cells after implantation. Consequently, the development of novel surface-mediated gene delivery strategies has been subject of increasing interest.

In this context, the general aim of this study is to develop surface coatings for metal substrates to directly anchor non-viral gene delivery particles on their surface and exert surface-mediated gene delivery.

AISI 316L stainless steel has been selected as metal substrate as it is the most commonly used alloy for stents.[44]

Stainless steel specimens were first electropolished, in order to obtain smoother metallic surfaces, without any apparent imperfections, and rich in oxides species. Two different strategies were designed in parallel to modify the metal surface, both exploiting the adhesive properties, the stability and the chemical reactivity of

polydopamine (PDA) coatings.[104] The first concerned the PDA coating only, while the second one a functionalization of the former with glutaric anhydride (GLU). The choice of these treatments was done according to the final aim of being able to deposit on them PEI-based polyplexes, positively charged sub-microparticles bearing amine groups at surface.

1) *Polydopamine coating (PDA)*

Considering that PEI-based polyplexes are characterized by free amine groups at surface, possible mechanisms of interaction with the created PDA adhesive layer include the Schiff base formation and the Michael type addition, which guarantee the formation of strong covalent bonds with the quinone structures of oxidized dopamine (Figure 3.1).
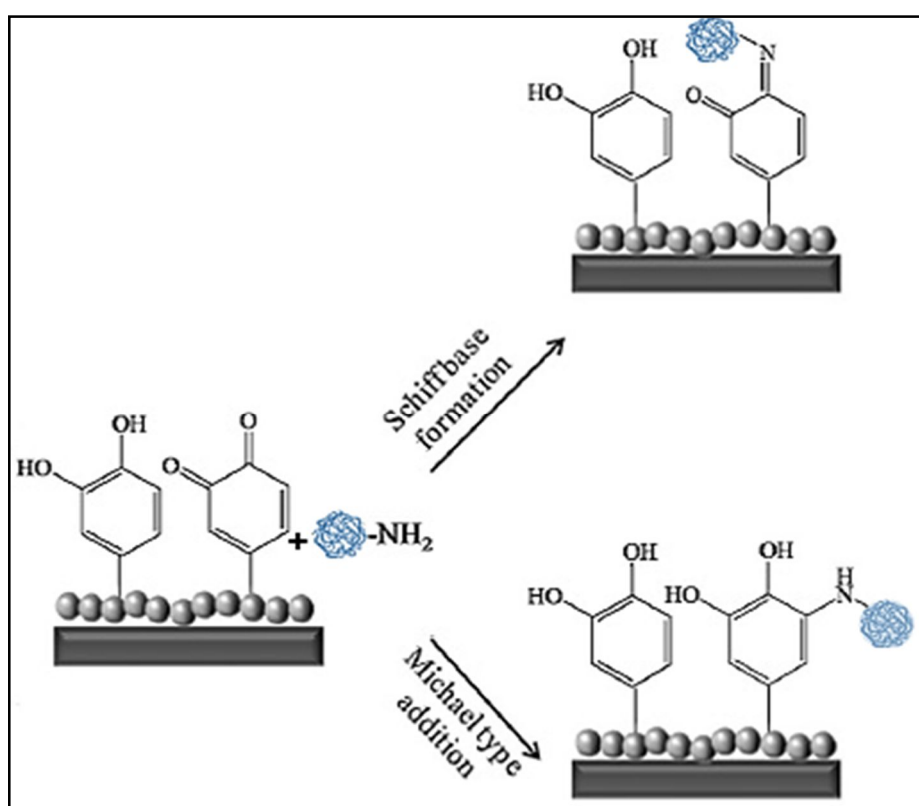
Figure 3.1: Possible reaction scheme of oxidized catechol groups with primary amines

2) *PDA functionalization with glutaric anhydride (GLU)*

Since polydopamine (PDA) features amine groups at surface, their functionalization with glutaric anhydride (GLU) and thus the enrichment of the surface with carboxylic groups represents an alternative proposed solution for promoting the immobilization of amino-based polyplexes. In this case, the interactions between the cationic carriers and the negatively charged carboxylic groups at neutral pH (Figure 3.2), will be of electrostatic nature.
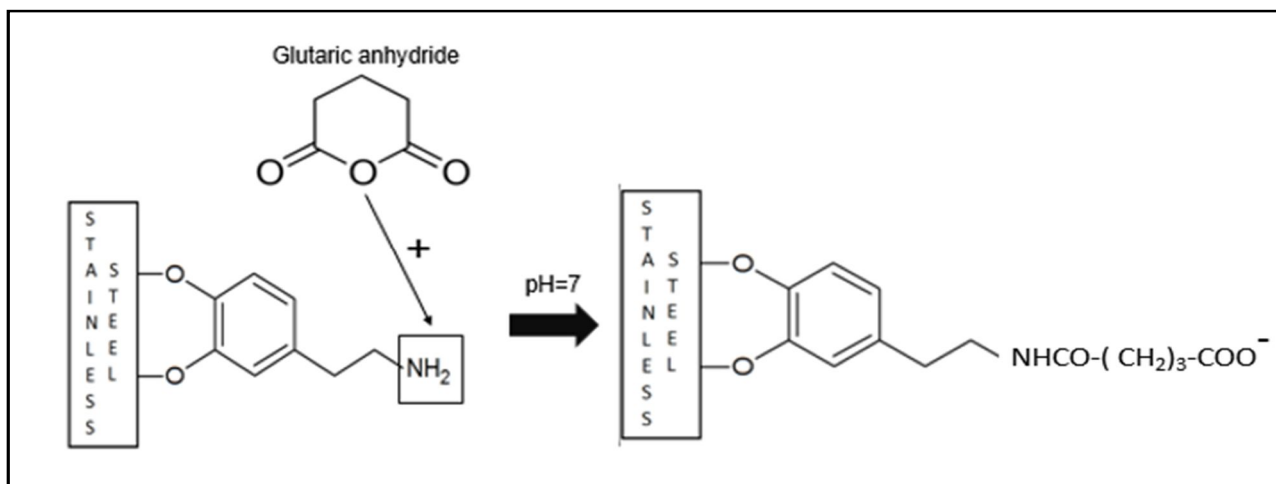
Figure 3.2: PDA functionalization with glutaric anhydride
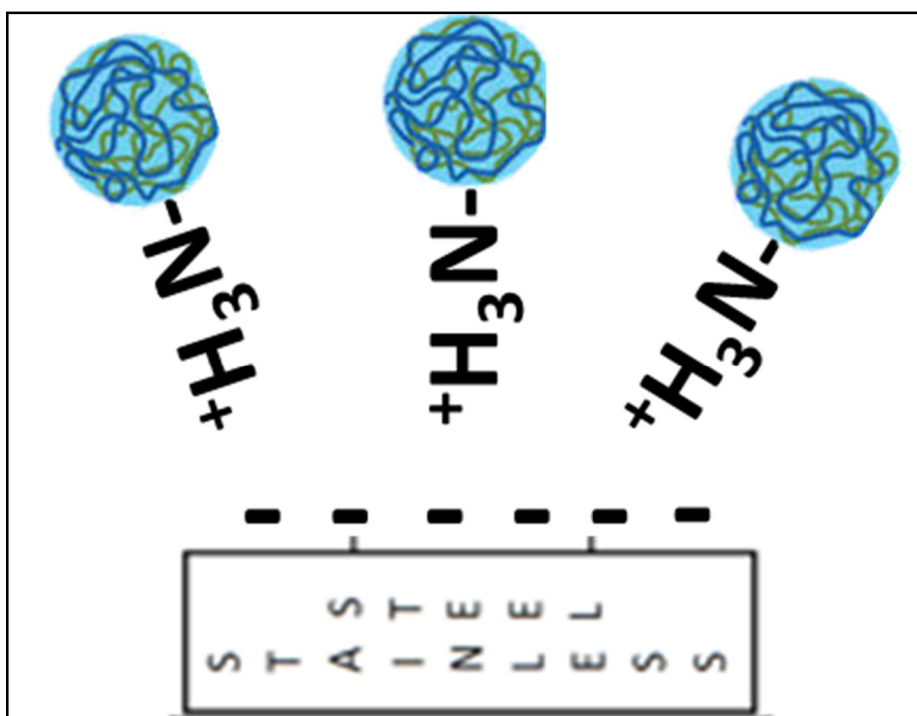
Figure 3.3: Schematic representation of the electrostatic interactions between the substrate and the protonated amine groups of the complexes

The developed surface treatments were thoroughly characterized in terms of morphological and physicochemical properties, and their ability to stably immobilize on the surface amine-bearing sub-micrometric particles was investigated.

Finally, preliminary surface-mediated transfection tests were performed using PEI-based polyplexes.

4. Materials and methods

4.1. Sample preparation

Raw samples were obtained by punching stainless steel AISI 316L foils (thickness = 0.5 mm) with a manual machine having a round cutter of 12.7 mm in diameter. Their composition provided by the suppliers (Goodfellow, Huntington, UK) is shown in the following Table 4.1:

ELEMENTS	Cr	Ni	Mo	C	Fe	Other
wt. (%)	18.00	10.00	3.00	<0.03	65	< 4.00

Table 4.1: SS316L elemental composition

After cutting, disc-shaped specimens were cleaned of gross contaminants by immersion in an acetone ultrasonic bath (frequency = 50KHz), double deionized water (ddH$_2$O) and methanol for 10 min each, and air-dried between each step. Finally, cleaned samples were kept in plastic boxes under vacuum until further use.[113]

4.1.1. Electropolishing

The electropolishing process (EP) was performed, according to previously developed protocols,[110,114] on cleaned samples in order to obtain smoother metallic surfaces, free from imperfections, and rich in oxides and hydroxides species.

Briefly, EP was carried out by dipping the samples in a first solution (Figure 4.1 (A)) containing 50% glycerol, 35% phosphoric acid and 15% ddH$_2$O at 90 °C, under 6 A of current for 3 minutes, followed by a further immersion in acidic bath (Figure 4.1 (B)) composed by 88% ddH$_2$O, 10% of nitric acid and 2% of hydrofluoric acid, at 50°C for 30 s. Finally, samples were rinsed with ddH$_2$O, dried out by compressed air flow and stored under vacuum in plastic boxes.
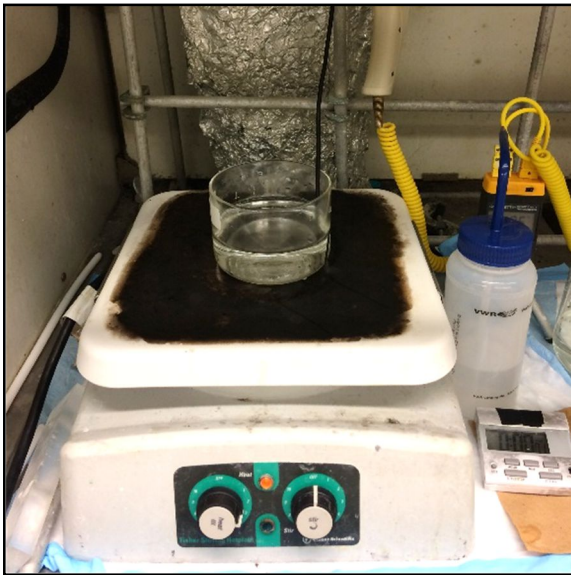
Figure 4.1: (A) Glycerol-based bath and (B) hydrofluoric acid-based solution for electropolishing process (Laboratory of biomaterials and bioengineering (LBB), Quebec City, Canada)

4.1.2. Coatings

A. Polydopamine coating

A quite thick ($\approx$ 50 nm)[110] polydopamine coating (PDA) was obtained on the surface of electropolished samples. Due to its chemical reactivity at slightly basic pH, such polymeric coating might work as anchor point for further immobilizations on it.

Briefly, metallic samples were placed into a 24-wells plate and covered with 2 mL of solution prepared by dissolving dopamine hydrochloride in 10 mM TRIS buffer, at a final concentration of 2 mg/mL, and incubated at room temperature (25°C, r.t.), for 16 hours, in the dark. Before the deposition, the pH of the solution was adjusted at 8.5 by the addition of 0.1M NaOH, in order to favor a spontaneous polymerization in alkaline environment.[115] Afterwards, stainless steel- polydopamine (SS-PDA) samples were washed 3 times (1 minute each washing) by vortexing in 10 mL of ddH$_2$O, air-dried and kept under vacuum until further use.[105]

B. Polydopamine coating functionalization with glutaric anhydride

The functionalization of the polydopamine coating (PDA) with glutaric anhydride (GLU) was performed in order to introduce carboxylic groups at surface, that, due to their ability of being deprotonated in neutral and acidic environments, might allow further electrostatic interactions with positively charged particles such as polyplexes.

In a glove box purified with dry nitrogen, functionalized SS-PDA samples were put in falcon tubes and covered with 5 mL of a saturated solution of GLU in acetone for 60 min on an orbital shaker at 160 rpm. Specifically,

since a 0.1 g/mL represents the saturation limit of GLU, 500 mg of GLU were added immediately before incubation with the samples and after 20 and 40 min, in order to guarantee the maintenance of a saturated solution despite GLU hydrolysis. At the end of the process, samples were rinsed with acetone and ddH$_2$O, before being dried with compressed air and stored under vacuum.[113]

4.2. Samples characterization

The realized surfaces were characterized from the topological, physical-chemical and biological points of views, to follow up the modifications obtained at each step, and to monitor the obtainment of the desired properties.

4.2.1. AFM: Atomic Force Microscopy
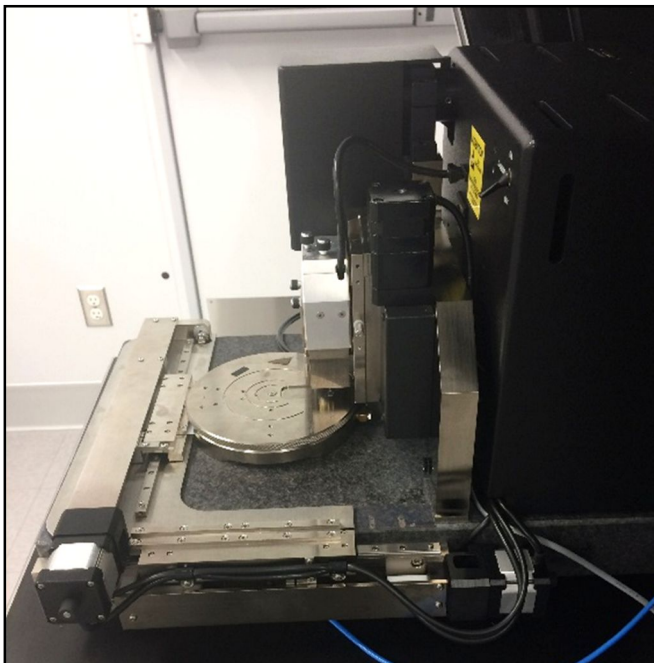
Superficial topologies were firstly observed using a Veeco Dimension TM3100 atomic force microscope (AFM) (Figure 4.2), Veeco, New York, USA), in tapping mode with an etched silicon tip (radius = 10 nm, Bruker, Billerica, USA). Areas of 40 x 40 µm^2 were analysed with Nanoscope Analysis v1.5, and afterwards, both average roughness (Ra) and root mean squared roughness (RMS) were evaluated using the software WSXM 5.0.

Figure 4.2: Veeco Dimension TM3100 atomic force microscope (Laboratory of biomaterials and bioengineering (LBB), Quebec City, Canada)

4.2.2. SEM: Scanning Electron Microscopy

Scanning electron microscopy (SEM) were performed in order to obtain high resolution images, referring to the superficial textures of the samples; a FEI Quanta 250 microscope (Figure 4.3, ThermoFisher Scientific, Hillsboro, USA) operating in low-vacuum modality was used.

Figure 4.3: FEI Quanta 250 microscope used for SEM imaging (Laboratory of biomaterials and bioengineering (LBB), Quebec City, Canada)

4.2.3. Contact angle

Static contact angle measurements were performed to evaluate the wettability of treated surfaces. In this regard, a video contact angle system (Figure 4.4, AST Products Inc. VCA 2500 XE, Billerica, USA) was used. The analysis was carried out in different parts of the same sample, at r.t. and using 1 µL droplets of double deionized water, deposited by means of a syringe.

Figure 4.4: VCA 2500 XE video system, used for static contact angle measurements (Laboratory of biomaterials and bioengineering (LBB), Quebec City, Canada)

4.2.4. XPS: X-Ray Photoelectron Spectroscopy
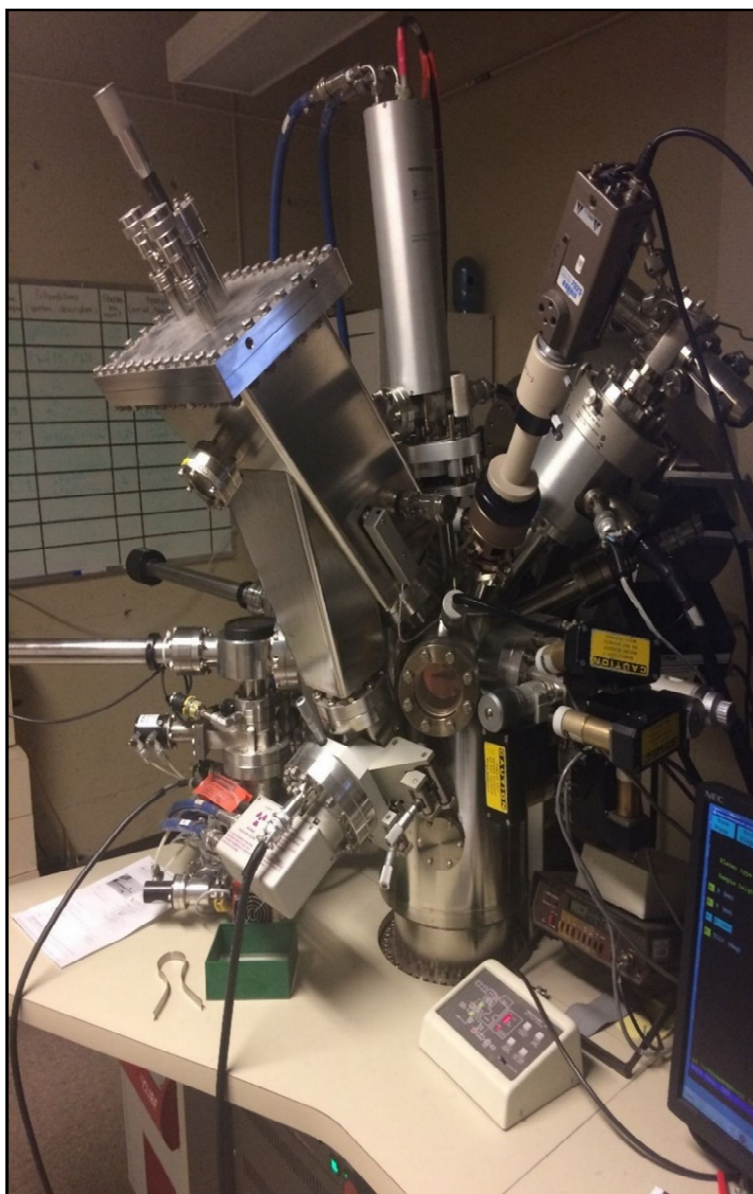
X-Ray photoelectron spectroscopy (XPS) was used to assess the superficial atomic composition of treated samples. The analysis was carried out by using a Physical Electronics PHI 5600-ci spectroscope (Figure 4.5), in two different modalities: the first using a standard aluminium X-ray source (1486.6 eV) at 300W to detect survey spectra; while, the second one employing a magnesium source (1253.6 eV), to record the high-resolution spectra of C(1s). The curve fitting for the high-resolution C(1s) peaks was determined by means of least-squares peak fitting using a 70%/30% Gaussian-Lorentzian peak shape with a Shirley background (using Casa XPS software). The C(1s) region was calibrated to the CF2 peak at 292 eV. Furthermore, the incident X-ray beam was regulated at 45° with respect to the normal surface, for the obtainment of a penetration depth of 5nm and an analysed area of 0,005 cm^2. For each surface at least 3 different regions were investigated.

Figure 4.5: Physical Electronics PHI 5600-ci spectroscope, used for XPS survey (Laboratory of biomaterials and bioengineering (LBB), Quebec City, Canada)

4.2.5. Chemical derivatization for the evaluation of superficial primary amines using TFMBA vapours

Chemical derivatization with vapours of 4-(Trifluoromethyl) benzaldehyde (TFMBA, Sigma-Aldrich, St. Louis, USA), was used for the evaluation of the presence of primary amines at samples surface. Firstly, 500mL of TFMBA were placed at the bottom of a Pyrex tube and separated from the sample thanks to few layers of inert soda-lime glass beads; then, the glass tube was tightly closed and the reaction with TFMBA vapours was performed for 2 hours at r.t. Finally, samples were outgassed in a heated vacuum chamber (40°C) and analysed at the XPS, using a standard aluminium X-ray source (187.85eV) at 300W to detect survey.

4.2.6. FT-IR: Fourier Transform-Infrared Spectroscopy
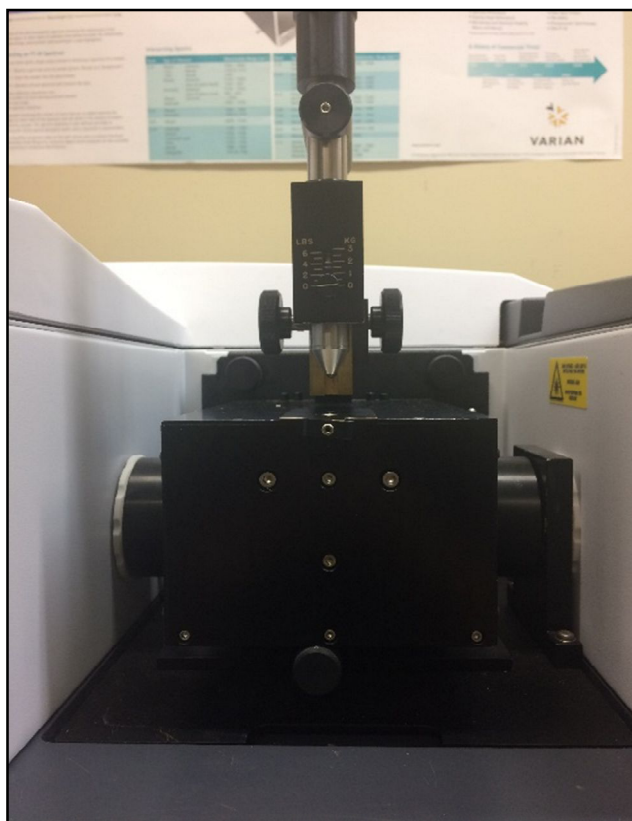
Infrared spectroscopy was performed to identify the presence of specific functional groups at the sample surfaces, from the analysis of their adsorption spectra. The analysis was performed using a Attenuated Total Reflectance (ATR) mode in FTIR (Figure 4.6, Agilent Cary 660 FTIR, Agilent technologies, Australia), equipped with a deuterated L-alanine-doped triglycine sulfate (DLa-TGS) detector and a Ge-coated KBr beam splitter. The depth of analysis was approximatively 1µm and 64 scans were routinely acquired at a spectral resolution of 4cm^{-1}.

Figure 4.6: Agilent Cary 660 FTIR, used for ATR analysis mode in FT-IR (Laboratory of biomaterials and bioengineering (LBB), Quebec City, Canada)

4.2.7. Colorimetry assays

Two different colorimetric assays were performed for the quantification of charged functional groups at surface.

In particular, a colorimetric assays based on Toluidine Blue O (TBO), which is a cationic compound that interacts electrostatically with negatively charged groups and can be easily detected by light absorption in the blue region, was used for the detection of anionic molecules, such as deprotonated carboxylic groups (COO$^-$), in alkaline conditions.[116]

A colorimetric assays based on Orange II sodium salt, which is, instead, an orange dye that interacts electrostatically with positively charged groups, was used for the detection of protonated primary amines, in acidic solution.[117]

A. Quantification of negatively charged groups on the surface using TBO dye

According to Noel et al,[117] a pH 10 solution was prepared in a glass bottle, thanks to the drop-by-drop addition of 1M NaOH into ddH$_2$O and TBO was added up to a final concentration of 5.10^{-4} M.

Then, samples were soaked in 10 mL of the TBO solution in 15 mL-tubes covered by aluminum foil and stirred for 6 hrs at 160 rpm.

After the 6 hr-incubation, samples were cleaned twice (1 minute each) by vortexing in 15 mL tubes containing 10 mL of ddH$_2$O, pH 10, and one time in fresh ddH$_2$O. Then, they were air-dried and TBO desorption was obtained by adding 2 mL of 50% v/v acetic acid inddH$_2$O to each sample.

Afterwards, 200 µL aliquots of the desorbed TBO solutions were placed in a transparent 96-well plate and their absorbance at λ = 633nm was read (in triplicate) by using a multiplate reader spectrophotometer (SpectraMax i3X, Molecular Devices). TBO quantification was performed by comparison with a calibration curve obtained by diluting different concentrations of TBO in 50% v/v acetic acid in ddH$_2$O.

B. Quantification of primary amine groups on the surface using ORANGE II dye

According to Ricciardi et al,[116] pH 3 and pH 12 solutions were prepared in two glass bottles, thanks to the drop-by-drop addition of 1M HCl and NaOH 1M into ddH$_2$O, respectively.

For the preparation of the dye solutions, ORANGE II sodium salt was added to ddH$_2$O pH 3 up to a final concentration of 14 mg/mL. Then, samples were submerged with 5 mL of ORANGE II solution in 15 mL-tubes covered by aluminum sheets, and put in incubator at 37°C for 30 minutes.

After the 30 minutes of incubation, samples were intensively rinsed 3 times, by hand shaking in 15 mL tubes containing 10 mL of ddH$_2$O pH 3, to remove the unbound dye. Then, they were air-dried, and ORANGE II desorption was obtained by adding 1 mL of ddH$_2$O pH 12 to each sample.

Afterwards, 200µL aliquots of the desorbed ORANGE II solutions were placed in a transparent 96-well plate and their absorbance at λ = 484 nm was read (in triplicate) by a multiplate reader spectrophotometer (SpectraMax i3X, Molecular Devices). ORANGE II quantification was performed by comparison with a calibration curve obtained by diluting different concentrations: each obtained value was inserted in the calibration curve obtained by diluting different concentrations of ORANGE II in ddH$_2$O pH 12.

4.2.8. Cytotoxicity tests

For the preliminary biological assessment of the surfaces, both direct and indirect cytotoxicity tests were performed using Alamar Blue viability assay (ThermoFisher Scientific, Hillsboro, USA) and according to the ISO 10993-5 standard. For each test, two different cell types, namely HeLa and HUVEC cells, were used.

HeLa cell line (American Type Culture Collection, ATCC, Manassas, USA) is derived from human epithelial ovarian carcinoma and is commonly used in transfectant development, thanks to their stable growth and to their ability to be easily transfected.[86]

Primary Human Umbilical Vein Endothelial Cells (HUVECs) were extracted from the endothelium of veins from the umbilical cord at LBB and were employed provide a classic model cell system for biomaterial studies in cardiovascular stent applications.[118]

HeLa cells were cultured in DMEM (Gibco 11995 by ThermoFisher Scientific) supplemented with 10% FBS and 1% Penicillin/Streptomycin solution (Complete DMEM HeLa) at 37°C in a H2O saturated atmosphere in a cell culture incubator.

HUVECs were cultured in DMEM supplemented with 5% FBS, 1% Penicillin/Streptomycin solution, 2 ng/ml fibroblast growth factor (FGF), 1 ng/ml epidermal growth factor (EGF), 1 µg/ml Ascorbic Acid, 1 µg/ml Hydrocortisone and 90 µg/ml Heparin (Complete DMEM HUVECs) at 37°C in a H2O saturated atmosphere in a cell culture incubator.

Alamar blue reagent is a redox indicator that yields a colorimetric change and a fluorescent signal in response to cellular metabolic activity, permitting to evaluate the relative cytotoxicity of different chemical agents. Live cells have a reducing environment within their cytosol. Resazurin, the active molecule of Alamar blue reagent, is a nontoxic, cell permeable compound that is blue in color and virtually non-fluorescent. Upon entering cells, resazurin is reduced to resorufin, a compound that is red in color and highly fluorescent (λ_{ex} = 545 nm, λ_{em} = 590 nm). Viable cells continuously convert resazurin to resorufin, therefore the level of fluorescence intensity is proportional to the metabolic activity of live cells.

A. Indirect cytotoxicity assay

The indirect assay allowed to evaluate the possible release of cytotoxic compounds from a material through the evaluation of the viability of cells, cultured in a culture medium conditioned by the material (material extract).

Samples were placed in a 24-wells plate and sterilized in 70% ethanol (EtOH) in dH2O. After 30 min, the 70% EtOH was completely removed, and samples dried under vacuum in sterile conditions. Samples were then incubated with 2 mL of complete DMEM HeLa or Complete DMEM HUVEC for 24 hrs at 37°C in a cell culture incubator. Afterwards, 2×10^4 cells/cm^2 were seeded in a transparent 96- wells plate (Corning^{TM}, Termo Fisher Scientific) in their own culture medium and incubated at 37°C. After 24 hrs, culture medium was replaced with 100 µL of sample extracts (eluates). After 24 hrs of incubation at 37°C in a cell culture incubator, Alamar Blue viability assay was performed. Briefly, 10×Alamar Blue stock solution was diluted 1:10 in fresh DMEM and 100 µL/well were added to cells. After 3 hrs of incubation at 37°C, the fluorescence of the culture medium was read at the spectrophotometer (λ_{ex} = 545nm; λ_{em} = 590nm) and the data were analysed with Excel. Cells cultured in non-conditioned medium were used as viability controls.

B. Direct cytotoxicity assay

The direct cytotoxicity assay allowed to determine the cell adhesion and proliferation on material surfaces over time.

Samples were placed in a 24-wells plate and sterilized in 70% EtOH. After 30 min, the 70% EtOH was completely removed, and samples dried under vacuum. Next, 1×10^4 HeLa cells/cm^2 or 1.5×10^4 HUVECs/cm^2 were seeded in their own culture medium directly onto the samples. After 24 hours of incubation at 37°C, the medium was replaced with 700 µL of 1× Alamar Blue solution in Complete DMEM and after 3 hrs of incubation at 37°C, 3×100 µL aliquots were taken from each well and put in a transparent 96-well plate for the fluorescence reading at the spectrophotometer (λ_{ex} = 545nm; λ_{em} = 590nm). The remaining Resazurin solution was completely removed with a vacuum pump and freshly new medium was added to cells; in this way, cell viability was measured also after 3 and 7 days of culture.

Cells seeded on culture wells were used as viability controls.

4.3. Microparticles deposition

In order to simulate the interaction between the developed surfaces and polyplexes (usually consisting of positively charged sub-micrometric particles exposing amines on the surface) superparamagnetic microparticles (screenMAG/G-Amine, Chemicell, Berlin, Germany) made of a silica core and superficially functionalized with amines (amination degree = 350 µmol of NH_2/g) and with a hydrodynamic diameter (D_H) of 500 nm, were deposited on the surface and subsequently quantified.

Samples were incubated in a microparticles suspension containing a number of microparticles sufficient to completely cover their surface (area=1.27cm^2). The particle aqueous stock suspension (50mg/mL) was diluted 200 times in buffer solutions prepared with either 10mM Hepes (pH=7) for the deposition on GLU samples or 10mM TRIS (pH=8.5) for the deposition on PDA samples. Non-coated electropolished samples were used as deposition controls.

Samples were placed in a 24-wells plate and soaked in 1 mL of microparticles suspension, at r.t. for 24 hrs. After the incubation, samples were rapidly rinsed in ddH$_2$O to remove the unbound particles, and dried in heated vacuum chamber (40°C) for 10 min. Particles covering the sample surfaces were observed under a stereo microscope (BX41M, Olympus) and digital images (n = 5 images per samples) were acquired at 10× magnification.

Once having collected a sufficient number of representative images, these were analysed with the software ImageJ, in order to quantify the % of the surface covered by microparticles.

4.3.1. Particle coating stability tests under shaking

For a preliminary analysis of the stability of the microparticles on the surface, samples were put under mechanical agitation (170 rpm, orbital shaking) in a 24-wells plate in PBS and, observed under a stereo microscope (BX41M, Olympus) as described above at different time points. Before imaging, samples were always rinsed in ddH$_2$O and dried in heated vacuum chamber (40°C) for 10 min.

Image analysis was performed by ImageJ as described hereinabove.

4.3.2. Particle coating dynamic stability tests

In order to simulate the stability of the submicrometric particles deposited on the surface in quasi-physiological conditions, a dynamic stability test was developed. Samples were placed in flow chambers (N Ibidi sticky-Slide I Luer), in which thanks to the mechanical action of a peristaltic pump, PBS was fluxed for recreating blood flow conditions occurring in healthy human coronary arteries:

1. Laminar flow: Reynolds' number < 2000; [119]
2. Shear stress at vessel wall: τ= 15 dyne/cm2= 1.5 Pa; [118,119]

The apparatus was designed to have a laminar flow sweeping the flat surface of a test specimen placed inside the Ibidi chamber (Figure 4.7), which is an apparatus typically employed for perfusion applications and applying defined shear stress and shear rates on cells inside the channel.

Figure 4.7: Sticky-Slide I Luer Ibidi chamber

Thus, a soft silicon sheet (1.5 mm thick) was cut with a puncher to obtain a 13mm diameter hole where samples were placed. The resulting silicon mask was placed over a microscope glass slide, the Ibidi chamber was placed over the system, the system was tightly closed with metal clamps, and finally the peristaltic pump was connected to the input and the output of the chamber (Figure 4.8).
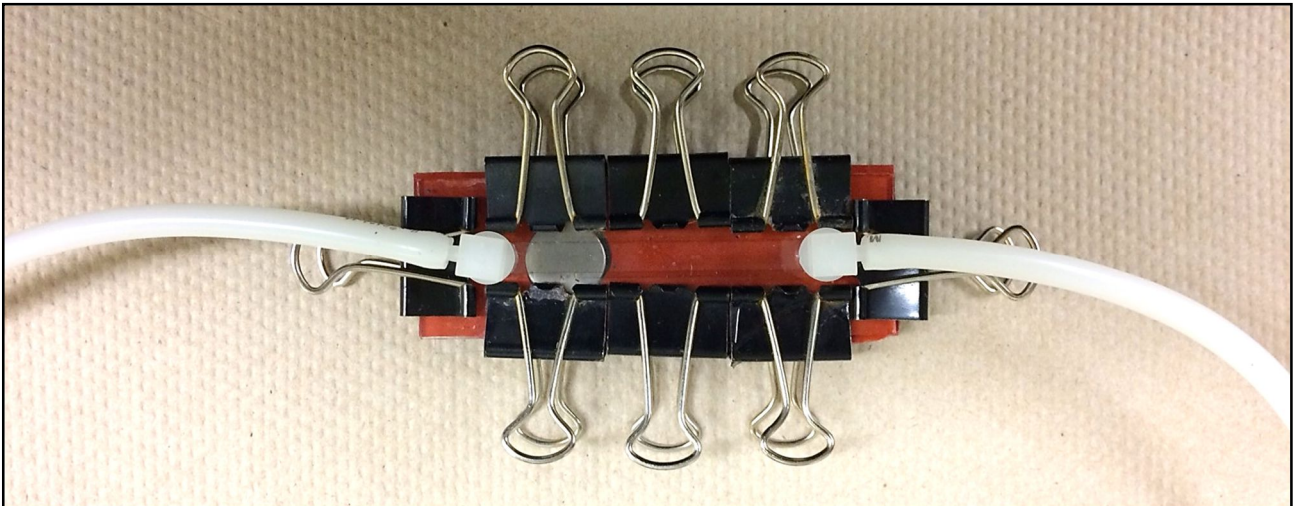
Figure 4.8: Representation of the modified Ibidi flow chamber, designed at LBB (Laboratory of biomaterials and bioengineering, Quebec City, Canada) for the realization of a particle coating dynamic stability test apparatus.

As reported in Figure 4.9, the geometrical parameters of the flow channel with rectangular section were: a=5mm, b=0.45mm and L=48.2 mm; thus, the hydrodynamic diameter was calculated as D_H= 2(a*b)/(a+b) = 0.826 mm.
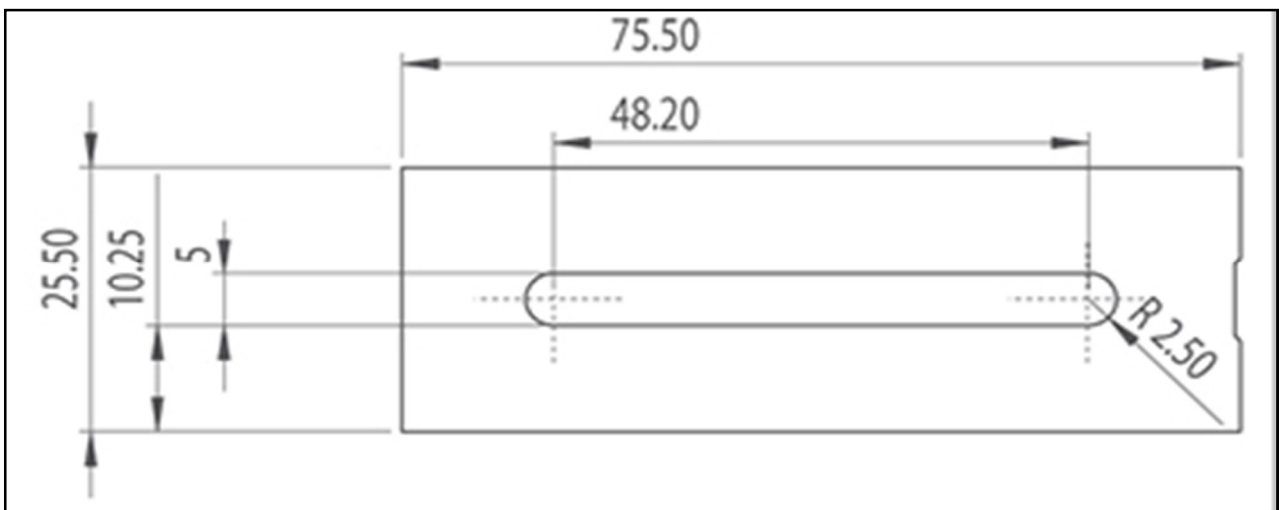
Figure 4.9: Schematization of the geometrical parameters of the flow channel.

For recreating a shear stress of 15 dyne/cm2 (= 1.5 Pa), which was representative of physiological arterial hemodynamic shear stress,[118,119] considering laminar flow, according to the manufacturer's instructions:

- $\tau = \eta * 104.7 * \varphi$ and $\varphi = \tau/104.7/\eta$

Imposing

- τ=15 dyne/cm2 = 1.5 Pa,

and considering for PBS at 25°C:

- dynamic viscosity η= 1cP= 0.001Pa*s= 0.01dyne*sec/cm2,

- density ρ= 1000 kg/m3.[120]

a flow rate φ = 14.33 ml/min= 0.239cm^3/sec was needed.

Moreover, to confirm the laminar flow condition, Reynolds' number was calculated as:

- Re=$\rho v D_H/\eta$= 87.7,

Since for φ = 14.33 ml/min, the average velocity in the pipe was:

- v= φ/area= 10.6 cm/s

Re= 87.7, which satisfied the first hypothesis.

The hydrodynamic length (L_H) was evaluated in order to correctly design the sample position inside the chamber (distance from the flow inlet port) and assure laminar flow.

According to Hülsbeck et al., for laminar flow:

- L_H>0.029*Re*DH,[121]

while according to Lévesque et al.:

- L_H>0.06*Re*DH.[122]

Considering the latter criteria as the most restrictive, using our data we obtained L_H >4.35 mm.

Hence, samples were placed at 35 mm from the inlet port, guaranteeing laminar flow.

Complexes were prepared at r.t. by mixing a bPEI-based polymer solution, at the desired bPEI concentration, with an aqueous plasmid solution of pGLuc-Basic Vector.

- Polymer solution: the starting polymer stock solution (bPEI, 250 kDa, [N] = 20 mM in dH$_2$O, Sigma-Aldrich) was diluted in 10 mM HEPES buffer (pH=7), in order to achieve the desired bPEI concentration, yielding to N/P=2.5.

- Plasmid solution: starting plasmid stock solution ((New England Biolabs© Inc, [pGLuc]= 0.25µg/µL). The pGLuc-Basic Vector contains the "humanized" coding sequence for the secreted Gaussia Luciferase (GLuc), for use in mammalian cells. GLuc possesses a natural secretory signal and upon expression is secreted into the cell medium of cultured mammalian

cells; this, allows for multiple samples to be assayed from the same transfected cells, as well as collecting data at different time points, through Luciferase assays.

Polyplex transfection solution was prepared in sterile Eppendorf tubes, by adding plasmid solution to polymer solution, without mixing. The volumes of the reagents were selected according to reach a final concentration of plasmids in transfection solution of 0.02 µg/µL, and a N/P ratio of 2.5. N/P is defined as the number of amines (N) of the cationic polymer which complexed the phosphate groups (P) of a given amount of DNA (1 µg of DNA carries 3.03 nmoles of phosphate groups). Then, the resulting suspensions were incubated for 30 min at r.t. (25 °C), prior to be deposited.

4.4. Deposition of bPEI-based polyplexes

Due to the good stability results obtained by the deposition of microparticles, polyplexes generated by mixing bPEI 250 kDa and pGLuc-Basic Vector at 0.25 µg/µl concentration, as previously described, were deposited on samples at different pH: PDA at pH=8.5 and GLU at pH=7, in both conditions EP samples were tested as negative control.

After 30 min of sterilization in pure EtOH, samples were covered with a silicone ring with an inner open circle with D = 10mm and were placed in a 12-well plate containing a water bath and a paper filter to keep the sample separated from water. Then, transfection solution was prepared by mixing b-PEI (250 kDa, 20 mM) and pGLuc (0.25 µg/µl), in order to obtain N/P=2.5 and plasmid concentration in solution = 0.02 µg/µl.

After 30 min of incubation at r.t poliplexes were deposited on EP and GLU samples at pH 7 by adding directly on the sample 100 µl/sample of the transfection solution; while, on EP and PDA after having adjusted the pH at 8.5. For the adjustment, 550 µl of the transfection solution were placed in a separate Eppendorf and 236 µl of 100 mM TRIS pH=8.5 were added (ratio v/v = 7:3) to reach the desired pH. Then, 143 µl of the resulting solution were placed on each sample.

Samples were incubated for 24 hrs at r.t. adding water in the spaces between the wells of the plate to limit evaporation. The plate was closed with parafilm.

4.5. HeLa cells transfection

The day after polyplex deposition samples were washed once in 10 mM Hepes, pH7 (rapid dipping in solution) and then placed in a 24 well plate, where immediately after 2×10^4 HeLa cells (P8)/cm2 were seeded in the wells in complete DMEM (DMEM Life Technologies, 11995-065, supplemented with 1% PenStrep (G1146 Sigma) and 10% Fetal Bovine Serum (Life Technologies, 12483-020)).

In order to evaluate the efficiency of the transfection process, Luc expression was assessed 24h, 72h, 5 days and 7 days after transfection. For the assay, 20 µL of the conditioned medium was mixed with 50 µL of

Luciferase substrate and the luminescence was immediately read at the spectrophotometer (λ=578 nm), in a white 96-well plate.

In parallel, a direct cytotoxicity test was performed in order to verify the cell adhesion and proliferation of transfected HeLa cells on material surfaces. Following the procedure already described in the previous chapters, the remaining conditioned medium was replaced with 700 µL of 1× Alamar Blue solution in Complete DMEM and after 3 hours of incubation at 37°C, 3×100 µL aliquots were taken from each well and put in a transparent 96-well plate for the fluorescence reading at the spectrophotometer (λ_{ex} = 545nm; λ_{em} = 590nm). The remaining Resazurin solution was completely removed with a vacuum pump and freshly new medium was added to cells; in this way, cell viability was measured at 24 hrs and 72 hrs of culture.

5. Results and discussion

In this study, innovative surface modification strategies for the development of novel gene delivery platforms, were investigated. The starting material was stainless steel AISI 316L, which was firstly electropolished and then superficially modified by two different strategies in parallel. The aim of the work was to modify the metal surface, to exploit both the adhesive properties, the stability and the chemical reactivity of polydopamine (PDA) coatings, for the realization of platforms on which immobilize PEI-based polyplexes, which are positively charged sub-microparticles bearing amine groups at surface. Particularly, the first approach involved the use of the PDA coating only, while the second one was based on the functionalization of the former with glutaric anhydride (GLU). In order to verify the success of the two coating processes and their potential as gene delivery surfaces, the developed samples were deeply characterized from physicochemical and biological points of view. In this chapter, the obtained results will be fully described and discussed.

5.1. Characterization of electropolished surfaces

The selection of the starting material was done according to a literature review, from which AISI 316L stainless steel emerged to be one of the most common used material in cardiovascular stent applications.[113,122]

Stainless steel raw samples were firstly electropolished, following a protocol previously developed at LBB (Laboratory of biomaterials and bioengineering, Quebec City, Canada), in order to obtain smoother metallic surfaces, free from imperfections, and rich in oxides species. In fact, as the final goal of this work is the realization of biomaterial substrates to be applied in cardiovascular stent applications, the most important requirement is the non-thrombogenicity of the surfaces, which is possibly obtained through the reduction of their roughness. As a matter of fact, AISI 316L stainless steel stents present on the market are electropolished. Moreover, the electropolishing process allowed to increase the reproducibility of the subsequent coating procedures and thus of the sample properties.

To evaluate the effect of the electropolishing process on stainless steel and validate its success, non-electropolished (non-EP) and electropolished (EP) samples were morphologically and physicochemically analysed and compared. For the morphological analysis, atomic force microscopy (AFM) and scanning electron microscopy (SEM) were employed to obtain high-resolution images of the surfaces; while contact angle measurements were performed for the evaluation of their hydrophilicity. Moreover, AFM pictures were analysed in terms of superficial roughness, calculated as the root mean square (RMS) of the surfaces measured microscopic peaks and valleys. Finally, concerning the physicochemical characterization, X-ray photoelectron spectroscopy (XPS) was used for the superficial elemental analysis.

5.1.1. Atomic force microscopy

Atomic force microscopy (AFM) was performed for evaluating the morphological changes obtained after the electropolishing process. In Figure 5.2. it is possible to appreciate the appearance of grain boundaries on EP

sample surfaces, which were not visible on non-EP ones (Figure 5.1). Thus, since this fact was already reported by other previous works, for example by the one of Haïdopoulos et al,[113] grain boundaries formation is a clear evidence of the successful performance of the process.

A. Imaging
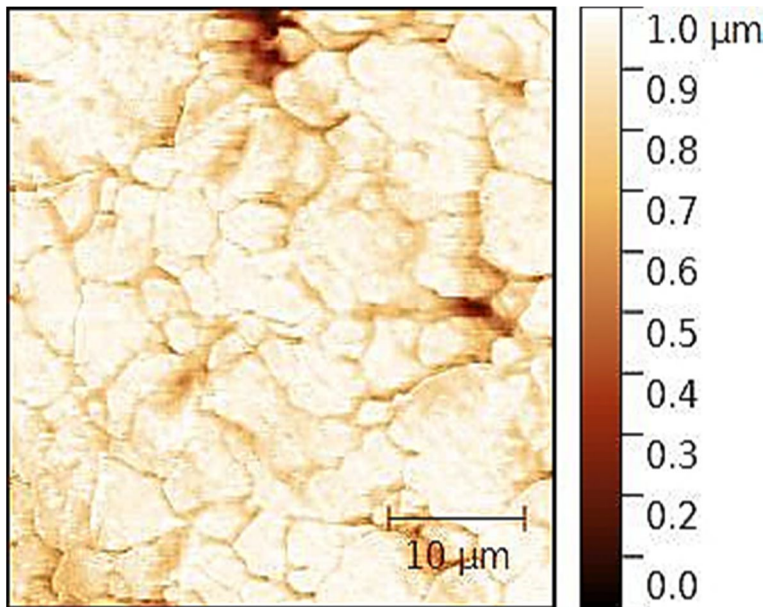
Figure 5.1: Superficial atomic force microscopy image of a non-electropolished stainless steel AISI 316L sample (non-EP). It was obtained by using an atomic force microscope (Veeco Dimension TM3100) in tapping mode, with an etched silicon tip. Areas of 40x40μm^2 were analysed with Nanoscope Analysis v1.5.

Figure 5.2: Superficial atomic force microscopy image of an electropolished stainless steel AISI 316L sample (EP). It was obtained by using an atomic force microscope (Veeco Dimension TM3100) in tapping mode, with an etched silicon tip. Areas of 40x40μm^2 were analysed with Nanoscope Analysis v1.5.

B. Roughness evaluation

After AFM imaging, pictures were analysed with the software WSXM 5.0, for the obtainment of detailed data concerning topology and roughness of non-electropolished (non-EP) and electropolished (EP) surfaces. In Figure 5.3, the evaluation of the root mean squared roughness (RMS) between non-EP and EP samples is reported.
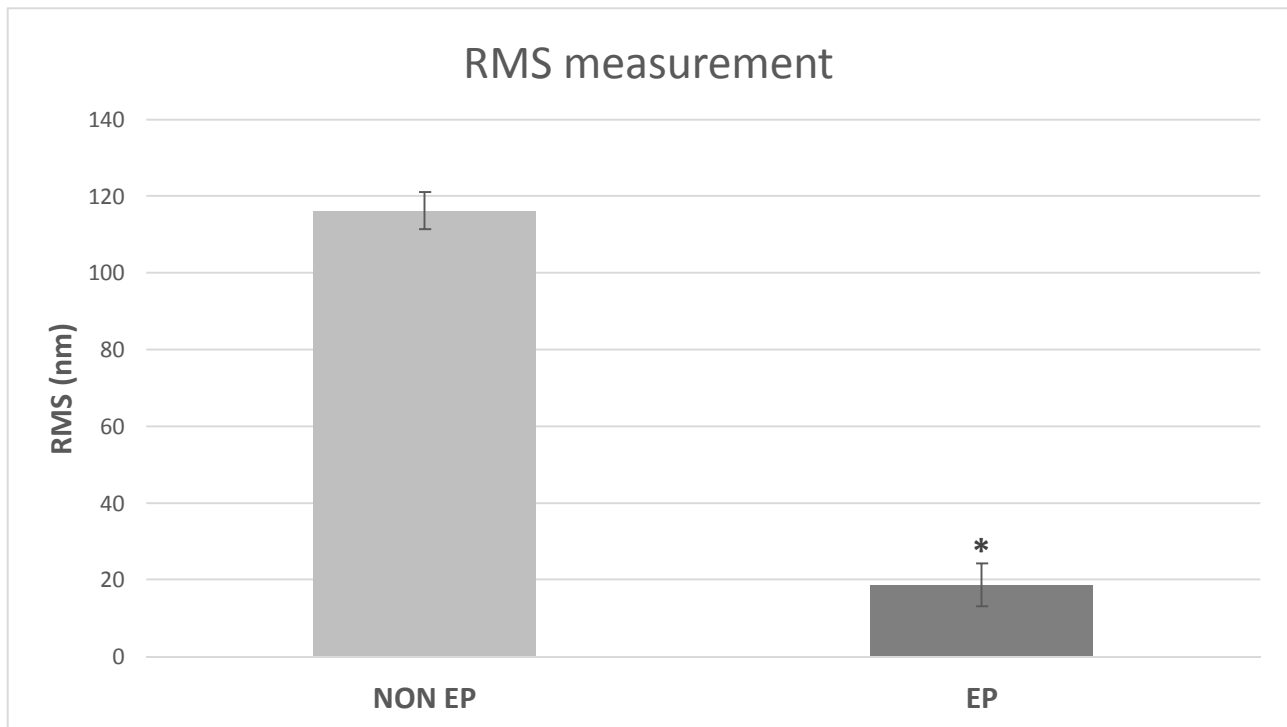
Figure 5.3: Evaluation and comparison of the superficial root mean squared (RMS) roughness measured on non- electropolished (non-EP) and electropolished (EP) samples of stainless steel AISI 316L. The analysis was performed on 4 samples per type and in 3 different points each, in order to obtain good reproducibility. Results are reported as mean ± standard deviation. *= significant statistical difference with respect to non-EP samples (p<0.001).

RMS represents the root mean squared average of the profile height deviations from the mean line, recorded within the evaluation length; thus, it allows to evaluate precisely the topology of a surface, accounting microscopic peaks and valleys. As expected, the RMS value after electropolishing notably decreased, in support of the fact that the EP process provided the obtainment of smoother surfaces. Furthermore, these results are in line with the ones obtained by other works in literature.[109,112]

5.1.2. Contact angle

Contact angle assay was performed in order to obtain information regarding the hydrophilicity and/or hydrophobicity of sample surface. In Figure 5.4 the comparison of the contact angle measurements between non-electropolished (non-EP) and electropolished (EP) samples is reported. A significant decrease in contact angle can be observed in EP samples, remarking an increase of their superficial hydrophilicity. Again, this is a proof of the success of the electropolishing process; in fact, as even reported in literature,[109] the formation of a smooth oxide layer at the surface leads to an increase of its hydrophilicity.
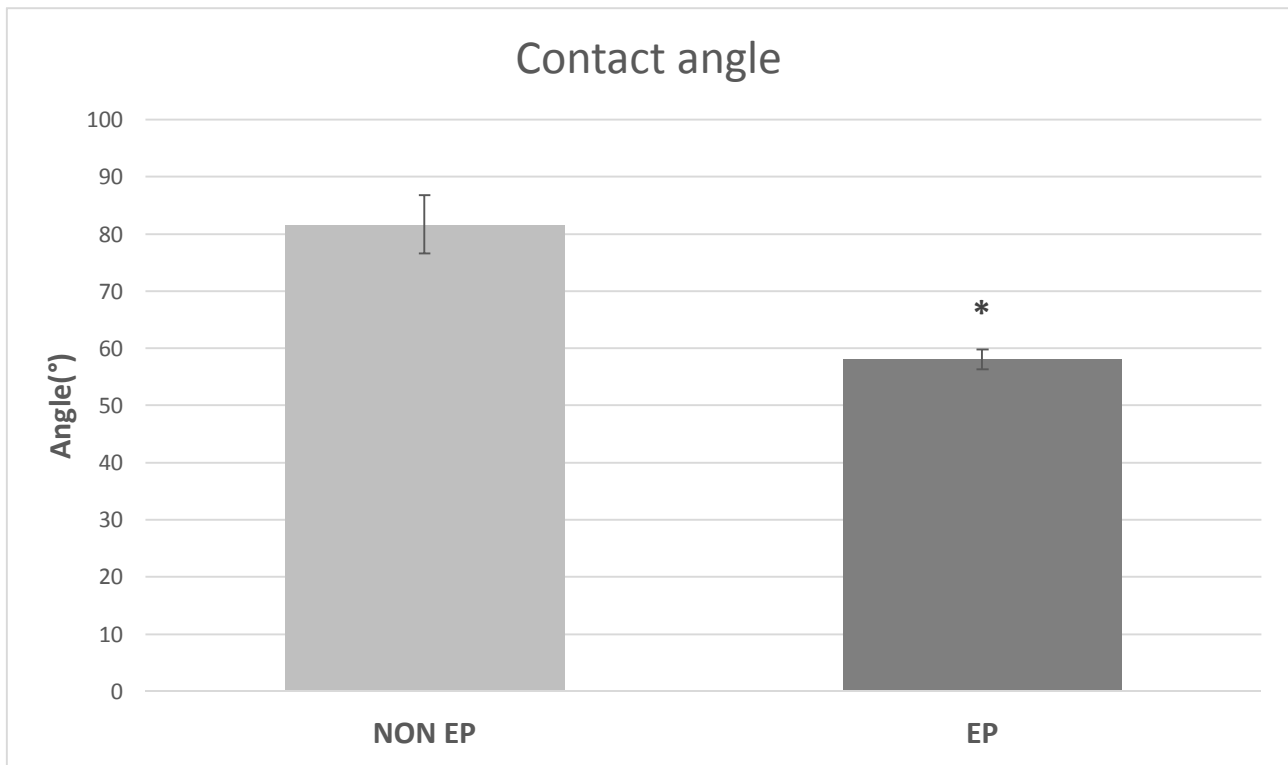
Figure 5.4: Evaluation and comparison of the superficial contact angle measurements performed on non-electropolished (non-EP) and electropolished (EP) samples of stainless steel AISI 316L. Measurements were obtained by using a video contact angle system (VCA 2500 XE), and the analysis was carried out on 4 samples per type, by depositing 1μL droplets of ddH$_2$O in 3 different points each, at room temperature. Results are reported as mean ± standard deviation. *= significant statistical difference with respect to non-EP samples (p<0.001).

5.1.3. Scanning electron microscopy

Scanning electron microscopy (SEM) was performed for the obtainment of detailed pictures, concerning the superficial morphology of non-electropolished (non-EP) and electropolished (EP) samples. In Figure 5.6, grain boundaries on surface of EP samples can be observed, which were not present on non-EP ones (Figure 5.5). Thus, as aforementioned for AFM analysis, the observation of grain boundaries at the surface, clearly smoother than the one of non-EP, is a clear evidence of the successful performance of the electropolishing process.
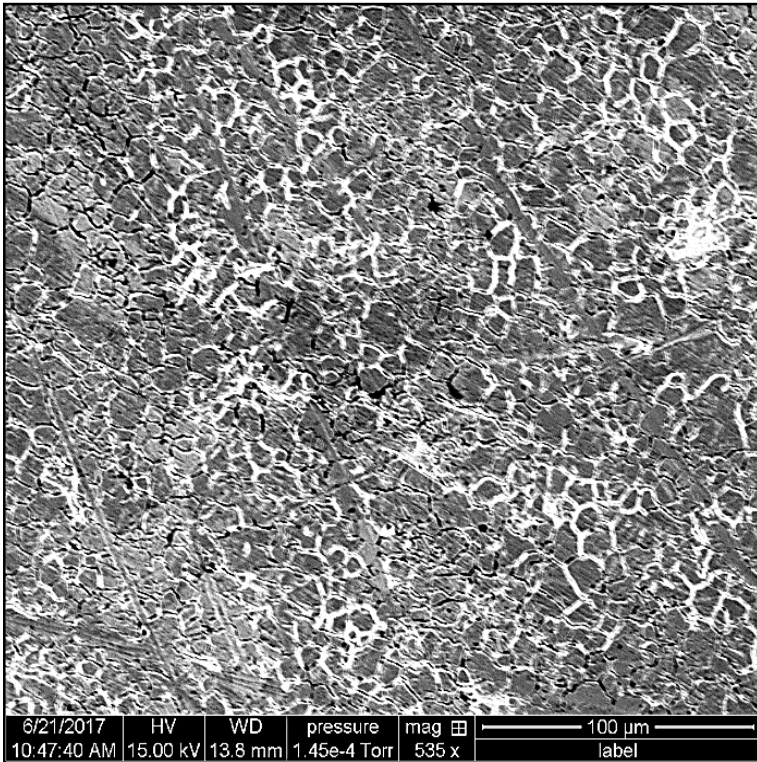
Figure 5.5: Scanning electron microscopy image of a non-electropolished stainless steel AISI 316L sample (non-EP), obtained with a FEI Quanta 250 microscope operating in low-vacuum mode.
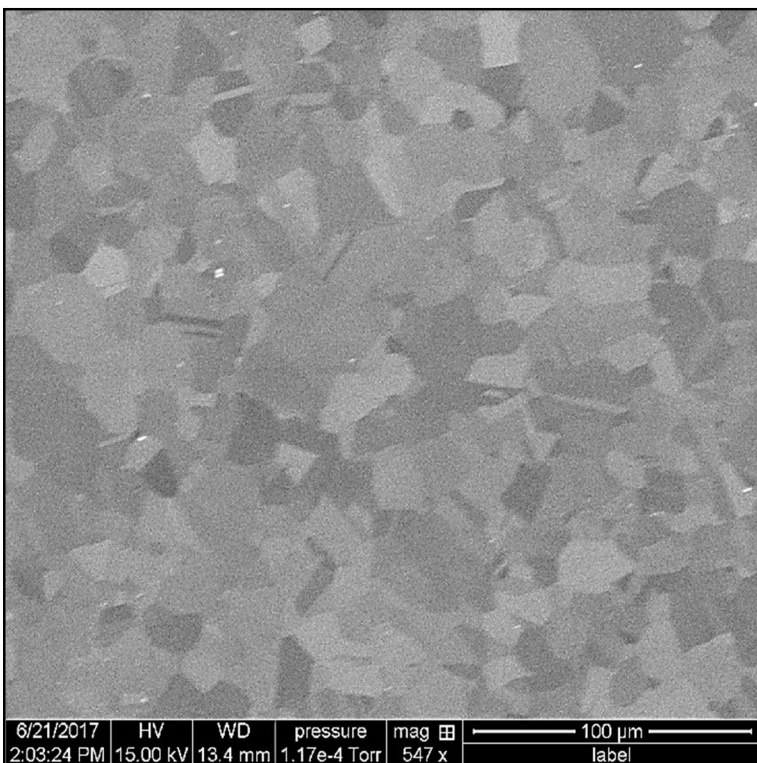
Figure 5.6: Scanning electron microscopy image of an electropolished stainless steel AISI 316L sample (EP), obtained with a FEI Quanta 250 microscope operating in low-vacuum mode.

5.1.4. X-ray photoelectron spectroscopy

X-ray photoelectron spectroscopy (XPS) was assessed in order to characterize and compare the elemental composition of non-EP and EP sample surfaces. As graphically reported in Figure 5.7, the elemental composition after the electropolishing process changed by increasing the contents of oxygen and metallic compounds, while decreasing the carbon one.
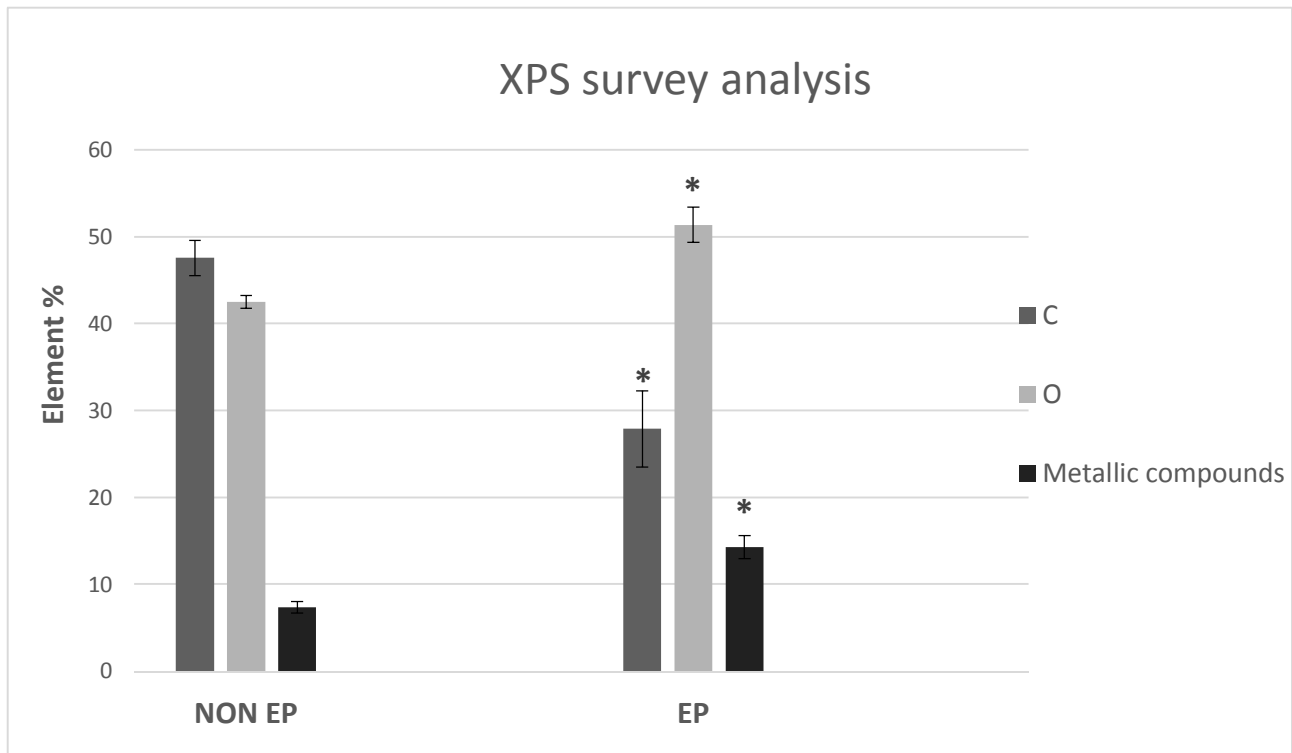
Figure 5.7: Survey analysis and comparison of the X-ray photoelectron spectroscopy results obtained on non-electropolished (non-EP) and electropolished (EP) samples of stainless steel AISI 316L, which was carried out on 3 samples per type and in 3 different points each, by using a Physical Electronics PHI 5600-ci spectroscope (standard aluminium X-ray source (1486.6 eV) at 300W). Results are reported as mean ± standard deviation. *= significant statistical difference with respect to the same elemental % of non-EP samples (p<0.001)

In light of these data, it is possible to state the successful obtainment, upon electropolishing, of a thick and homogeneous oxide layer at the surface, mainly composed by chromium, which was originally present in lower amount, in the thinner superficial oxide layer of non-EP material (typically 10-50 Å thick).[113] Moreover, as the metal oxide layer grows at surface, increasing the surface content of oxygen and metallic compounds, it screens the substrate of stainless steel from the XPS scanning (limited at 5 nm in depth), determining a decrease of the detected carbon fraction. These observations are consistent with other works that are present in literature.[43,123]

In conclusion, from the obtained data is it possible to confirm the success of the electropolishing process, with high reproducibility of results.

5.2. Development and characterization of polydopamine coatings and of polydopamine coatings functionalized with glutaric anhydride

Once verified the goodness of the electropolishing process, EP samples were treated to obtain a superficial polydopamine coating (PDA) that was further functionalized by reaction with glutaric anhydride (GLU), according to the strategies described in Chapter 3. Since the final goal of this work is the development of novel surface coatings to be employed as surface-mediated gene delivery platforms for cardiovascular stent applications, the developed surface treatments were thoroughly characterized in terms of biological, morphological and physicochemical properties. Moreover, their ability to stably immobilize on the surface amine-bearing sub-micrometric particles (modelling gene delivery particles) was investigated with either static and dynamic stability tests. Finally, preliminary surface-mediated transfection tests were performed using bPEI-based polyplexes immobilized on the developed surfaces.

5.2.1. Atomic force microscopy

Atomic force microscopy (AFM) was performed for evaluating the morphological changes obtained after superficial modification of EP samples, through PDA coating and PDA further functionalization with glutaric anhydride (GLU). In Figure 5.8 and Figure 5.9 it is possible to appreciate the appearance of protrusions (white spots) on the PDA and GLU surfaces, which were not present on EP samples (Figure 5.2). Even if the nature of these protrusions is still not clear, their formation is a preliminary evidence of successful surface modifications, as they have already been reported for PDA coatings in different works present in literature.[104,109]
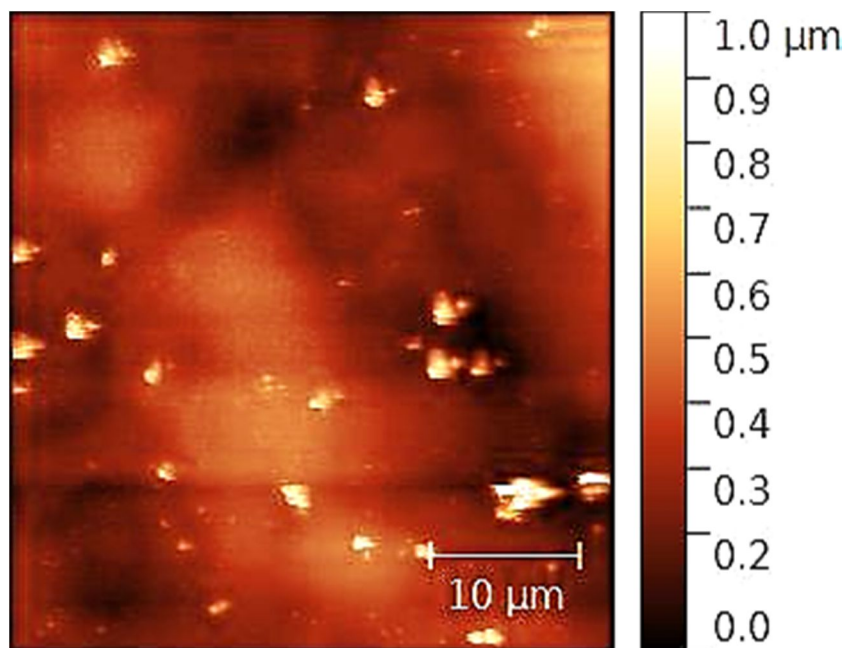
Figure 5.8: Superficial atomic force microscopy image of a polydopamine-coated sample (PDA). It was obtained by using an atomic force microscope (Veeco Dimension TM3100) in tapping mode, with an etched silicon tip. Areas of 40x40µm² were analysed with Nanoscope Analysis v1.5.

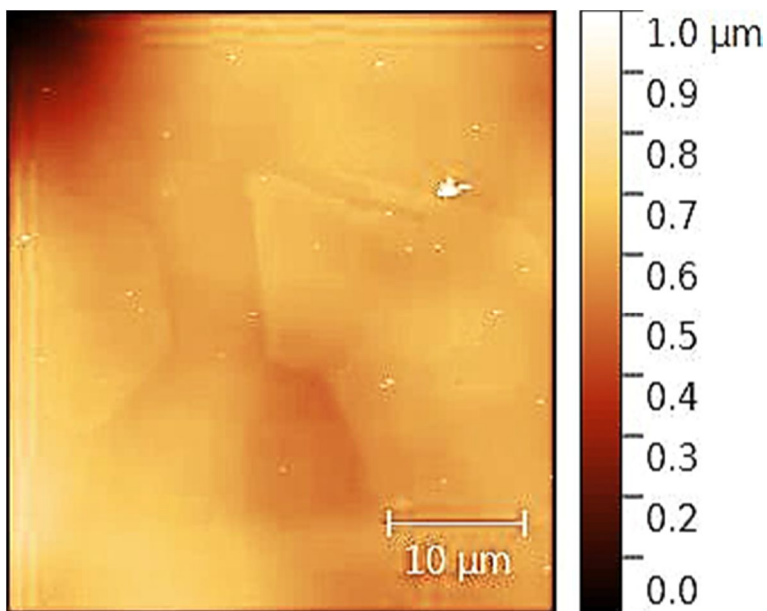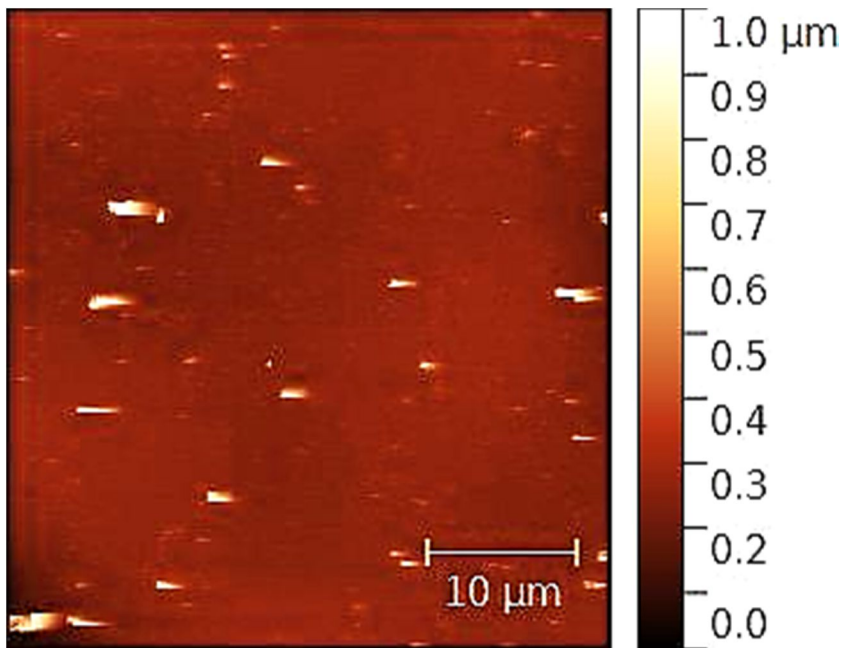*Figure 5.9: Superficial atomic force microscopy image of a polydopamine-coated sample (PDA) functionalized with glutaric anhydride (GLU). It was obtained by using an atomic force microscope (Veeco Dimension TM3100) in tapping mode, with an etched silicon tip. Areas of $40x40\mu m^2$ were analysed with Nanoscope Analysis v1.5.*

5.2.1.1. Roughness evaluation

After AFM imaging, pictures were analysed with WSXM 5.0 software, to obtain detailed data concerning topology and roughness of the surfaces. In Figure 5.10, the comparison of the RMS roughness mong electropolished (EP), polydopamine-coated (PDA) and PDA-functionalized with glutaric anhydride (GLU) samples is reported.

As expected, due to the formation of small protrusions at surface after superficial modifications, RMS measurement slightly increases after PDA coating and abruptly after GLU functionalization. These data support the speculation done on the basis of the qualitative analysis of AFM images. It is worth to note that, even if roughness increases in GLU samples, it is still importantly lower compared to non-EP samples.
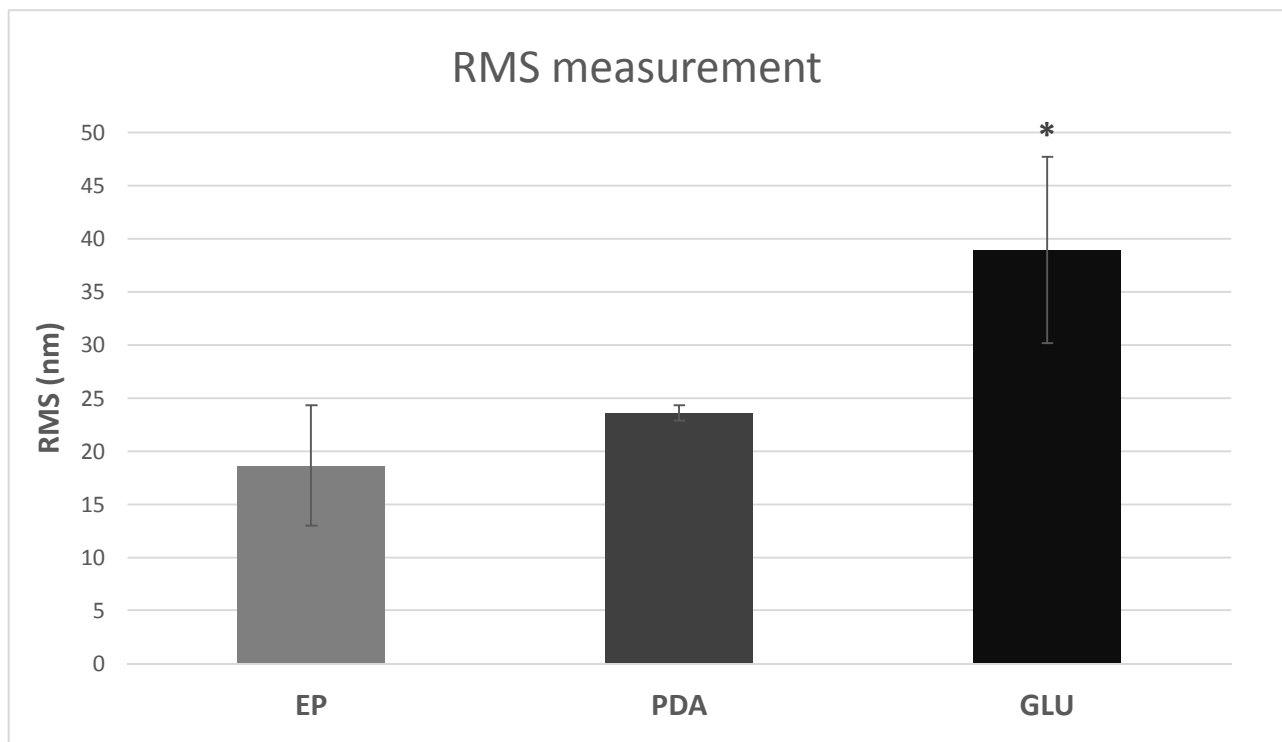
Figure 5.10: Evaluation and comparison of the superficial root mean squared (RMS) roughness measured on electropolished (EP), polydopamine-coated (PDA) and PDA-functionalized with glutaric anhydride (GLU) samples. The analysis was performed on 4 samples per type and in 3 different points each, in order to evaluate reproducibility. Results are reported as mean ± standard deviation. *= significant statistical difference with respect to non-EP samples (p<0.05)

5.2.2. Scanning electron microscopy

Scanning electron microscopy was performed to obtain detailed pictures of the superficial morphology of PDA and GLU samples. In both cases (Figure 5.11 and Figure 5.12, respectively), it is still possible to observe the grain boundaries texture typical of EP surfaces, indicating that thin coatings were obtained and that they did not excessively altered surface morphology. In fact, as reported in literature,[106] PDA treatment typically provides 50 nm thick coatings. In addition, only in the case of GLU there is the appearance of white spots, already observed in AFM images, whose nature is still not certain.

.
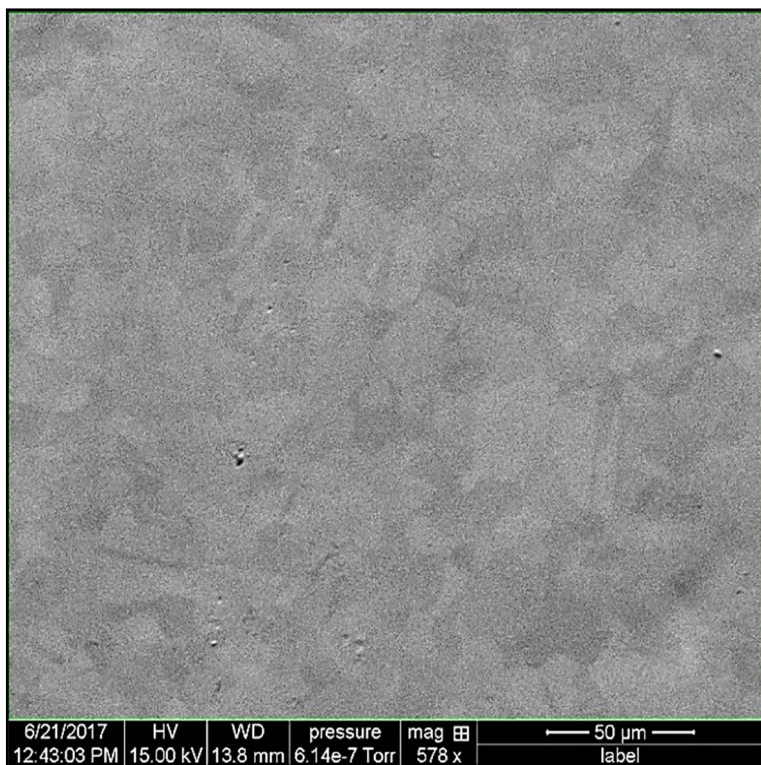
Figure 5.11: Scanning electron microscopy image of a polydopamine-coated sample (PDA), obtained with a FEI Quanta 250 microscope operating in low-vacuum modality
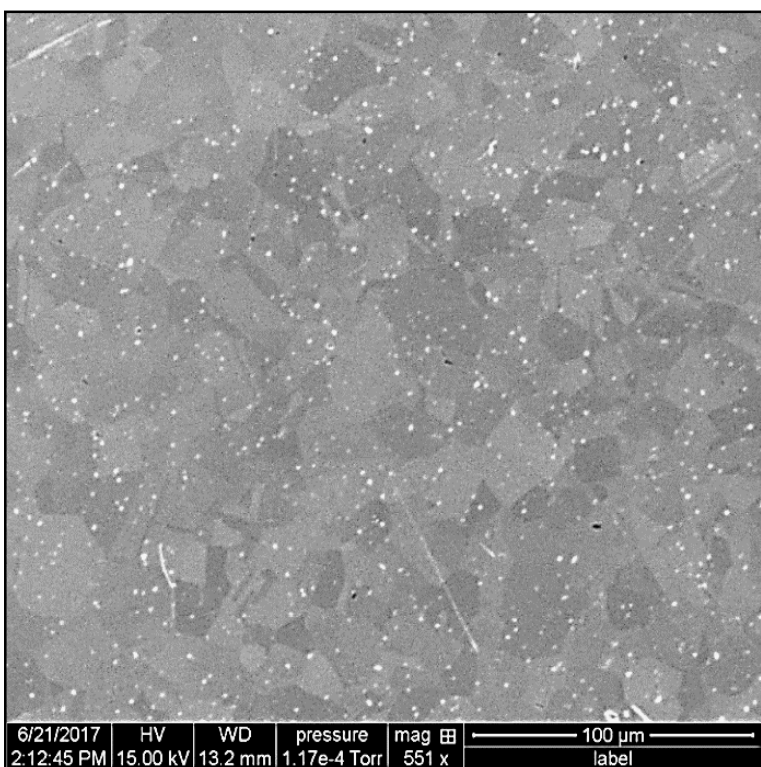
Figure 5.12: Scanning electron microscopy image of a polydopamine-coated sample (PDA) functionalized with glutaric anhydride (GLU), obtained with a FEI Quanta 250 microscope operating in low-vacuum modality.

5.2.3. Contact angle

Contact angle assay was performed in order to obtain information regarding the hydrophilicity of treated surfaces. In Figure 5.13, the comparison of contact angle measurements between EP, PDA and GLU surfaces is reported. A moderate but significant decrease in contact angle and so an increase in hydrophilicity, was observed for PDA and GLU surfaces with respect to EP samples, as expected due to the enrichment of hydrophilic groups on the surface, such as $NH3^+$ and COO^-. No significant difference could be instead observed between PDA and GLU ($p > 0.05$).
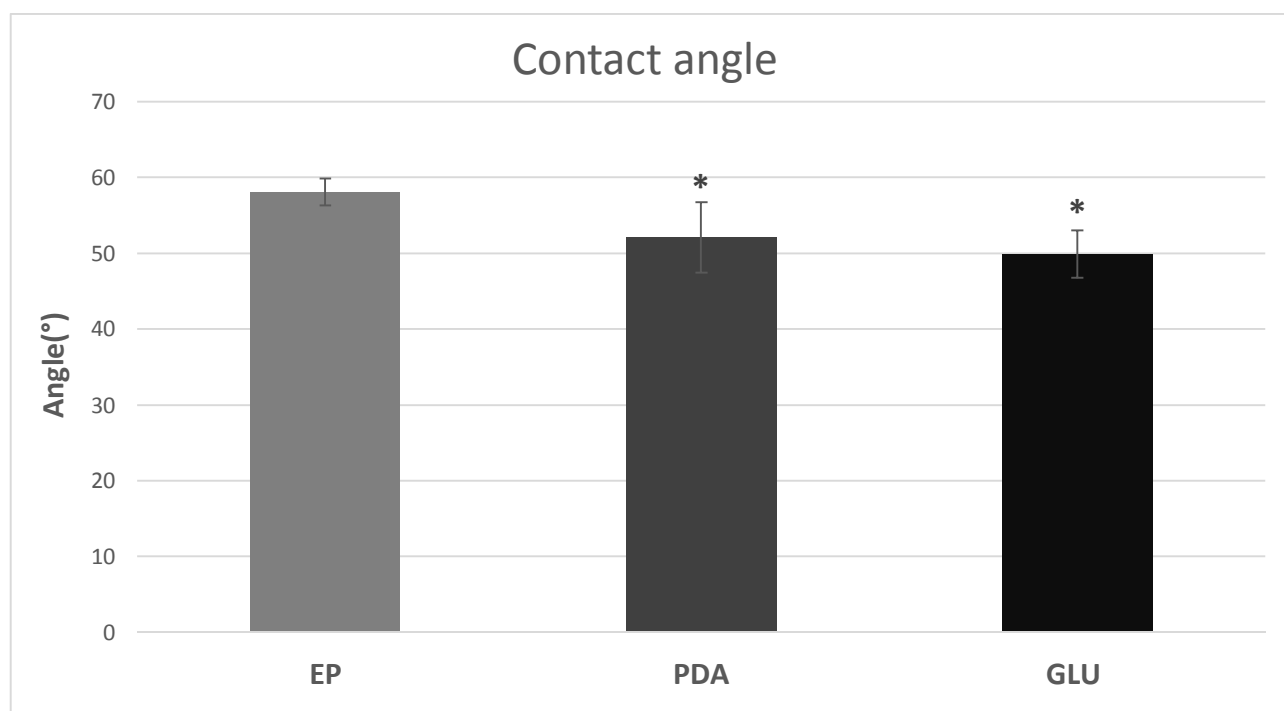
Figure 5.13: Evaluation and comparison of the superficial contact angle measurements performed on electropolished (EP), polydopamine-coated (PDA) and PDA-functionalized with glutaric anhydride (GLU) samples. Measurements were obtained by using a video contact angle system (VCA 2500 XE), and the analysis was carried out on 4 samples per type, by depositing 1μL droplets of ddH$_2$O in 3 different points each, at room temperature. Results are reported as mean ± standard deviation. *= significant statistical difference with respect to EP samples (p<0.001).

5.2.4. Fourier Transform Infrared Spectroscopy

Fourier transform infrared (FTIR) spectra of EP, PDA and GLU surfaces were recorded using Attenuated Total Reflectance (ATR) mode in FTIR (Agilent Cary 660 FTIR, Agilent technologies, Australia), equipped with a deuterated L-alanine-doped triglycine sulfate (DLa-TGS) detector and a Ge-coated KBr beam splitter. Figure 5.14 shows the overlay of the three FTIR spectra, from which it emerges that, as confirmed by other literature works,[124–127] new bands appear after surface modification by PDA coatings of EP samples at 1210 cm^{-1}, 1620 cm^{-1}, 3100 cm^{-1} and 3400 cm^{-1}. Nevertheless, since the FTIR penetration analysis (~1μm) is much higher than the PDA coating thickness (~50 nm), the differences are limited and difficult to appreciate since great part of

the signal/noise was due to the stainless-steel substrate. Some examples of possible changes in the absorbance spectra can be observed within 1200-1500 cm^{-1} (C-C, C-O, C-N region), at 1510 cm^{-1} (N-H shearing vibration), 1539 cm^{-1} (N-H bending) 1611 cm^{-1} (C=C stretching of an aromatic amine), 1662 cm^{-1} (C=O stretching) and within 3100-3600 cm^{-1} (N-H or O-H stretching vibration) The same observations are valid for the GLU surfaces where the grafting of a linker of 3 carbons length and a terminal carboxyl group should be only few Å thicker than in PDA. Consequently, GLU spectra closely resemble the PDA ones, without allowing to clearly observe the appearance of new bands with respect to PDA.
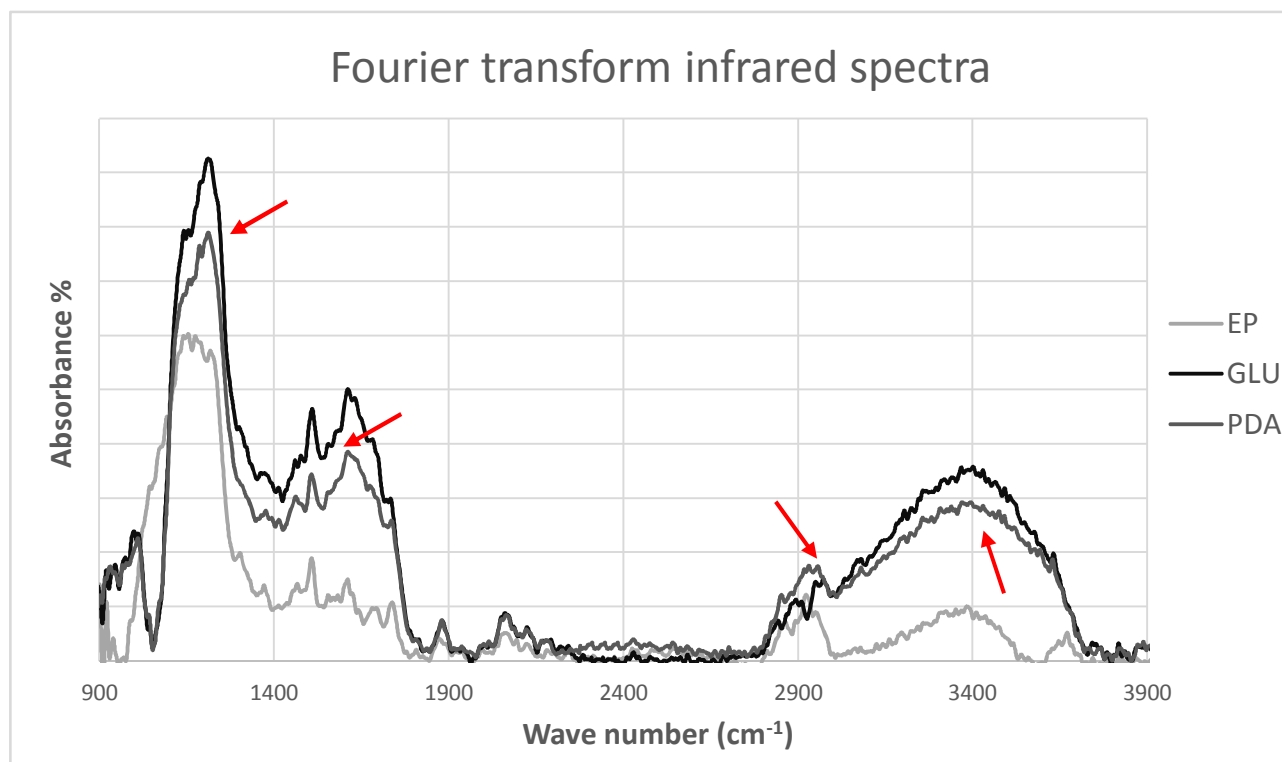
Figure 5.14:FTIR overlay spectra, recorded on electropolished (EP), polydopamine-coated (PDA) and PDA-functionalized with glutaric anhydride (GLU) samples, using Transform Infrared Spectroscopy (Agilent Cary 660 FTIR, Agilent technologies, Australia). The assay was carried out on 3 samples per type and in 3 different points each.

5.2.5. X-ray photoelectron spectroscopy

X-ray photoelectron spectroscopy (XPS) was performed in order to characterize PDA and GLU surfaces in terms of elemental composition. As reported in Figure 5.15, PDA and GLU coatings provided an increase in carbon and nitrogen contents as suggested by the chemical organic nature of the PDA coating, while decreasing the ones of oxygen and metallic compounds due to the deposition of an about 50 nm thick layer of polydopamine at surface, which screens the stainless-steel substrate from the XPS survey (maximum depth of analysis = 5 nm). Even though the treatment with glutaric anhydride is supposed to enrich the surface with COOH groups, no significant difference between PDA and GLU could be observed.
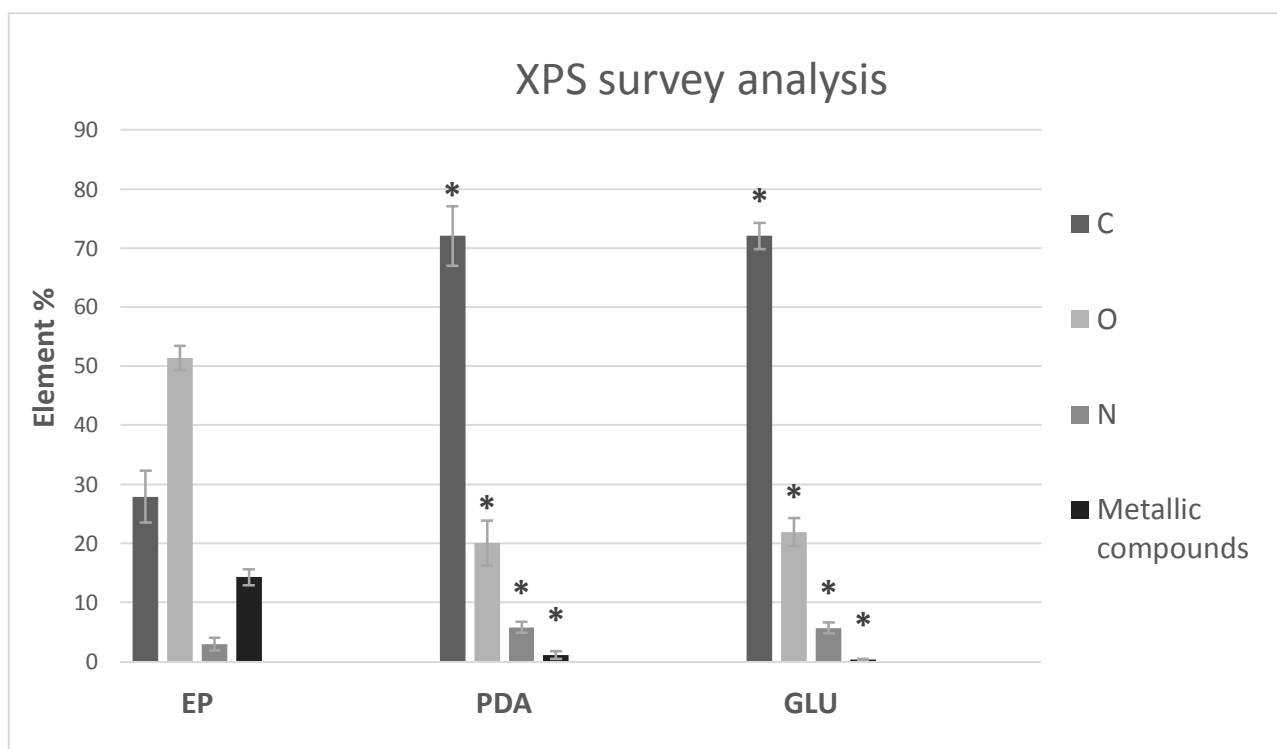
*Figure 5.15: Survey analysis and comparison of the X-ray photoelectron spectroscopy results obtained on electropolished (EP), polydopamine-coated (PDA) and PDA-functionalized with glutaric anhydride (GLU) samples. It was carried out on 3 samples per type and in 3 different points each, by using a Physical Electronics PHI 5600-ci spectroscope (standard aluminium X-ray source (1486.6 eV) at 300W). Results are reported as mean ± standard deviation. *= significant statistical difference with respect to the same elemental % of EP samples (p<0.001).*

5.2.5.1. Evaluation of the quantity of primary amines on the surface through chemical derivatization

Chemical derivatization with vapours of 4-(Trifluoromethyl) benzaldehyde was used for the evaluation of the presence of superficial primary amines on PDA and GLU surfaces. In this assay, primary amines specifically reacted with aldehyde derivatives containing fluorine, which allowed to indirectly quantify their amount. In Figure 5.16 the comparison between the two typologies of samples is reported. As expected, an important amount of primary amines (fluorine content after chemical derivatization) is observed on PDA samples while fluorine content (F1s %) was almost completely nullified upon PDA functionalization with GLU, demonstrating that glutaric anhydride reacts with all the primary amines available at the surface.
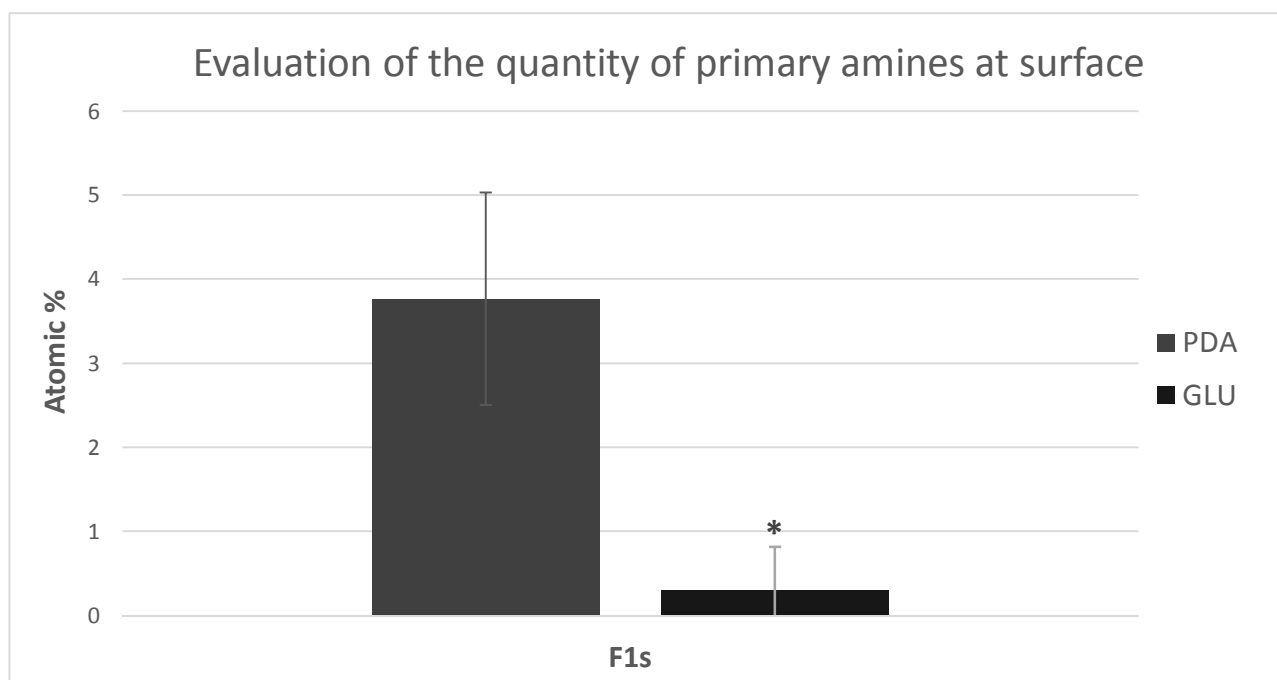
Figure 5.16: Analysis and comparison of the amine derivatization obtained through X-ray photoelectron spectroscopy on polydopamine-coated (PDA) and PDA functionalized with glutaric anhydride (GLU) samples. After functionalization of the surfaces with vapours of 4-(Trifluoromethyl) benzaldehyde (2h at r.t.), which is a compound able to react only with primary amine groups present at surfaceXPS analyses were performed on 3 samples per type and in 3 different points each. Results are reported as mean ± standard deviation. *= significant statistical difference with respect to PDA samples (p<0.001).

5.2.6. Quantification of charged groups at the surface by colorimetric assays

A. ORANGE II: superficial amine groups quantification

Orange II sodium salt, which is an orange dye that interacts electrostatically with positively charged groups, was employed for the detection of protonated primary amines at surface, in acidic solution. In table 5.1 the quantification of positively charged groups on the surface of EP and PDA samples, normalized over the surface area, is reported. A great increase of positive groups/nm^2 after PDA coating can be clearly observed.

SAMPLES	EP	PDA
[positively charged groups] (Molecules/nm^2)	1.27 ± 0.40	14.81 ± 1.08

Table 5.1: Orange II assay for the quantification of positively charged groups on electropolished (EP) and polydopamine-coated (PDA) surfaces. Results are reported as mean ± standard deviation. N= 8 tested samples per type

B. TBO: superficial negatively charged groups quantification

Toluidine Blue O (TBO), which is a cationic compound that interacts electrostatically with negatively charged groups and can be easily detected by light absorption in the blue region, was used for the detection of superficial anionic molecules, in alkaline conditions.

Table 5.2 shows that the concentration of negatively charged molecules such as deprotonated carboxylic groups (COO^-), strongly increases on GLU samples reaching average values of about 15 negative groups/nm^2, even if with a non-negligible variability (standard deviation higher than 3 negative groups/nm^2) This result confirmed the introduction of carboxylic acids expected by the GLU treatment. Interestingly, an increase in negative groups was also observed when the simple PDA coating was performed, with respect to EP samples, indicating that negatively charged groups could be present in the complex structure of polydopamine.

SAMPLES	EP	PDA	GLU
[negatively charged groups] (Molecules/nm^2)	0.31 ± 1.59	5.01 ± 2.31	14.62 ± 3.04

Table 5.2: TBO assay for the quantification of anionic groups at electropolished (EP), polydopamine-coated (PDA) and PDA functionalized with glutaric anhydride (GLU) surfaces. Results are reported as mean ± standard deviation. N= 10 tested samples per type.

5.2.7. Cytotoxicity tests

For the biological analysis of the surfaces and to evaluate the cytocompatibility of the developed coatings both direct and indirect cytotoxicity tests were performed using Alamar Blue viability assay (ThermoFisher Scientific, Hillsboro, USA) and according to the ISO 10993-5 standard, which describes the test methods to assess the *in vitro* cytotoxicity of medical devices. These methods evaluate the possible cytotoxicity of materials by the incubation of cultured cells in contact with a material or with extracts of the material itself. In particular, they are designed to determine the biological response of mammalian cells *in vitro* using appropriate biological parameters. Moreover, for each test, two different cell types were tested: HeLa and HUVECs. According to their stable growth and to their ability to be easily transfected, HeLa cells are commonly used in transfection systems development.[85] While, since HUVECs are the first cells that come in contact with stents devices, they provide a classic model cell system for biomaterial studies in cardiovascular field of applications.

Since poly-styrene (PS) cell culture plates reproduce the ideal conditions for cells adhesion and proliferation, they were considered as the positive viability controls and were compared with the developed surfaces in cytotoxicity assays.

5.2.7.1. Indirect cytotoxicity assay

The indirect assay allows to evaluate the possible release of cytotoxic compounds from a material through the evaluation of the viability of cells, cultured in a culture medium (Complete DMEM HeLa or Complete DMEM HUVECs) conditioned by the material. In this case, viabilities of HeLa and HUVECs were tested upon incubation with material extracts obtained from EP, PDA and GLU surfaces (24 h of extraction time).

A. HeLa cells

Figure 5.17 shows the results of the indirect cytotoxicity test obtained for HeLa cells. From the analysis it was evident that extracts from EP, PDA and GLU samples did not affect the cellular viability, which was in fact comparable to the one obtained using non-conditioned culture medium (CTRL). Hence, as expected, no cytotoxic compound is released from the developed materials.
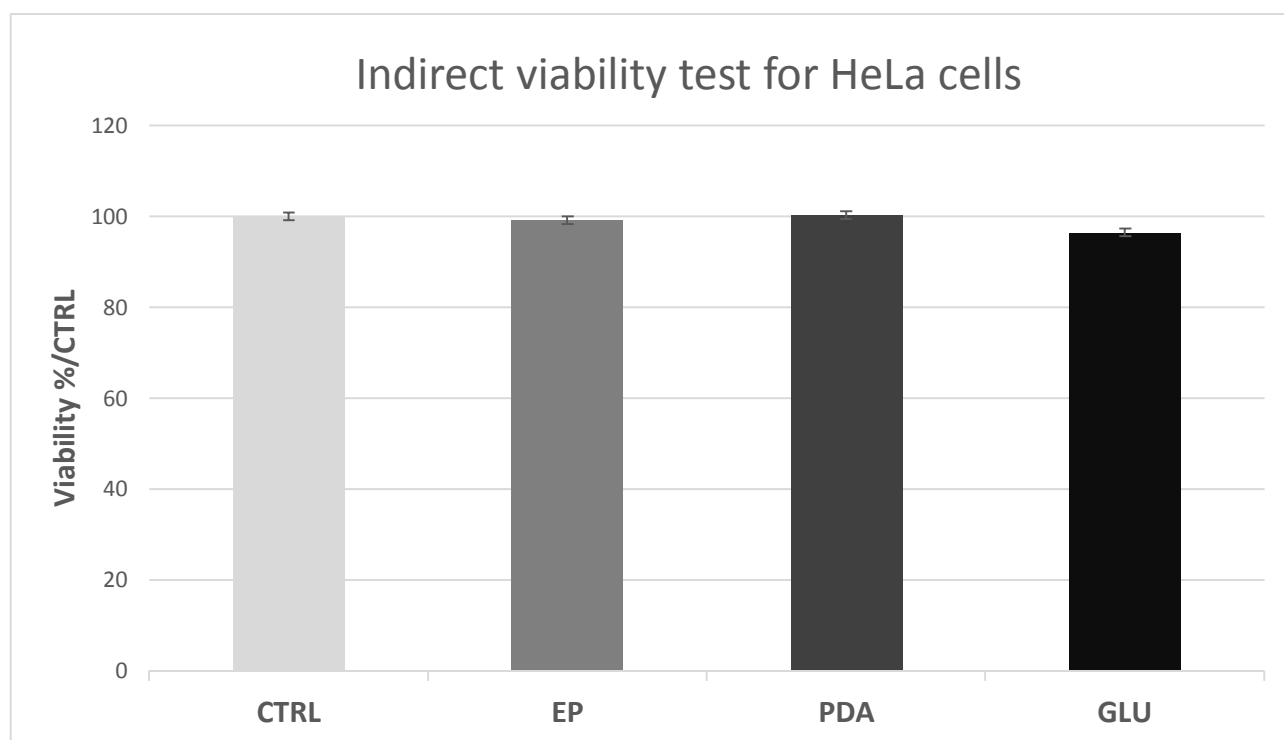
Figure 5.17: Indirect cytotoxicity test performed on electropolished (EP), polydopamine-coated (PDA) and PDA functionalized with glutaric anhydride (GLU) samples. HeLa cells were cultured with material extracts and non-conditioned fresh cell culture medium was considered as positive viability control (CTRL). The assay was performed on 4 samples per type, analyzing 3*100 μL aliquotes each. Results are reported as mean ± standard deviation.

B. Endothelial cells (HUVECs)

Figure 5.18 shows the results of the indirect cytotoxicity test obtained for HUVECs. From the analysis it was evident that, similarly to HeLa cells, extracts from EP, PDA and GLU samples did not affect the cellular viability, which was in fact comparable to the one of CTRL wells. These results, obtained on the more sensitive HUVEC primary vascular cells confirm that not cytotoxic compound is released from the developed materials, making them promising candidates for cardiovascular stent applications.
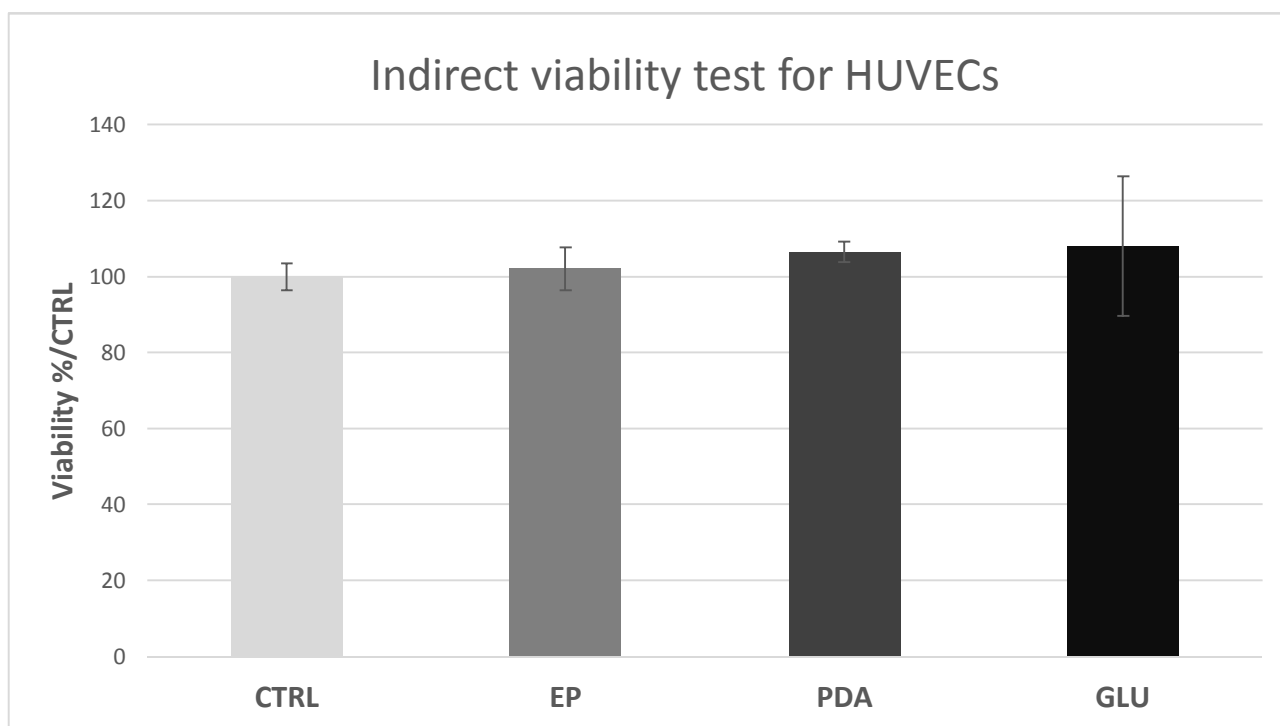
Figure 5.18: Indirect cytotoxicity test performed on electropolished (EP), polydopamine-coated (PDA) and PDA functionalized with glutaric anhydride (GLU) samples. HUVECs were cultured with material extracts and non-conditioned fresh cell culture medium was considered as positive viability control. The assay was performed on 4 samples per type, analyzing 3*100 µL aliquotes. Results are reported as mean ± standard deviation. each.

5.2.7.2 Direct cytotoxicity assay: cell adhesion and proliferation on material surface

The direct cytotoxicity assay allows to determine both cell adhesion and proliferation on material surfaces. Cell adhesion and proliferation of HeLa and HUVECs were tested by directly seeding cells on the material surface and evaluating viability after 24h and 72h of incubation by Alamar Blue assay.

A. HeLa cells

Figure 5.19 shows the results of the direct cytotoxicity test obtained for HeLa cells cultured onto different surfaces, up to 3 days of incubation. EP, PDA and GLU treatments affected the overall cellular viability if compared with cell culture wells, considered as positive CTRL. Nevertheless, it is worth to note that cell culture surfaces are optimized for cell adhesion and proliferation and no difference in viability could be observed between the developed surface treatments and electropolished stainless steel that is the most commonly employed biomaterial in stent applications.
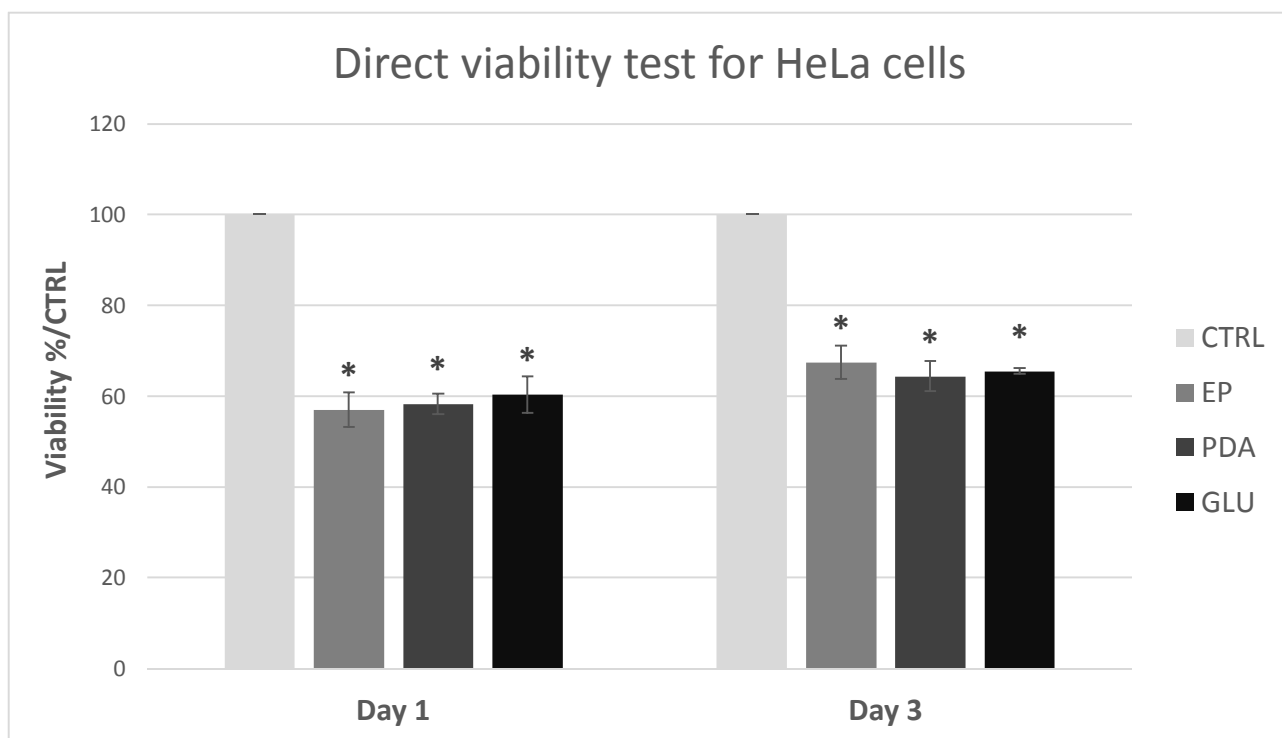
Figure 5.19: Direct cytotoxiciity test performed on electropolished (EP), polydopamine-coated (PDA) and PDA functionalized with glutaric anhydride (GLU) samples. HeLa cells were seeded on the samples and the cell culture plate was considered as positive control (CTRL). The assay was performed on 4 samples per type, analyzing 3*100 μL aliquotes each. * = significant statistical difference with respect to CTRL (p<0.01). Results are reported as mean ± standard deviation.

B. Endothelial cells (HUVECs)

Figure 5.20 shows the results of the direct cytotoxicity test obtained for HUVECs cultured onto different surfaces, up to 3 days of incubation. PDA and GLU treatments affected the overall cellular viability if compared to the CTRL. Nevertheless, these data are promising if compared to the electropolished stainless steel. In fact, EP samples showed a viability of about 30 and 20% after 1 and 3 days of culture respectively; while, values higher than 50% were observed for PDA and GLU surfaces, even if the difference was not statistically significant, due to a high variability of the obtained results. These results, together with those obtained for HeLa cells, suggest that the developed materials are not cytotoxic and could potentially even

improve cell adhesion and proliferation of vascular cells, with respect to EP, the most commonly used material in cardiovascular stent applications.
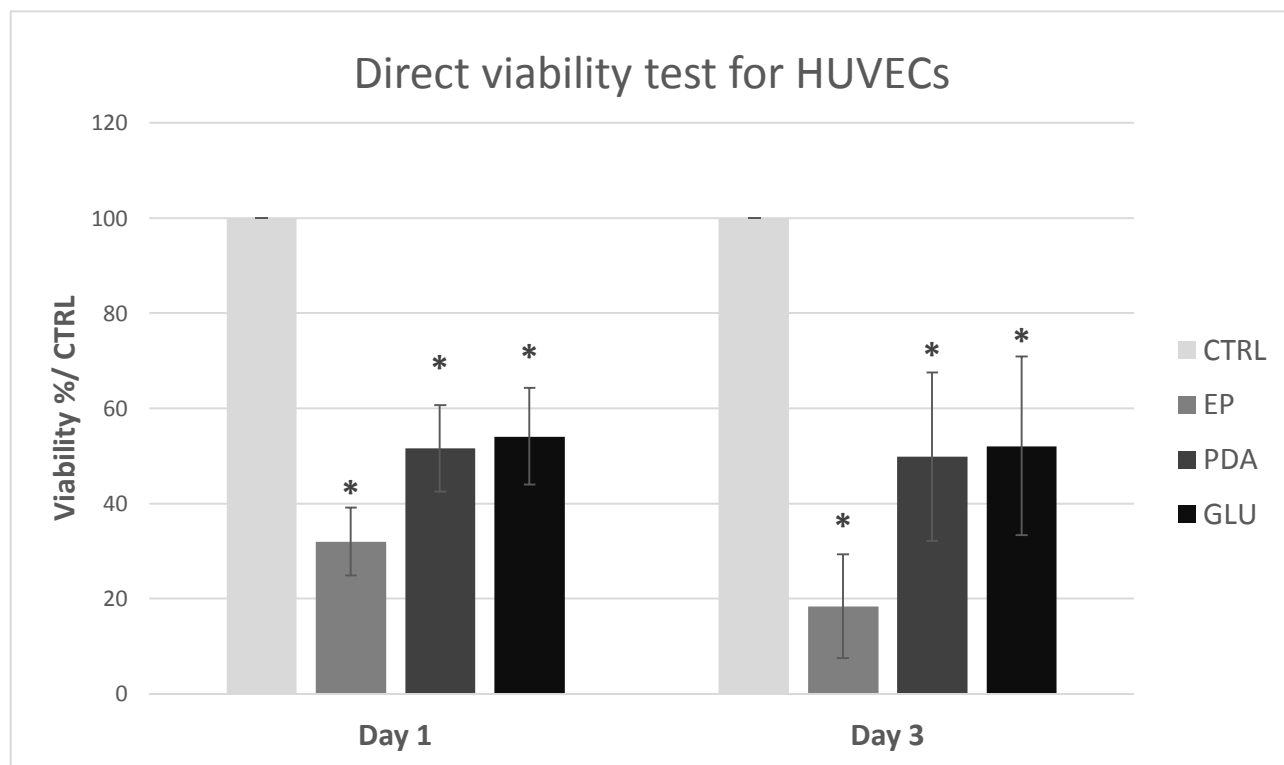
Figure 5.20: Direct cytotoxicity test performed on electropolished (EP), polydopamine-coated (PDA) and PDA functionalized with glutaric anhydride (GLU) samples. HUVECs were seeded on the samples and the cell culture plate was considered as positive control (CTRL).
The assay was performed on 4 samples per type, analyzing 3*100 μL aliquotes each. * = significant statistical difference with respect to CTRL (p<0.01). Results are reported as mean ± standard deviation.

5.3. Deposition and analysis of the stability of amine-bearing sub-micrometric particles

In order to simulate the interaction between the treated surfaces and gene delivery particles, in particular cationic polymer/nucleic acid complexes (polyplexes), usually consisting of positively charged sub-micrometric particles exposing amines on the surface, amine-bearing sub-micrometric particles were used and deposited on the developed surfaces and subsequently quantified. Moreover, to evaluate the strength of the adhesion of particles on the surfaces, further stability tests were performed, firstly by simple washing in PBS and then under flow reproducing quasi-physiological shear stresses occurring *in vivo* in coronary arteries.

5.3.1. Particle deposition

For particle deposition, samples were placed in a 24-wells plate and incubated in 1 mL of microparticle solution (0.25 mg/mL) for 24 hours, which contained a number of microparticles sufficient to completely cover their surface.

After the incubation, samples were rapidly rinsed in double deionized water to remove the unbound particles, dried in heated vacuum chamber (40°C) for at least 10 minutes. In the following macroscopic representative

pictures (Figure 5.21), which were taken on dried samples, the effectiveness of the deposition is made clear by the orange coloration that appeared on the surfaces. On EP no macroscopic presence of particles could be easily observed. Oppositely, a pale orange colour, not homogeneously distributed, was observed on PDA surfaces demonstrating that the deposition was successfully obtained. Finally, the best results were clearly obtained on GLU samples, where the deposition provided a strong homogeneous covering on the whole surface.

A) **B)** **C)**

Figure 5.21: amine-bearing sub-micrometric particles deposited at (A) electropolished (EP), (B) polydopamine-coated (PDA) and (C) PDA functionalized with glutaric anhydride (GLU) surfaces

5.3.2. Washing stability test

After these macroscopic observations, further analyses were performed by visible light microscopy (10x magnification) before and after washing in PBS (Figures 5.22-5.27). Images were acquired with greyscale settings, and the black regions represent the areas covered by the particles.

For a preliminary analysis of the stability of the microparticles on the surface, samples were put under mechanical agitation (170 rpm, orbital shaking) in PBS and observed under a stereo microscope immediately after deposition and after 7 days of washing. Before imaging, samples were always rinsed in double deionized water and dried in heated vacuum chamber (40°C) for at least 10 minutes.
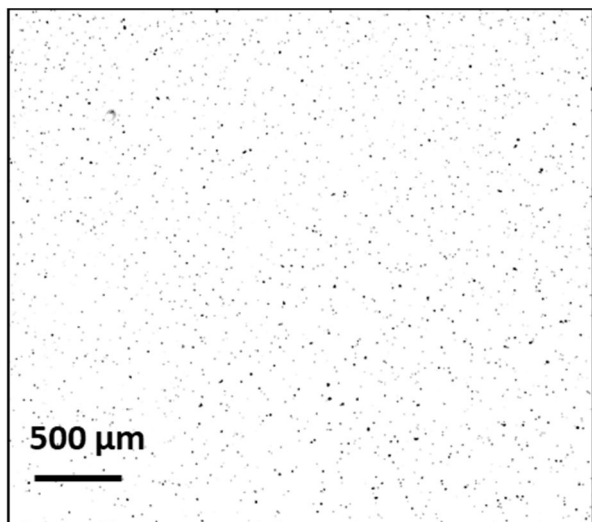
Figure 5.22: Optical image microscopy of the surface of an electropolished sample (EP), obtained with a stereo microscope (BX41M, Olympus, 10x magnification), immediately after deposition of amines functionalized sub-microparticles at surface.
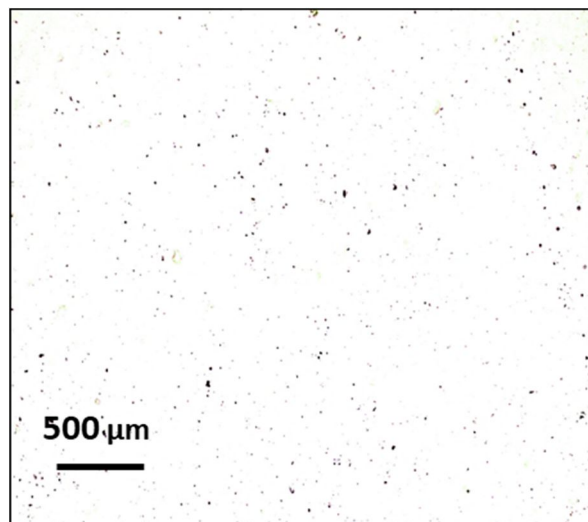
Figure 5.23: Optical image microscopy of the surface of an electropolished sample (EP), obtained with a stereo microscope (BX41M, Olympus, 10x magnification), after deposition of amines functionalized sub-microparticles at surface and 7 days of washing in PBS under mechanical agitation (170rpm).
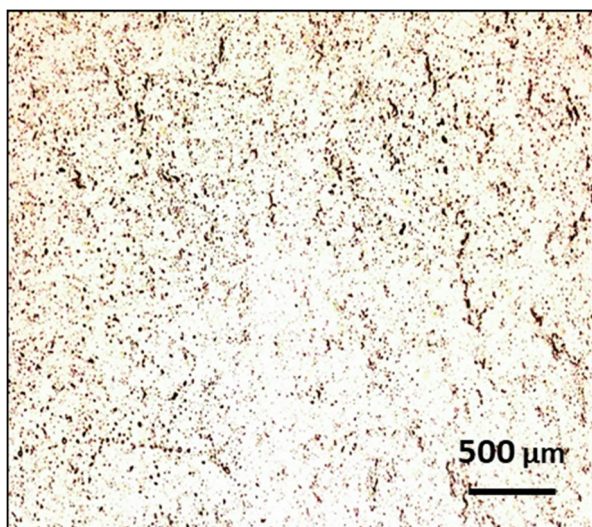
Figure 5.24: Optical image microscopy of the surface of a polydopamine-coated sample (PDA), obtained with a stereo microscope (BX41M, Olympus, 10x magnification), immediately after deposition of amines functionalized sub-microparticles at surface.
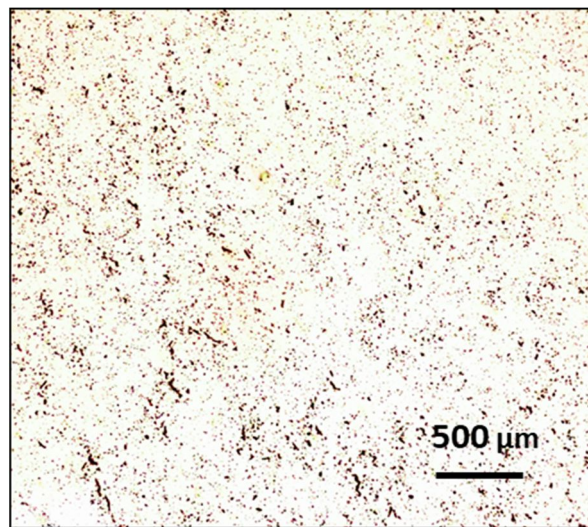
Figure 5.25: Optical image microscopy of the surface of a polydopamine-coated sample (PDA), obtained with a stereo microscope (BX41M, Olympus, 10x magnification), after deposition of amines functionalized sub-microparticles at surface and 7 days of washing in PBS under mechanical agitation (170rpm).
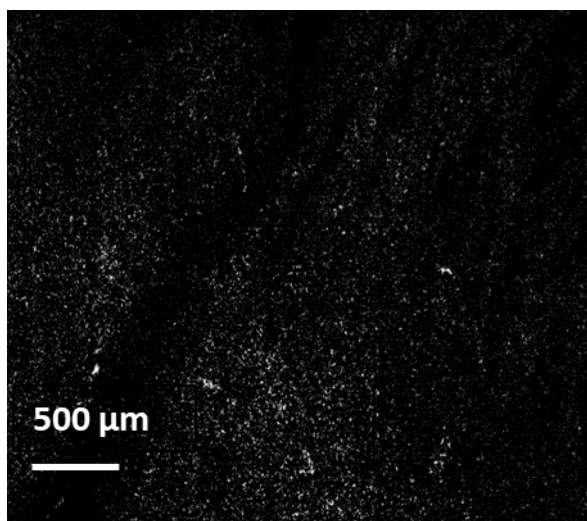
Figure 5.26: Optical image microscopy of the surface of a PDA-functionalized with glutaric anhydride sample (GLU), obtained with a stereo microscope (BX41M, Olympus, 10x magnification), immediately after deposition of amines functionalized sub-microparticles at surface.
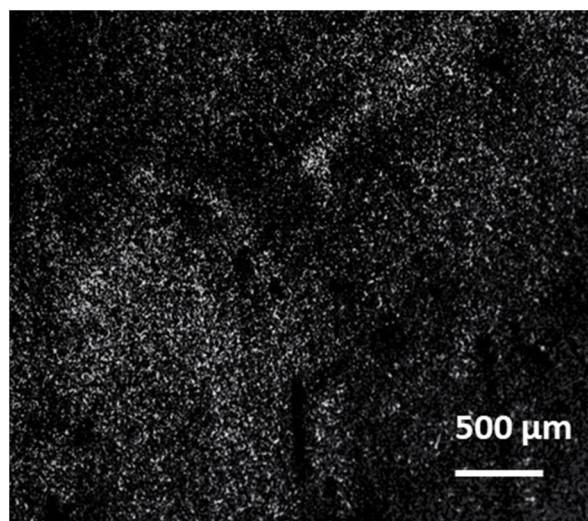
Figure 5.27: Optical image microscopy of the surface of a PDA-functionalized with glutaric anhydride sample (GLU), obtained with a stereo microscope (BX41M, Olympus, 10x magnification), after deposition of amines functionalized sub-microparticles at surface and 7 days of washing in PBS under mechanical agitation (170rpm).

The same images were analysed with ImageJ in order to quantify the amount of sub-micrometric particles effectively deposited at surface, and the stability upon washing in PBS under orbital mechanical agitation (170 rpm). The differences in particle deposition observed macroscopically were confirmed by microscopy and by the analysis of the percentage of surface area covered by particles (Figure 5.28). Immediately after the deposition it is possible to notice how on the EP samples particle attachment was fairly low (about 5% of the surface) while on PDA and even more on GLU, it was far more effective, reaching coverage values of about 20 and 80% respectively (on, $p<0.001$, EP vs. PDA, EP vs. GLU and PDA vs. GLU).

These results confirmed that the strategies designed for the immobilization of amine-bearing particles by PDA and GLU were successful. Particularly, GLU coating increased by four times the immobilization ability of PDA, suggesting that, in the developed coatings, exploiting the electrostatic interactions between the negatively charged coating and the protonated amine groups carried by the microparticles, is the optimal approach for particle deposition on the surface.

Furthermore, after 7 days of washing in PBS, the decrease of the covered area on both GLU and PDA was not statistically significant, highlighting the stability of both the binding strategies, while on the EP almost everything was released. It is worth to highlight that quite big standard deviations for the surface coverage were obtained, this was due to the non-perfect homogeneity of the deposition and to a not very high reproducibility of results in different samples for both the PDA and GLU coatings. Furthermore, it can be

speculated that the convexity of the metal samples, due to the punching procedure from the stainless-steel sheet, could influence the homogeneity of the deposition.

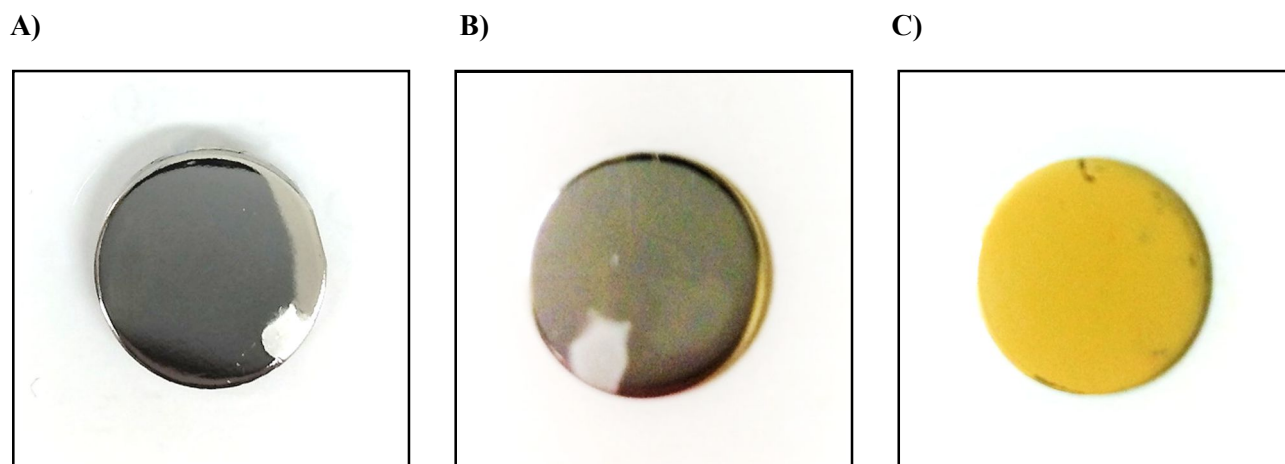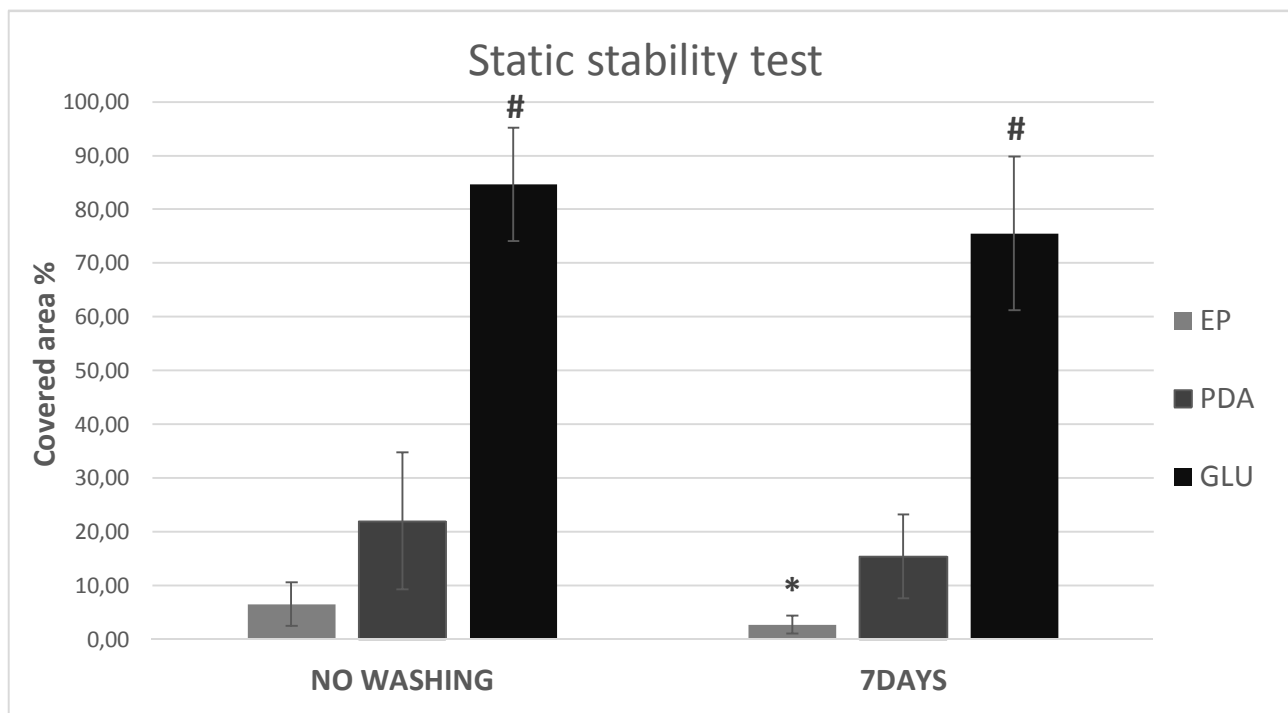*Figure 5.28: Evaluation of the surface coverage by amine-bearing sub-microparticles depositedon electropolished (EP), polydopamine-coated (PDA) and PDA functionalized with glutaric anhydride (GLU) surfaces, immediately after deposition and upon PBS washing for 7 days.. The test was performed on 10 samples per type and 6 images per sample were taken and analyzed by ImageJ software. Results are reported as mean ± standard deviation. *= significant statistical difference with respect to the covered area of the same typology of coating before washing (p<0.001). #= significant statistical difference with respect to the covered area obtained on PDA samples at the same time point (p<0.001).*

5.3.3. Dynamic stability test

In order evaluate the stability of the adhesion of the sub-micrometric particles on the surface of the developed materials in quasi-physiological flow conditions, a dynamic stability test was performed. For the deposition procedure, the same protocol, previously described, was followed. Then, samples were placed in flow chambers (N Ibidi sticky-Slide I Luer), in which thanks to a peristaltic pump, PBS was fluxed over the samples aiming to recreate shear stress conditions occurring in healthy human coronary arteries due to blood flow: laminar flow regime and shear wall stress τ= 15 dyne/cm^2= 1.5 Pa. Then, images of the sample surface were taken with a stereo microscope after 3 and 7 days of washing. Before imaging, samples were always rinsed by fluxing 70% pure ethanol for 3 minutes at the same flux conditions, and then dried in heated vacuum chamber (40°C) for 30 minutes.

After imaging, pictures were analysed with the software ImageJ, following the same protocol previously described for the static stability test. As shown in Figure 5.29, at day 3all the particles detached from the EP samples and almost nothing could be observed on them, oppositely, on both PDA and GLU coatings, the

decrease in area coverage was minimum, and no statistical difference was noticed with respect to day 0 (immediately after deposition). At day 7, although the decrease was low if compared with day 3, a statistical difference was noticed in comparison with the measurements obtained at day 0 for both PDA and GLU, with a total coverage decrease of 41 and 26 % respectively.
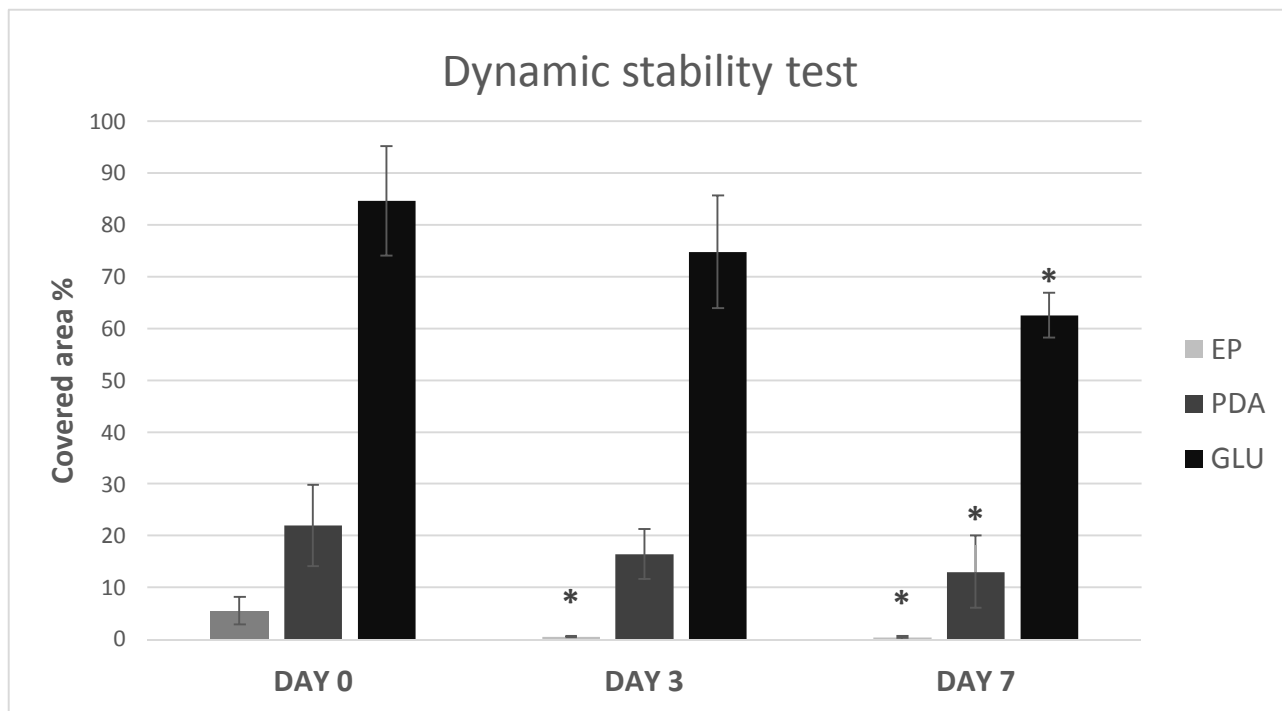
Figure 5.29: Evaluation of the stability of deposition of amines functionalized sub-microparticle at electropolished (EP), polydopamine-coated (PDA) and PDA functionalized with glutaric anhydride (GLU) surfaces, by dynamic flow tests. The covered area was evaliated at different time points. The test was performed on 4 samples per type and 6 images each sample were taken and analyzed by ImageJ software. Results are reported as mean ± standard deviation. *= significant statistical difference with respect to the covered area of the same typology of coating at day 0 (p<0.001)

In conclusion, through the analysis of the results obtained by the dynamic stability test, it is possible to state that the developed coatings allow the stable deposition of amine-bearing particles on stainless steel sample surfaces. The stability of the interaction (supposedly covalent for PDA and electrostatic for GLU) between particles and surfaces demonstrated under quasi-physiological flow conditions make the developed approaches promising for cardiovascular applications.

5.4. HeLa cells transfection

Once demonstrated that amine-bearing sub-micrometric particles can be stably deposited on the developed surface coatings, preliminary surface-mediated transfection experiments were performed. In this work, the pGLuc-Basic Vector was employed as reporter gene plasmid for expression in mammalian cells, because Gaussia Luciferase (GLuc) is a protein encoded by a "humanized" sequence that is easy to quantify by a simple luminescence assay and it contains a native signal peptide that allows it to be secreted from mammalian cells

into the cell culture medium. Moreover, since the activity of GLuc is high and very stable in the cell culture medium, the GLuc activity detected through the Luciferase assay reflects the amount of GLuc secreted by the transfected cells over a period of several days. Polyplexes prepared by mixing 250 kDa bPEI and pGLuc-Basic Vector at N/P=2.5 (plasmid concentration in solution = 0.02 μg/μL), were deposited on electropolished (EP) and treated (PDA and GLU) samples. The day after polyplex deposition samples were washed once in 10 mM Hepes ph7 (rapid dipping in solution) and then placed in a 24 well plate. Then 20000 HeLa cells/cm^2 were seeded directly on the samples, with the aim of evaluating their potential as gene delivery surfaces. In this concern, Luciferase expression was assessed 24h, 72h, 5 days and 7 days after transfection. Luciferase assay is commonly used in biological research as a tool to assess the transcriptional activity in cells that are transfected with a genetic construct containing the luciferase gene. Moreover, it is widely used because it is convenient, relatively inexpensive, and gives quantitative measurements instantaneously. For the detection, aliquots of the conditioned medium taken after 1, 3, 5 and 7 days of culture were mixed with the Luciferase substrate and the luminescence was immediately read at the spectrophotometer (λ=578 nm).

As reported in Figure 5.30, a luciferase signal was obtained in all the sample tested but at low levels (luciferase expression levels in classical transfections in solution with 250 kDa bPEI at N/P 2.5 are in the order of 10000 RLU) and stable in time. Luc expression was comparable among the three different surfaces. These results suggest that further optimization of the polyplex type and of the polyplex deposition is necessary to take advantage of the properties of the developed coatings for surface-mediated gene delivery.
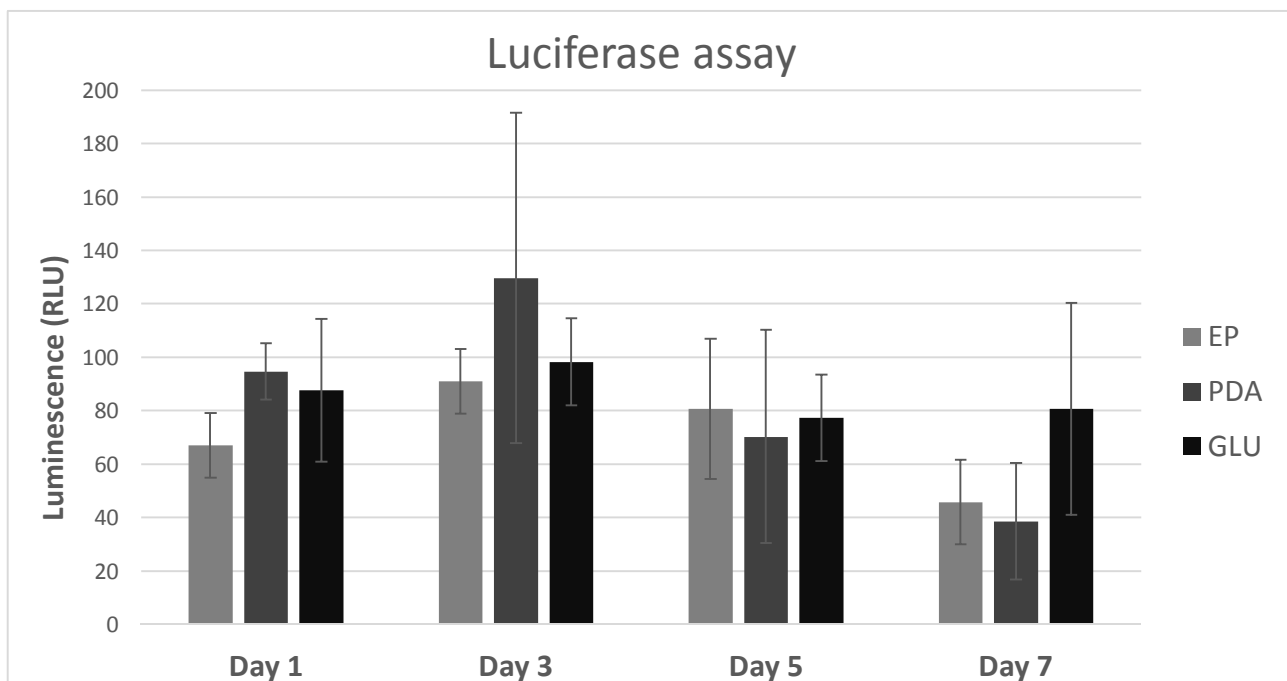
Figure 5.30: Luciferase expression assay carried out on electropolished (EP), polydopamine-coated (PDA) and PDA functionalized with glutaric anhydride (GLU) samples, after bPEI-based complexes deposition and HeLa cells seeding. The assay was carried ouy on 4 samples per type of coating. Results are reported as mean ± standard deviation.

However, it is worth to note that, according to the cytotoxicity test performed at 24h and 72 hours of culture (Figure 5.31) no sign of cytotoxicity can be observed due to the deposition of polyplexes on the surface.
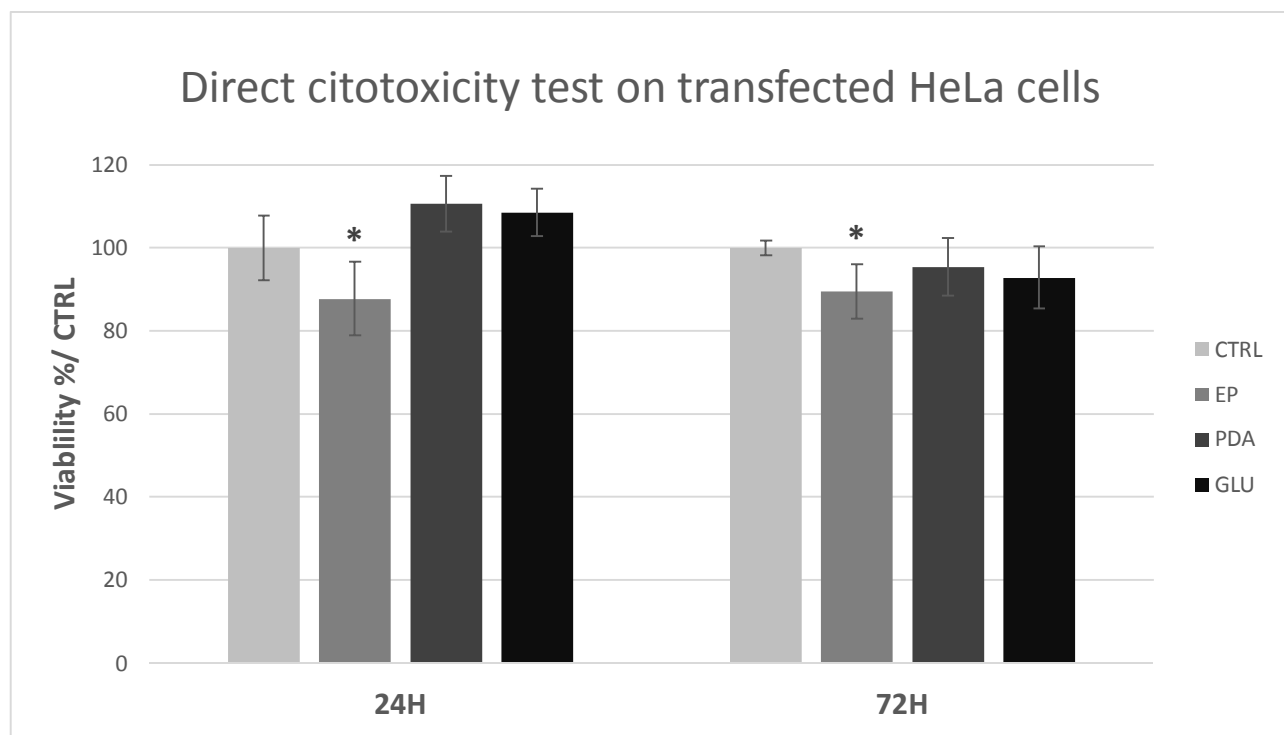
Figure 5.31: Direct viability test performed on electropolished (EP), polydopamine-coated (PDA) and PDA functionalized with glutaric anhydride (GLU) samples after deposition of 250 kDa bPEI/pGLuc N/P 2.5 polyplexes. HeLa were employed and samples without deposited polyplexes were considered as controls (CTRL). The assay was performed on 4 samples per type, analyzing 3*100 µL aliquotes each. Results are reported as mean ± standard deviation. * = significant statistical difference with respect to CTRL (p<0.01).

6. Conclusions and perspectives

Nowadays, percutaneous coronary interventions (PCIs) play an increasingly important role in the management of patients with coronary artery disease (CHD). More than one million procedures are in fact currently performed in the US each year, and this number continues to increase annually.[20] Among them, coronary stenting, angioplasty performed with either bare metal stents (BMS) or drug-eluting stents (DES), accounts for 70% of all PCIs.[128] Nevertheless, restenosis remains a major limitation to the long-term success of coronary angioplasty. In fact, although if compared to BMS, DES achieve better outcomes related to early and mid-term arterial patency, in many studies they have been linked to a higher rate of late stent thrombosis.[38] In this context, the demand for new strategies for the treatment of cardiovascular diseases is rapidly growing worldwide. Recently, gene-eluting stents (GES), have been proposed as a potential treatment strategy for the prevention of restenosis, in alternative to DES. Their innovative concept relies in the stent surface-mediated delivery of therapeutic nucleic acid-based drugs, which are nucleic acid sequences that, once internalized by cells, can provide benefits by either promoting the expression of therapeutic proteins or by blocking the expression of deleterious ones. Altogether the GES system is composed by a metallic stent, whose subsequent superficial functionalization must allow the entrapment of gene carriers on its surface. The major challenge toward the development of reliable functional GES is the realization of a stable, biocompatible and anti-thrombogenic biomaterials surfaces on which gene delivery vectors can be immobilized, in order to promote and sustain their activity on the surrounding cells after implantation (surface-mediated gene delivery). Nowadays, common superficial modifications involve the application of inorganic or organic coatings by, for example the layer-by-layer technique, and physico-chemical modifications often obtained through physical vapour deposition (PVD), chemical vapour deposition (CVD) or plasma treatments. In this context, the overall goal of this research is to develop surface coatings for metal substrates to directly anchor non-viral gene delivery particles on their surface and exert surface-mediated gene delivery. Stainless steel AISI 316L has been selected as starting material, since it is the most commonly used alloy for stents, and two different strategies were designed in parallel to modify the metal surface, exploiting the adhesive properties, the stability and the chemical reactivity of polydopamine (PDA) coatings. The first was based on a classic PDA coating, while the second envisaged the functionalization of the PDA coating with glutaric anhydride (GLU). The main hypothesis of this work is that PDA allows the immobilization of gene delivery non-viral particles (in particular cationic polymer-DNA complexes, polyplexes), that are usually characterized by free amine groups at surface and by a net positive charge, by the formation of strong covalent bonds with the reactive PDA coating and by electrostatic interaction with the GLU functionalized coating, enriched of negatively charged surface carboxylic groups.

The experimental work of this thesis was conducted at the Laboratoire de Biomatériaux et Bioingénierie (LBB, Québec, Canada), and its specific aims are divided in the following four different phases:

1) Obtainment of electropolished (EP) substrates, starting from stainless-steel AISI 316L;

2) Development and characterization of either polydopamine (PDA) coating and PDA-functionalized with GLU;

3) Deposition of amine-bearing sub-micrometric particles at both surfaces, for validating the hypothesis of either covalent binding or electrostatic interactions;

4) Preliminary transfection on HeLa cells, using bPEI-based polyplexes.

Concerning the first phase, aiming to obtain smooth metallic stainless-steel surfaces, free from imperfections and rich in oxides species, an EP process was performed, following a protocol previously developed at LBB. Atomic force microscopy (AFM) and scanning electron microscopy (SEM) confirmed the success of the process showing smooth surfaces and the appearance of grain boundaries. Moreover, a decrease in both the RMS roughness and contact angle values, highlighted the obtainment of smoother surfaces, more hydrophilic, and thus, well EP. Finally, X-ray photoelectron spectroscopy (XPS) analysis confirmed the obtainment of a thick and homogeneous oxide layer at surface due to the EP process, demonstrating an increase in oxygen and metallic compounds contents at the surface.

Concerning the second phase of this work, both PDA and GLU surfaces were analysed morphologically, physico-chemically and even biologically, according to the final aim of applying them as coatings for gene-eluting stent applications. From AFM imaging, it is possible to appreciate the appearance of protrusions (white spots) on the PDA and GLU surfaces, which were not present on EP samples; while, from SEM analysis, it is still possible to observe the grain boundaries texture typical of EP surfaces, indicating that thin coatings were obtained and that they did not excessively altered surface morphology. In addition, only in the case of GLU there is the appearance of white spots, which were already observed in AFM images. RMS analysis obtained from AFM images, showed a slight increase of values after PDA coating and an abrupt one after GLU functionalization. This is due to the formation of protrusions at surface after superficial modifications, and it is remarked by contact angle measurements, which moderately decrease for PDA and GLU surfaces with respect to EP samples, highlighting the superficial enrichment in hydrophilic compounds such as $NH3^+$ and COO^-. Colorimetry assays were performed in order to quantify the real amount of compounds deposited at surface, but no information about their chemical nature were provided. Thus, Fourier-transform infrared spectroscopy (FT-IR) and XPS were employed for obtaining information about the superficial elemental composition. Particularly, the former analysis showed the appearance of new bands, typical of PDA coatings; while, the latter recorded an increase in carbon and nitrogen contents, as suggested by the chemical organic nature of both coatings, and a decrease in the ones of oxygen and metallic compounds, which is a clear evidence of the fact that a thick layer (about 50 nm, according to literature records) of PDA was deposited at surface. Moreover, XPS analysis performed after chemical derivatization with vapours of 4-(Trifluoromethyl) benzaldehyde highlighted, as expected, an important amount of primary amines on PDA samples, which almost completely disappeared upon PDA functionalization with GLU. Finally, biocompatibility and cytotoxicity of both PDA and GLU were tested through direct and indirect viability tests, using HeLa and HUVEC cells. No differences were noticed between the two cell types, where both the treatments appeared non-cytotoxic and

showed promising results in terms of cell adhesion and proliferation, especially on endothelial cells, the cells that are in direct contact with stents. As future perspective, the same tests should be done at longer time points (7 and 14 days), and on other cellular lines, such as smooth muscle cells (SMCs), which are involved in the arterial restenosis processes. Particularly, the treatments should block their adhesion and proliferation, in order to reduce the occurrence of neointimal hyperplasia.

Once the surfaces were developed and fully characterized, amine-bearing sub-micrometric particles were deposited onto them, in order to simulate the interaction between the treated surfaces and polyplexes. As confirmed by visible light microscopy, good results were obtained in terms of attachment, particularly on GLU samples, where deposition was increased by about four times with respect to simple PDA coatings. Furthermore, on both PDA and GLU, high strength of adhesion was noticed after 7 days of testing in PBS under flow reproducing quasi-physiological shear stresses occurring *in vivo* in coronary arteries.

In light of these very promising results in terms of particle deposition and stability, the last phase of this work consisted in preliminary surface-mediated transfection experiments on HeLa cells, for which on polyplexes prepared by mixing 250 kDa bPEI and pGLuc-Basic Vector at N/P=2.5 were deposited on PDA and GLU surfaces. Luciferase assay was used to assess the transfection efficiency. Unexpectedly, from the analysis recorded at 24h, 72h, 5 days and 7 days after transfection, quite low signals were obtained in all the sample tested, without differences with respect to simple EP samples. These results, that are low if compared to the ones obtained in classical transfections in solution, suggest that further optimization of the polyplex type and of the polyplex deposition is necessary. In this work in fact, only preliminary tests were performed, employing only one type of cationic polymers as synthetic non-viral gene carriers and testing their efficiency only on one typology of cells. Supposing that bPEI is the best choice, as it is considered the gold standard cationic polymer for gene delivery applications, its characteristics should be modulated in order to achieve higher transfection efficiencies. For instance, future works will focus on testing bPEI at different molecular weights, and complexing DNA at different N/Ps. Moreover, stability tests on polyplexes immobilized at surface are ongoing, with the aim of confirming the promising results obtained with of sub-micrometric particles.

In conclusion, although further improvements are needed, in this work two superficial modifications, i.e. PDA and GLU, were developed and characterised showing promising results for their future application as surface mediated gene-delivery platforms. In fact, the protocols employed for the realization of the coatings allowed to obtain reproducible cytocompatible coatings, even if with some variability in their properties, capable to effectively immobilize positively charged amine-based submicrometric particles, mimicking polyplex particles. Nevertheless, the protocol developed for the DNA complexation and polyplexes deposition at surface, still needs to be modified in order to increase their surface-mediated transfection ability, with respect to the limited results obtained in the very first transfection experiments.

7. Bibliography

1. Bailey, R. Circulatory System. *biology.about.com*

2. SEER Training:Classification & Structure of Blood Vessels. Available at: https://training.seer.cancer.gov/anatomy/cardiovascular/blood/classification.html. (Accessed: 2nd August 2017)

3. Deng Q., Huo Y. & Luo J. Endothelial mechanosensors: the gatekeepers of vascular homeostasis and adaptation under mechanical stress. *Sci. China Life Sci.* **57,** 755–762 (2014).

4. TeachPE.com - Free Resource for Physical Education and Sports Coaching. Available at: http://www.teachpe.com/. (Accessed: 2nd August 2017)

5. Camaré C., Pucelle M., Nègre-Salvayre A. & Salvayre R. Angiogenesis in the atherosclerotic plaque. *Redox Biol.* **12,** 18–34 (2017).

6. TeachPE.com - Free Resource for Physical Education and Sports Coaching. Available at: http://www.teachpe.com/. (Accessed: 2nd August 2017)

7. WHO | Cardiovascular diseases (CVDs). *WHO* Available at: http://www.who.int/cardiovascular_diseases/en/.

8. Shanthi Mendis, Pekka Puska & Bo Norrving. *WHO | Global atlas on cardiovascular disease prevention and control*. (World Health Organization in collaboration with the World Heart Federation and the World Stroke Organization, 2011).

9. McGorrian C. *et al.* Estimating modifiable coronary heart disease risk in multiple regions of the world: the INTERHEART Modifiable Risk Score. *Eur. Heart J.* **32,** 581–589 (2011).

10. Yu Q., Shao H., He P. & Duan Z. World scientific collaboration in coronary heart disease research. *Int. J. Cardiol.* **167,** 631–639 (2013).

11. Wang E.Y., Dixson J., Schiller N. B. & Whooley M. A. Causes and Predictors of Death in Patients With Coronary Heart Disease (from the Heart and Soul Study). *Am. J. Cardiol.* **119,** 27–34 (2017).

12.   Ross R. Atherosclerosis — An Inflammatory Disease. *N. Engl. J. Med.* **340,** 115–126 (1999).

13.   Insull W. The Pathology of Atherosclerosis: Plaque Development and Plaque Responses to Medical Treatment. *Am. J. Med.* **122,** S3–S14 (2009).

14.   Falk E. Plaque rupture with severe pre-existing stenosis precipitating coronary thrombosis. Characteristics of coronary atherosclerotic plaques underlying fatal occlusive thrombi. *Heart* **50,** 127–134 (1983).

15.   Della Rocca D. G. & Pepine C. J. Endothelium as a Predictor of Adverse Outcomes. *Clin. Cardiol.* **33,** 730–732 (2010).

16.   W. T. Woods. Patent: APPARATUS AND METHOD FOR ANGIOPLASTY AND FOR PREVENTING RE-STENOSIS.

17.   Yin R.-X., Yang D.-Z. & Wu J.-Z. Nanoparticle Drug- and Gene-eluting Stents for the Prevention and Treatment of Coronary Restenosis. *Theranostics* **4,** 175–200 (2014).

18.   Abdul-Mohsen M. Medical angioplasty - Hope and expectations: An optimistic overview. *J. Fam. Community Med.* **18,** 101 (2011).

19.   Douce S. *et al.* Stent Placement to Prevent Restenosis After Angioplasty in Small Coronary Arteries. *Circulation* **104,** 2029–2033 (2001).

20.   Holmes D. R. *et al.* Restenosis after percutaneous transluminal coronary angioplasty (PTCA): A report from the PTCA registry of the national heart, lung, and blood institute. *Am. J. Cardiol.* **53,** C77–C81 (1984).

21.   Schwartz S. M. Perspectives series: cell adhesion in vascular biology. Smooth muscle migration in atherosclerosis and restenosis. *J. Clin. Invest.* **99,** 2814–2816 (1997).

22.   Orford J. L., Selwyn A. P., Ganz P., Popma J. J. & Rogers, C. The comparative pathobiology of atherosclerosis and restenosis. *Am. J. Cardiol.* **86,** 6H–11H (2000).

23.   Hannan E. L. *et al.* A comparison of short- and long-term outcomes for balloon angioplasty and coronary stent placement. *J. Am. Coll. Cardiol.* **36,** 395–403 (2000).

24.   Kastrati A. *et al.* Predictive Factors of Restenosis After Coronary Stent Placement. *J. Am. Coll. Cardiol.* **30,** 1428–1436 (1997).

25.   Simflex^TM CoCr Stent Delivery System.

26.   Serruys P. W. *et al.* A Comparison of Balloon-Expandable-Stent Implantation with Balloon Angioplasty in Patients with Coronary Artery Disease. *N. Engl. J. Med.* **331,** 489–495 (1994).

27.   Mattos M. A. *et al.* Vascular stents. *Curr. Probl. Surg.* **36,** 909–1053 (1999).

28.   Hao H. *et al.* Drug-Eluting Stent. *Circ. J.* **75,** 1548–1558 (2011).

29.   Zijpp Y. J. T., Van der Poot A. A. & Feijen J. Endothelialization of Small-Diameter Vascular Prostheses. *Arch. Physiol. Biochem.* **111,** 415–427 (2003).

30.   Mani G., Feldman M. D., Patel D. & Agrawal C. M. Coronary stents: A materials perspective. *Biomaterials* **28,** 1689–1710 (2007).

31.   Stainless Steel - AISI 316L Foil - online catalogue source - supplier of research materials in small quantities - Goodfellow. Available at: http://www.goodfellow.com/E/Stainless-Steel-AISI-316L-Foil.html. (Accessed: 3rd November 2017)

32.   Haudrechy P., Foussereau J., Mantout B. & Baroux B. Nickel release from 304 and 316 stainless steels in synthetic sweat. Comparison with nickel and nickel-plated metals. Consequences on allergic contact dermatitis. *Corros. Sci.* **35,** 329–336 (1993).

33.   Kastrati A., Schomig A., Dietz R., Neumann F.-J. & Richardt G. Time Course of Restenosis During the First Year After Emergency Coronary Stenting. *Circulation* **87,** 1498–1505 (1993).

34.   Lüscher T. F. *et al.* Drug-Eluting Stent and Coronary Thrombosis: Biological Mechanisms and Clinical Implications. *Circulation* **115,** 1051–1058 (2007).

35.   Stefanini G. G. & Holmes D. R. J. Drug-Eluting Coronary-Artery Stents. *N. Engl. J. Med.* **368,** 254–265 (2013).

36.   Dangas G. D. *et al.* In-Stent Restenosis in the Drug-Eluting Stent Era. *J. Am. Coll. Cardiol.* **56,** 1897–1907 (2010).

37.   Burke S. E., Kuntz R. E. & Schwartz L. B. Zotarolimus (ABT-578) eluting stents. *Adv. Drug Deliv. Rev.* **58,** 437–446 (2006).

38.   Bonello L. *et al.* Vascular Brachytherapy for Patients with Drug-Eluting Stent Restenosis. *J. Intervent. Cardiol.* **21,** 528–534 (2008).

39.   Fishbein I. *et al.* Endovascular Gene Delivery from a Stent Platform: Gene- Eluting Stents. *Angiol. Open Access* **1,** (2013).

40.   Ganly S. *et al.* Liposomal surface coatings of metal stents for efficient non-viral gene delivery to the injured vasculature. *J. Controlled Release* **167,** 109–119 (2013).

41.   Martinez A. W. & Chaikof E. L. Microfabrication and nanotechnology in stent design. *Wiley Interdiscip. Rev. Nanomed. Nanobiotechnol.* **3,** 256–268 (2011).

42.   Godin B. *et al.* Emerging applications of nanomedicine for the diagnosis and treatment of cardiovascular diseases. *Trends Pharmacol. Sci.* **31,** 199–205 (2010).

43.   Tepe G. *et al.* Reduced thrombogenicity of nitinol stents—In vitro evaluation of different surface modifications and coatings. *Biomaterials* **27,** 643–650 (2006).

44.   Haïdopoulos M., Turgeon S., Sarra-Bournet C., Laroche G. & Mantovani D. Development of an optimized electrochemical process for subsequent coating of 316 stainless steel for stent applications. *J. Mater. Sci. Mater. Med.* **17,** 647–657 (2006).

45.   Lekshmi K. M., Che H.-L., Cho C.-S. & Park I.-K. Drug- and Gene-eluting Stents for Preventing Coronary Restenosis. *Chonnam Med. J.* **53,** 14–27 (2017).

46.   Foldvari M. *et al.* Non-viral gene therapy: Gains and challenges of non-invasive administration methods. *J. Controlled Release* **240,** 165–190 (2016).

47.   Ibraheem D., Elaissari A. & Fessi H. Gene therapy and DNA delivery systems. *Int. J. Pharm.* **459,** 70–83 (2014).

48.   Gupt K., Singh S. & Garg K. N. Gene therapy in dentistry: Tool of genetic engineering. Revisited. *Arch. Oral Biol.* **60,** 439–446 (2015).

49. Su C.-H., Wu Y.-J., Wang H.-H. & Yeh H.-I. Nonviral gene therapy targeting cardiovascular system. *Am. J. Physiol. - Heart Circ. Physiol.* **303,** H629–H638 (2012).

50. Central Dogma Reversed. *Nature* **226,** 2261198a0 (1970).

51. Central dogma of molecular biology. *Wikipedia* (2017).

52. Fox S. W. Biological replication of macromolecules. *J. Chem. Educ.* **36,** A706 (1959).

53. Kilberg M. S., Hutson R. G. & Laine R. O. Amino acid-regulated gene expression in eukaryotic cells. *FASEB J.* **8,** 13–19 (1994).

54. Ylä-Herttuala S. & Baker A. H. Cardiovascular Gene Therapy: Past, Present, and Future. *Mol. Ther.* **25,** 1095–1106 (2017).

55. Isner J. M. *et al.* Clinical evidence of angiogenesis after arterial gene transfer of phVEGF165 in patient with ischaemic limb. *The Lancet* **348,** 370–374 (1996).

56. Adeel M. Y. & Sharif F. Advances in stent-mediated gene delivery. *Expert Opin. Drug Deliv.* **13,** 465–468 (2016).

57. Mason D., Chen Y.-Z., Krishnan H. V. & Sant S. Cardiac gene therapy: Recent advances and future directions. *J. Controlled Release* **215,** 101–111 (2015).

58. Manjila S. B. *et al.* Novel gene delivery systems. *Int. J. Pharm. Investig.* **3,** 1–7 (2013).

59. Pezzoli D., Chiesa R., De Nardo L. & Candiani G. We still have a long way to go to effectively deliver genes. *J Appl Biomater Funct Mater* **10,** 82–91 (2012).

60. Pezzoli D. & Candiani G. Non-viral gene delivery strategies for gene therapy: a "ménage à trois" among nucleic acids, materials, and the biological environment. *J. Nanoparticle Res.* **15,** 1523 (2013).

61. Hayes M. E. *et al.* Genospheres: self-assembling nucleic acid-lipid nanoparticles suitable for targeted gene delivery. *Gene Ther.* **13,** 646–651 (2005).

62. Cavalli R., Bisazza A. & Lembo D. Micro- and nanobubbles: A versatile non-viral platform for gene delivery. *Int. J. Pharm.* **456,** 437–445 (2013).

63. Lechardeur D. & Sohn K.J. Metabolic instability of plasmid DNA in the cytosol: a potential barrier to gene transfer. *Publ. Online 01 April 1999 Doi101038sjgt3300867* **6,** (1999).

64. One Central Press » Polymer nanoparticles for targeted gene delivery.

65. Khalil I. A., Kogure K., Akita H. & Harashima H. Uptake Pathways and Subsequent Intracellular Trafficking in Nonviral Gene Delivery. *Pharmacol. Rev.* **58,** 32–45 (2006).

66. Wan K., Kievit F. M. & Zhang M. Nanoparticles for cancer gene therapy: Recent advances, challenges, and strategies. *Pharmacol. Res.* **114,** 56–66 (2016).

67. Lu Y. & Madu C. O. Viral-based gene delivery and regulated gene expression for targeted cancer therapy. *Expert Opin. Drug Deliv.* **7,** 19–35 (2010).

68. Nayak S. & Herzog R. W. Progress and prospects: immune responses to viral vectors. *Gene Ther.* **17,** 295–304 (2010).

69. Tros de Ilarduya C., Sun Y. & Düzgüneş N. Gene delivery by lipoplexes and polyplexes. *Eur. J. Pharm. Sci.* **40,** 159–170 (2010).

70. Felgner P. L. *et al.* Lipofection: a highly efficient, lipid-mediated DNA-transfection procedure. *Proc. Natl. Acad. Sci.* **84,** 7413–7417 (1987).

71. Aied A., Greiser U., Pandit A. & Wang W. Polymer gene delivery: overcoming the obstacles. *Drug Discov. Today* **18,** 1090–1098 (2013).

72. Wu G. Y. & Wu C. H. Receptor-mediated in vitro gene transformation by a soluble DNA carrier system. *J. Biol. Chem.* **262,** 4429–4432 (1987).

73. Safinya C. R. Structures of lipid–DNA complexes: supramolecular assembly and gene delivery. *Curr. Opin. Struct. Biol.* **11,** 440–448 (2001).

74. Chen M. *et al.* Enhanced gene delivery of low molecular weight PEI by flower-like ZnO microparticles. *Mater. Sci. Eng. C* **69,** 1367–1372 (2016).

75. Fein D. E. *et al.* Novel Cationic Lipids with Enhanced Gene Delivery and Antimicrobial Activity. *Mol. Pharmacol.* **78,** 402–410 (2010).

76.   Oliveira C., Silveira I., Veiga F. & Ribeiro A. J. Recent advances in characterization of nonviral vectors for delivery of nucleic acids: impact on their biological performance. *Expert Opin. Drug Deliv.* **12,** 27–39 (2015).

77.   Nonviral gene therapy: promises and challenges. *Publ. Online 17 January 2000 Doi101038sjgt3301110* **7,** (2000).

78.   Felgner P. L. *et al.* Nomenclature for Synthetic Gene Delivery Systems. *Hum. Gene Ther.* **8,** 511–512 (1997).

79.   Prévost S. *et al.* Colloidal Structure and Stability of DNA/Polycations Polyplexes Investigated by Small Angle Scattering. *Biomacromolecules* **12,** 4272–4282 (2011).

80.   Pack D. W., Hoffman A. S., Pun S. & Stayton P. S. Design and development of polymers for gene delivery. *Nat. Rev. Drug Discov.* **4,** 581–593 (2005).

81.   Gebhart C. L. & Kabanov A. V. Evaluation of polyplexes as gene transfer agents. *J. Controlled Release* **73,** 401–416 (2001).

82.   O'Rorke S., Keeney M. & Pandit A. Non-viral polyplexes: Scaffold mediated delivery for gene therapy. *Prog. Polym. Sci.* **35,** 441–458 (2010).

83.   Mastrobattista E. & Hennink W. E. Polymers for gene delivery: Charged for success. *Nat. Mater.* **11,** 10–12 (2012).

84.   Pezzoli D., Giupponi E., Mantovani D. & Candiani G. Size matters for *in vitro* gene delivery: investigating the relationships among complexation protocol, transfection medium, size and sedimentation. *Sci. Rep.* **7,** srep44134 (2017).

85.   Fischer D., Li Y., Ahlemeyer B., Krieglstein J. & Kissel T. In vitro cytotoxicity testing of polycations: influence of polymer structure on cell viability and hemolysis. *Biomaterials* **24,** 1121–1131 (2003).

86.   Malloggi C. *et al.* Comparative evaluation and optimization of off-the-shelf cationic polymers for gene delivery purposes. *Polym. Chem.* **6,** 6325–6339 (2015).

87. Bengali Z., Rea J. C., Gibly R. F. & Shea L. D. Efficacy of immobilized polyplexes and lipoplexes for substrate-mediated gene delivery. *Biotechnol. Bioeng.* **102,** 1679–1691 (2009).

88. Chang F.-H. *et al.* Surfection: a new platform for transfected cell arrays. *Nucleic Acids Res.* **32,** e33 (2004).

89. Jewell C. M. & Lynn D. M. Surface-mediated delivery of DNA: Cationic polymers take charge. *Curr. Opin. Colloid Interface Sci.* **13,** 395–402 (2008).

90. Pannier A. K. & Shea L. D. Controlled release systems for DNA delivery. *Mol. Ther.* **10,** 19–26 (2004).

91. Segura T., Chung P. H. & Shea L. D. DNA delivery from hyaluronic acid-collagen hydrogels via a substrate-mediated approach. *Biomaterials* **26,** 1575–1584 (2005).

92. Wang, X. & Li, W. Biodegradable mesoporous bioactive glass nanospheres for drug delivery and bone tissue regeneration. *Nanotechnology* **27,** 225102 (2016).

93. Jewell C. M. & Lynn D. M. Multilayered polyelectrolyte assemblies as platforms for the delivery of DNA and other nucleic acid-based therapeutics. *Adv. Drug Deliv. Rev.* **60,** 979–999 (2008).

94. Lvov Y., Decher G. & Sukhorukov G. Assembly of thin films by means of successive deposition of alternate layers of DNA and poly(allylamine). *Macromolecules* **26,** 5396–5399 (1993).

95. Vázquez E., Dewitt D. M., Hammond P. T. & Lynn D. M. Construction of Hydrolytically-Degradable Thin Films via Layer-by-Layer Deposition of Degradable Polyelectrolytes. *J. Am. Chem. Soc.* **124,** 13992–13993 (2002).

96. Bertrand P., Jonas A., Laschewsky A. & Legras R. Ultrathin polymer coatings by complexation of polyelectrolytes at interfaces: suitable materials, structure and properties. *Macromol. Rapid Commun.* **21,** 319–348 (2000).

97. Ren K., Ji J. & Shen J. Construction and enzymatic degradation of multilayered poly-l-lysine/DNA films. *Biomaterials* **27,** 1152–1159 (2006).

98.   Segura T. & Shea L. D. Surface-Tethered DNA Complexes for Enhanced Gene Delivery. *Bioconjug. Chem.* **13,** 621–629 (2002).

99.   Bielinska A. U. *et al.* Application of membrane-based dendrimer/DNA complexes for solid phase transfection in vitro and in vivo. *Biomaterials* **21,** 877–887 (2000).

100.   Zheng J., Manuel W. S. & Hornsby P. J. Transfection of Cells Mediated by Biodegradable Polymer Materials with Surface-Bound Polyethyleneimine. *Biotechnol. Prog.* **16,** 254–257 (2000).

101.   Ye Q., Zhou F. & Liu W. Bioinspired catecholic chemistry for surface modification. *Chem. Soc. Rev.* **40,** 4244–4258 (2011).

102.   Lee H., Dellatore S. M., Miller W. M. & Messersmith P. B. Mussel-Inspired Surface Chemistry for Multifunctional Coatings. *Science* **318,** 426–430 (2007).

103.   Rice C. R., Ward M. D., Nazeeruddin M. K. & Grätzel M. Catechol as an efficient anchoring group for attachment of ruthenium–polypyridine photosensitisers to solar cells based on nanocrystalline TiO2 films. *New J. Chem.* **24,** 651–652 (2000).

104.   Xu C. *et al.* Dopamine as A Robust Anchor to Immobilize Functional Molecules on the Iron Oxide Shell of Magnetic Nanoparticles. *J. Am. Chem. Soc.* **126,** 9938–9939 (2004).

105.   Saidin S., Chevallier P., Abdul Kadir M. R., Hermawan H. & Mantovani D. Polydopamine as an intermediate layer for silver and hydroxyapatite immobilisation on metallic biomaterials surface. *Mater. Sci. Eng. C* **33,** 4715–4724 (2013).

106.   Yu M., Hwang J. & Deming T. J. Role of l-3,4-Dihydroxyphenylalanine in Mussel Adhesive Proteins. *J. Am. Chem. Soc.* **121,** 5825–5826 (1999).

107.   Faure E. *et al.* Catechols as versatile platforms in polymer chemistry. *Prog. Polym. Sci.* **38,** 236–270 (2013).

108.   Kim, K.-Y. *et al.* Polydopamine coating effects on ultrafiltration membrane to enhance power density and mitigate biofouling of ultrafiltration microbial fuel cells (UF-MFCs). *Water Res.* **54,** 62–68 (2014).

109. Liu, Y., Ai, K. & Lu, L. Polydopamine and Its Derivative Materials: Synthesis and Promising Applications in Energy, Environmental, and Biomedical Fields. *Chem. Rev.* **114,** 5057–5115 (2014).

110. Campelo C. S., Chevallier P., Vaz J. M., Vieira R. S. & Mantovani D. Sulfonated chitosan and dopamine based coatings for metallic implants in contact with blood. *Mater. Sci. Eng. C* **72,** 682–691 (2017).

111. Malisova B., Tosatti S., Textor M., Gademann K. & Zürcher S. Poly(ethylene glycol) Adlayers Immobilized to Metal Oxide Substrates Through Catechol Derivatives: Influence of Assembly Conditions on Formation and Stability. *Langmuir* **26,** 4018–4026 (2010).

112. Dalsin J. L. *et al.* Protein resistance of titanium oxide surfaces modified by biologically inspired mPEG-DOPA. *Langmuir ACS J. Surf. Colloids* **21,** 640–646 (2005).

113. Montaño-Machado V. *et al.* A comparison of adsorbed and grafted fibronectin coatings under static and dynamic conditions. *Phys. Chem. Chem. Phys.* **18,** 24704–24712 (2016).

114. Haïdopoulos M., Turgeon S., Laroche G. & Mantovani D. Surface modifications of 316 stainless steel for the improvement of its interface properties with RFGD-deposited fluorocarbon coating. *Surf. Coat. Technol.* **197,** 278–287 (2005).

115. Liao Y. *et al.* Antibacterial surfaces through dopamine functionalization and silver nanoparticle immobilization. *Mater. Chem. Phys.* **121,** 534–540 (2010).

116. Ricciardi S. *et al.* Surface functionalization by poly-acrylic acid plasma-polymerized films for microarray DNA diagnostics. *Surf. Coat. Technol.* **207,** 389–399 (2012).

117. Noel S., Liberelle B., Robitaille L. & De Crescenzo G. Quantification of Primary Amine Groups Available for Subsequent Biofunctionalization of Polymer Surfaces. *Bioconjug. Chem.* **22,** 1690–1699 (2011).

118. Loy C. *et al.* A planar model of the vessel wall from cellularized-collagen scaffolds: focus on cell–matrix interactions in mono-, bi- and tri-culture models. *Biomater. Sci.* **5,** 153–162 (2016).

119.   Doriot P.A. *et al.* In-vivo measurements of wall shear stress in human coronary arteries. [Miscellaneous Article]. *Coron. Artery Dis.* **11,** 495–502 (2000).

120.   Jun Kang Y., Yeom E. & Lee S.J. A microfluidic device for simultaneous measurement of viscosity and flow rate of blood in a complex fluidic network. *Biomicrofluidics* **7,** (2013).

121.   Müller-Hülsbeck S., Grimm J., Jahnke T., Häselbarth G. & Heller M. Flow patterns from metallic vascular endoprostheses: in vitro results. *Eur. Radiol.* **11,** 893–901 (2001).

122.   Levesque J. Conception et validation d'un banc d'essai pour évaluer la dégradation d'alliages de magnésium dans des conditions quasi-physiologiques. (2004).

123.   Shih C.C. *et al.* Effect of surface oxide properties on corrosion resistance of 316L stainless steel for biomedical applications. *Corros. Sci.* **46,** 427–441 (2004).

124.   Haïdopoulos, M., Turgeon, S., Laroche, G. & Mantovani, D. Chemical and Morphological Characterization of Ultra-Thin Fluorocarbon Plasma-Polymer Deposition on 316 Stainless Steel Substrates: A First Step Toward the Improvement of the Long-Term Safety of Coated-Stents. *Plasma Process. Polym.* **2,** 424–440 (2005).

125.   Ginic-Markovic, M. *et al.* A versatile approach to grafting biofouling resistant coatings from polymeric membrane surfaces using an adhesive macroinitiator. *RSC Adv.* **5,** 63017–63024 (2015).

126.   Cong, Y. *et al.* Mussel-inspired polydopamine coating as a versatile platform for synthesizing polystyrene/Ag nanocomposite particles with enhanced antibacterial activities. *J. Mater. Chem. B* **2,** 3450–3461 (2014).

127.   Iqbal, Z., Lai, E. P. C. & Avis, T. J. Antimicrobial effect of polydopamine coating on Escherichia coli. *J. Mater. Chem.* **22,** 21608–21612 (2012).

128.   Zhang, M., He, X., Chen, L. & Zhang, Y. Preparation of IDA-Cu functionalized core–satellite Fe3O4/polydopamine/Au magnetic nanocomposites and their application for depletion of abundant protein in bovine blood. *J. Mater. Chem.* **20,** 10696–10704 (2010).

129.   Arjomand, H., Turi, Z. G., McCormick, D. & Goldberg, S. Percutaneous coronary intervention: historical perspectives, current status, and future directions. *Am. Heart J.* **146,** 787–796 (2003).